

PENNSSTATE



Radiation Science and Engineering Center
College of Engineering
The Pennsylvania State University
Breazeale Nuclear Reactor Building
University Park, PA 16802-2301

(814) 865-6351
Fax: (814) 863-4840

Annual Operating Report, FY 04-05
PSBR Technical Specifications 6.6.1
License R-2, Docket No. 50-5

December 15, 2005

U. S. Nuclear Regulatory Commission
Attention: Document Control Desk
Washington, D. C. 20555

Dear Sir:

Enclosed please find the Annual Operating Report for the Penn State Breazeale Reactor (PSBR). This report covers the period from July 1, 2004 through June 30, 2005, as required by technical specifications requirement 6.6.1. Also included are any changes applicable to 10 CFR 50.59.

A copy of the Fiftieth Annual Progress Report of the Penn State Radiation Science and Engineering Center is included as supplementary information.

Sincerely yours,

C. Frederick Sears
Director, Radiation Science
and Engineering Center

Enclosures

tlf

cc. E. J. Pell
D. N. Wormley
L. C. Burton
E. J. Boeldt
M. Mendonca
T. Dragoun

AO20
-AUD1

PENN STATE BREAZEAL REACTOR

Annual Operating Report, FY 04-05
PSBR Technical Specifications 6.6.1
License R-2, Docket No. 50-5

Reactor Utilization

The Penn State Breazeale Reactor (PSBR) is a TRIGA Mark III facility capable of 1 MW steady state operation, and 2000 MW peak power pulsing operation. Utilization of the reactor and its associated facilities falls into two major categories:

EDUCATION utilization is primarily in the form of laboratory classes conducted for graduate and undergraduate students and numerous high school science groups. These classes vary from neutron activation analysis of an unknown sample to the calibration of a reactor control rod. In addition, an average of 2500 visitors tour the PSBR facility each year.

RESEARCH/SERVICE accounts for a large portion of reactor time which involves Radionuclear Applications, Neutron Radiography, a myriad of research programs by faculty and graduate students throughout the University, and various applications by the industrial sector.

The PSBR facility operates on an 8 AM - 5 PM shift, five days a week, with an occasional 7 AM - 7 PM or 8 AM - 12 Midnight shift to accommodate laboratory courses or research/service projects.

Summary of Reactor Operating Experience - Tech Specs requirement 6.6.1.a.

Between July 1, 2004 and June 30, 2005, the PSBR was		
critical for	1034 hours	or 3.7 hrs/shift
subcritical for	450 hours	or 1.6 hrs/shift
used while shutdown for	621 hours	or 2.2 hrs/shift
not available	47 hours	or 0.1 hrs/shift
Total usage	2155 hours	or 7.6 hrs/shift

The reactor was pulsed a total of 152 times with the following reactivities:

< \$2.00	12
\$2.00 to \$2.50	127
> \$2.50	13

The square wave mode of operation was used 39 times to power levels between 100 and 500 KW.

Total energy produced during this report period was 657 MWH with a consumption of 34 grams of U-235.

Unscheduled Shutdowns - Tech Specs requirement 6.6.1.b.

The three unplanned shutdowns during the July 1, 2004 to June 30, 2005 period are described below.

On August 20, 2004, a reactor operator inadvertently bumped a button on the Reactor Safety System Power Range drawer causing a non-operate indication and a reactor scram from a power level of 3 kW.

On August 25, 2004, a reactor operator inadvertently pushed the regulating rod scram button instead of the regulating rod up button during a rod calibration procedure, resulting in a reactor scram from a power level of ~100 watts. As a result of the August 20 and August 25 events (and another event similar to that of August 25 that occurred prior to a reactor startup on July 1), hinged covers were placed over the buttons on the wide range and power range channels, the control rod scram buttons, and the building evacuation alarm button.

On January 11, 2005, a reactor scram occurred during a reactor startup (reactor in manual and period still infinite). The Fast Neutron Irradiator rotator alarm sounded during the startup. The operator stood up and reached across the console wide range drawer to manipulate the rotator switch, and about that time the scram occurred. An investigation revealed that pushing the 100 khz button can generate the same message and the same historical trends generated by the scram. It was also demonstrated that the 100 khz button could be depressed by pushing on its protective cover (a plexiglass flap). New protective covers were placed around the switches on the power range and wide range drawers. These covers are raised plexiglass with cutouts to provide access to the switches.

Major Maintenance With Safety Significance - Tech Specs requirement 6.6.1.c.

On March 21 following the 4th pulse of a NE 497F class, an observation of the control rod mimic display suggested that the TR took longer than normal to bottom. An as found measurement confirmed that the drop time was approximately 1.4 sec. Thus the PSBR was in violation of TS 3.2.6, "The time from the SCRAM initiation to the full insertion of any control rod from a full up position shall be less than 1 second." CCP-9, Transient Rod Drive and Air Supply Inspection, and then CCP-1, Control Rod Speed and Scram Time Checks, were initiated and following the cleaning and lubrication, the drop time was measured in the mid-700 mSec range (the last annual check on August 19, 2004, found it to be 680 mSec). The NRC was notified and operations resumed, with the requirement to repeat the CCP-1 the next Monday, the 28th. On the 28th, the drop time was in the mid-800 mSec range. Based on the 21st and 28th measurements, further cleaning and lubrication was conducted, but the drop times actually increased. The TR system was dis-assembled and it was found that a Teflon seal inside of an O-ring was almost totally separated, and the TR rod piston was dragging on the O-ring instead of moving freely inside the Teflon seal. The Teflon seal and O-ring were replaced, and the TR piston was mechanically cleaned with diamond paper, acetone, and ethyl alcohol to remove any traces of the Mobil I lubricant that had been used for the last few years. The TR was re-assembled and lubricated with krytox, a previously used lubricant that provides good drop times but may increase air leakage from the system (not a safety concern). CCP-1 drop times were now in the mid-600 mSec range. CCP-1 frequency was increased pending further assessment of TR performance. The last complete teardown of the TR mechanism and seal replacement was approximately five years prior to this event. Procedure changes were made to increase the frequency of scram time checks and Transient Rod system teardown and inspection.

Major Changes Reportable Under 10 CFR 50.59 - Tech Specs requirement 6.6.1.d.

Facility Changes -

During August 2 to August 5, 2004, an upgrade of the reactor console hardware and software was completed. The original AECL/GammaMetrics Control Console was installed in 1992. The digital Protection, Control, and Monitoring System (PCMS) provides reactor control, historical data storage, and a Local Area Network (LAN) for remote monitoring of reactor parameters. The console provides a hard-wired Reactor Safety System (RSS) analog system to meet Tech Specs

requirements. There were no changes to the RSS. The PCMS has provided a high degree of reliability and flexibility. The upgrade consisted of two parts. First the computer hardware was upgraded to more modern equipment. The control software was upgraded to include issues raised over the last eleven years by Penn State and other AECL customers. The 50.59 review revealed no new safety issues.

Procedures -

Procedures are normally reviewed biennially, and on an as needed basis. Changes during the year were numerous and no attempt will be made to list them.

New Tests and Experiments -

None

Radioactive Effluents Released - Tech Specs requirement 6.6.1.e.

Liquid

There were no planned liquid effluent releases under the reactor license for the report period.

Liquid radioactive waste from the radioisotope laboratories at the PSBR is under the University byproduct materials license and is transferred to the Radiation Protection Office for disposal with the waste from other campus laboratories. Liquid waste disposal techniques include storage for decay, release to the sanitary sewer as per 10 CFR 20, and solidification for shipment to licensed disposal sites.

Gaseous

Gaseous effluent Ar-41 is released from dissolved air in the reactor pool water, air in dry irradiation tubes, air in neutron beam ports, and air leakage to and from the carbon-dioxide purged pneumatic sample transfer system. During the year, an unplanned release of Ar-41 occurred during the production of Ar-41 for a commercial customer, and is included in the calculations for the year.

The amount of Ar-41 released from the reactor pool is very dependent upon the operating power level and the length of time at power. The release per MWH is highest for extended high power runs and lowest for intermittent low power runs. The concentration of Ar-41 in the reactor bay and the bay exhaust was measured by the Radiation Protection staff during the summer of 1986. Measurements were made for conditions of low and high power runs simulating typical operating cycles. Based on these measurements, an annual release of between 498 mCi and 1511 mCi of Ar-41 is calculated for July 1, 2004 to June 30, 2005, resulting in an average concentration at ground level outside the reactor building that is 0.8 % to 2.4 % of the effluent concentration limit in Appendix B to 10 CFR 20.1001 - 20.2402. The concentration at ground level is estimated using only dilution by a 1 m/s wind into the lee of the 200 m² cross section of the reactor bay.

During the report period, several irradiation tubes were used at high enough power levels and for long enough runs to produce significant amounts of Ar-41. The calculated annual production was 427 mCi. Since this production occurred in a stagnant volume of air confined by close fitting shield plugs, much of the Ar-41 decayed in place before being released to the reactor bay. The reported releases from dissolved air in the reactor pool are based on measurements made, in part, when a dry irradiation tube was in use at high power levels; some of the Ar-41 releases from the tubes are part of rather than in addition to the release figures quoted in the previous paragraph. Even if all of the 427 mCi were treated as a separate release, the percent of the Appendix B limit given in the previous paragraph would still be no more than 3.1 %. During the year, an

unplanned release of 120 mCi of Ar-41 occurred during the production of Ar-41 for a commercial customer. Including this release would increase the previous 3.1% figure to 3.3%.

Production and release of Ar-41 from reactor neutron beam ports was minimal. Beam port #7 has only three small collimation tubes (each 1 cm² area) exiting the port and any Ar-41 production in these small tubes is negligible. Beam port #4 has an aluminum cap installed inside the outer end of the beam tube to prevent air movement into or out of the tube as the beam port door is opened or closed. The estimated Ar-41 production in beam port #4 for all beam port operations is 37 mCi. With the aforementioned aluminum cap in place, it is assumed that this Ar-41 decayed in place. Radiation Protection Office air measurements have found no presence of Ar-41 during beam port #4 reactor operations with the beam port cap in place.

The use of the pneumatic transfer system was minimal during this period and any Ar-41 release would be insignificant since the system operates with CO-2 as the fill gas.

Tritium release from the reactor pool is another gaseous release. The evaporation rate of the reactor pool was checked previously by measuring the loss of water from a flat plastic dish floating in the pool. The dish had a surface area of 0.38 ft² and showed a loss of 139.7 grams of water over a 71.9 hour period giving a loss rate of 5.11 g ft⁻² hr⁻¹. Based on a pool area of about 395 ft² the annual evaporation rate would be 4680 gallons. This is of course dependent upon relative humidity, temperature of air and water, air movement, etc. For a pool ³H concentration of 33633 pCi/l (the average for July 1, 2004 to June 30, 2005) the tritium activity released from the ventilation system would be 596 μCi. A dilution factor of 2 x 10⁸ ml s⁻¹ was used to calculate the unrestricted area concentration. This is from 200 m² (cross-section of the building) times 1 m s⁻¹ (wind velocity). These are the values used in the safety analysis in the reactor license. A sample of air conditioner condensate a previous year showed no detectable ³H. Thus, there is probably very little ³H recycled into the pool by way of the air conditioner condensate and all evaporation can be assumed to be released.

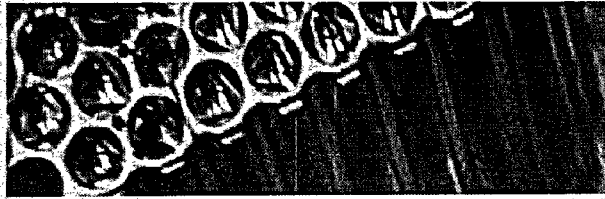
³ H released	596 μC
Average concentration, unrestricted area	9.45 x 10 ⁻¹⁴ μCi/ml
Permissible concentration, unrestricted area	1 x 10 ⁻⁷ μCi/ml
Percentage of permissible concentration	9.45 x 10 ⁻⁵ %
Calculated effective dose, unrestricted area	4.72 x 10 ⁻⁵ mRem

Environmental Surveys - Tech Specs requirement 6.6.1.f.

The only environmental surveys performed were the routine TLD gamma-ray dose measurements at the facility fence line and at control points in two residential areas several miles away. This reporting year's gross measurements (in millirems) tabulated below represent the July 1, 2004 to June 30, 2005 period.

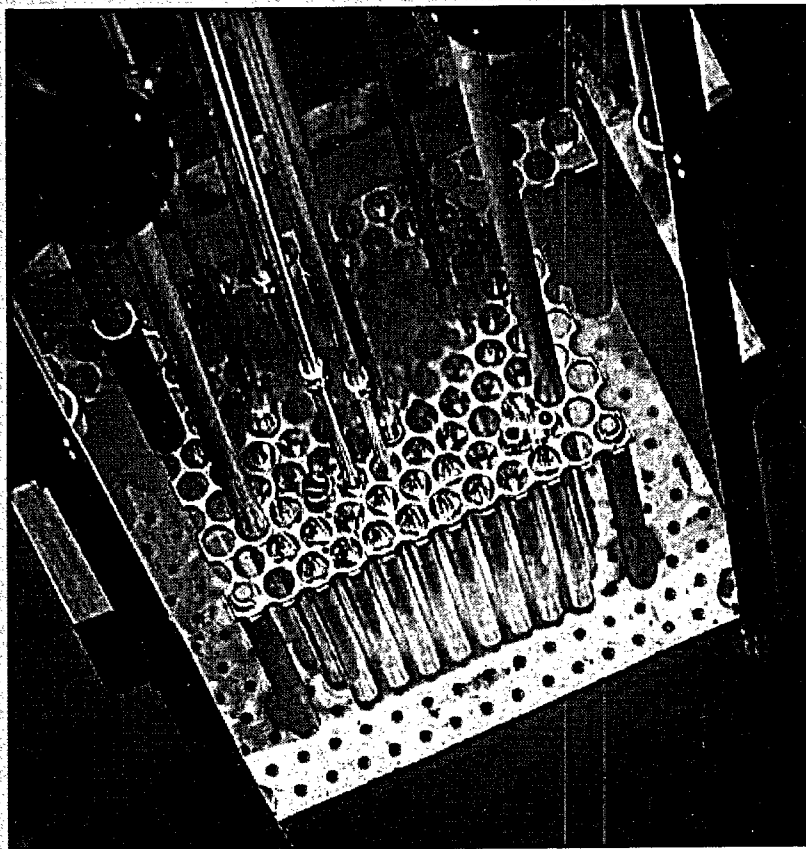
	<u>3rd Qtr '04</u>	<u>4th Qtr '04</u>	<u>1st Qtr '05</u>	<u>2nd Qtr '05</u>	<u>Total</u>
Fence North	27.8	28.7	26.3	30.4	113.2
Fence South	28.7	30.6	23.9	29.3	112.5
Fence East	28.8	30.0	20.8	31.5	111.1
Fence West	25.7	30.7	30.8	29.6	116.8
Control	25.8	31.0	22.9	30.0	109.7
Control	22.4	25.5	18.4	24.0	90.3

PENNSTATE



Radiation Science and Engineering Center (RSEC)

50th Annual Progress Report



**College of Engineering
Breazeale Nuclear Reactor
University Park, PA 16802**

December 2005

50TH ANNUAL PROGRESS REPORT

PENN STATE RADIATION SCIENCE & ENGINEERING CENTER

July 1, 2004 to June 30, 2005

Submitted to:

United States Department of Energy

and

Penn State

By:

C. Frederick Sears (Director)
Kenan Ünlü (Associate Director for Research)
Terry L. Flinchbaugh (Associate Director for Operations)
Wendy Belinc (Staff Assistant, Editor)
Radiation Science and Engineering Center
Penn State
University Park, PA 16802

December 2005
Contract DE-AC07-99ID13727
Contract 0036822
U.Ed. ENG 06-50

*Penn State is committed to affirmative action, equal opportunity,
and the diversity of its workforce.*

	<u>Page</u>
PREFACE - T.L. Flinchbaugh	iv
I. INTRODUCTION - K. Ünlü	1
II. PERSONNEL – T.L. Flinchbaugh	4
III. REACTOR OPERATIONS – T.L. Flinchbaugh	8
IV. GAMMA IRRADIATION FACILITY – C. C. Davison	12
V. EDUCATION AND TRAINING – C. C. Davison	15
VI. NEUTRON BEAM LABORATORY – K. Ünlü	19
VII. RADIONUCLEAR APPLICATIONS LABORATORY	
A. Service – T.H. Daubenspeck	21
B. Research – K. Ünlü	22
VIII. NEW CLASSROOM	23
IX. ANGULAR CORRELATIONS LABORATORY – G.L. Catchen	24
X ENVIRONMENTAL HEALTH AND SAFETY – D.Bertocchi	25
XI. RADIATION SCIENCE AND ENGINEERING CENTER RESEARCH AND SERVICE UTILIZATION	
A. Penn State Research and Service Utilizing the Facilities of the Penn State Radiation Science & Engineering Center – K. Ünlü, S. M. Çetiner, A.A. Talley	28
B. Other Universities, Organizations and Companies Utilizing the Facilities of the Penn State Radiation Science & Engineering Center – T.L. Flinchbaugh	93
XII. PUBLICATIONS – K. Ünlü	94
APPENDIX A. Faculty, Staff, Students, and Industries Utilizing the Facilities of the Penn State Radiation Science & Engineering Center - T.L. Flinchbaugh	96
APPENDIX B. Formal Tour Groups – A.A.Talley	100

TABLES

	<u>Page</u>
1. Personnel	5
2. Penn State Reactor Safeguards Committee	6
3. Reactor Operation Data	10
4. Reactor Utilization Data	11
5. Summary of Current Gamma Irradiation Facilities	13
6. Cobalt-60 Utilization Data	13
7. Academic Instruction Data	17

FIGURES

	<u>Page</u>
1. Organization Chart	7
2. Gamma Irradiation Uses and Examples	14
3. Educational Institutions Visiting the RSEC	18

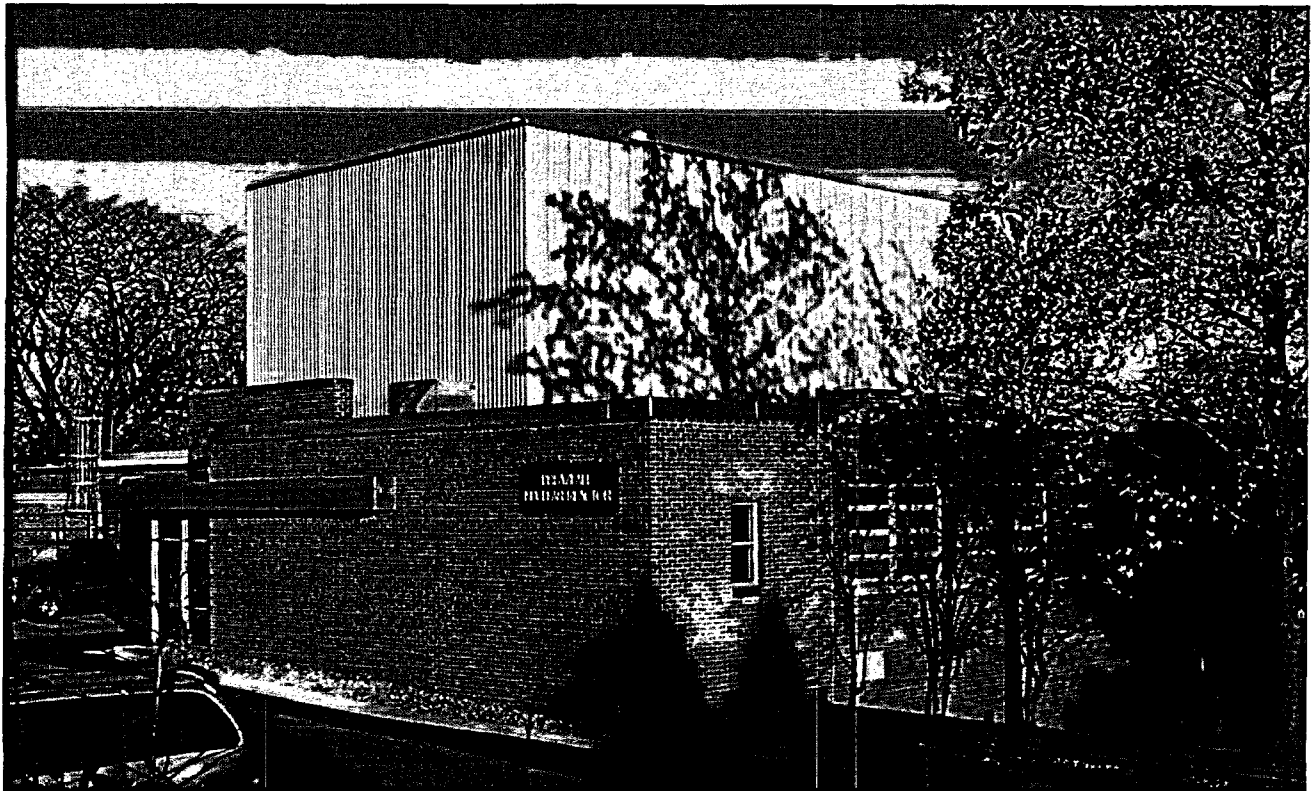
PREFACE

Administrative responsibility for the Radiation Science and Engineering Center (RSEC) resides in the College of Engineering. Overall responsibility for the reactor license resides with the Vice President for Research and the Dean of the Graduate School. The reactor and associated laboratories are available to all Penn State colleges for education and research programs. In addition, the facility is made available to assist other educational institutions, government agencies and industries having common and compatible needs and objectives, providing services that are essential in meeting research, development, education, and training needs.

The Penn State University Radiation Science and Engineering Center's 50th Annual Progress Report (July 2004 through June 2005) is submitted in accordance with the requirements of Contract DE-AC07-99ID13727 between the United States Department of Energy and Bechtel (BWXT Idaho), and their Contract 00036822 with The Pennsylvania State University. This report also provides the University administration with a summary of the utilization of the facility for the past year.

Numerous individuals are to be recognized and thanked for their dedication and commitment in this report, especially Wendy Belinc, Sacit Çetiner, and Ashley Talley. Special thanks are extended to those responsible for the individual sections as listed in the table of contents and to the individual facility users whose research summaries are compiled in Section X.

INTRODUCTION



MISSION

The mission of The Penn State Radiation Science and Engineering Center (RSEC), in partnership with faculty, staff, students, alumni, government, and corporate leaders, is to safely utilize nuclear technology to benefit society through education, research, and service.

The RSEC facilities have a diverse and dedicated staff with a commitment to safety, excellence, quality, user satisfaction, and education by example and teaching.

VISION

It is the vision of the faculty and staff of the Radiation Science and Engineering Center to become a leading national resource and make significant contributions in the following areas:

- Safety** Actively promote nuclear and personal safety in everything we do.
- Education** Develop and deliver innovative educational programs to advance societal knowledge of nuclear science and engineering through resident instruction and continuing education for students of all ages and their educators.
- Research** Expand leading edge research that increases fundamental knowledge of nuclear science and engineering particularly in the area of materials research applications of nuclear techniques.
- Service** Expand and build a diverse array of services and users by maintaining excellence, quality, user satisfaction, and efficient service to supplement university funding and enhance education and research.

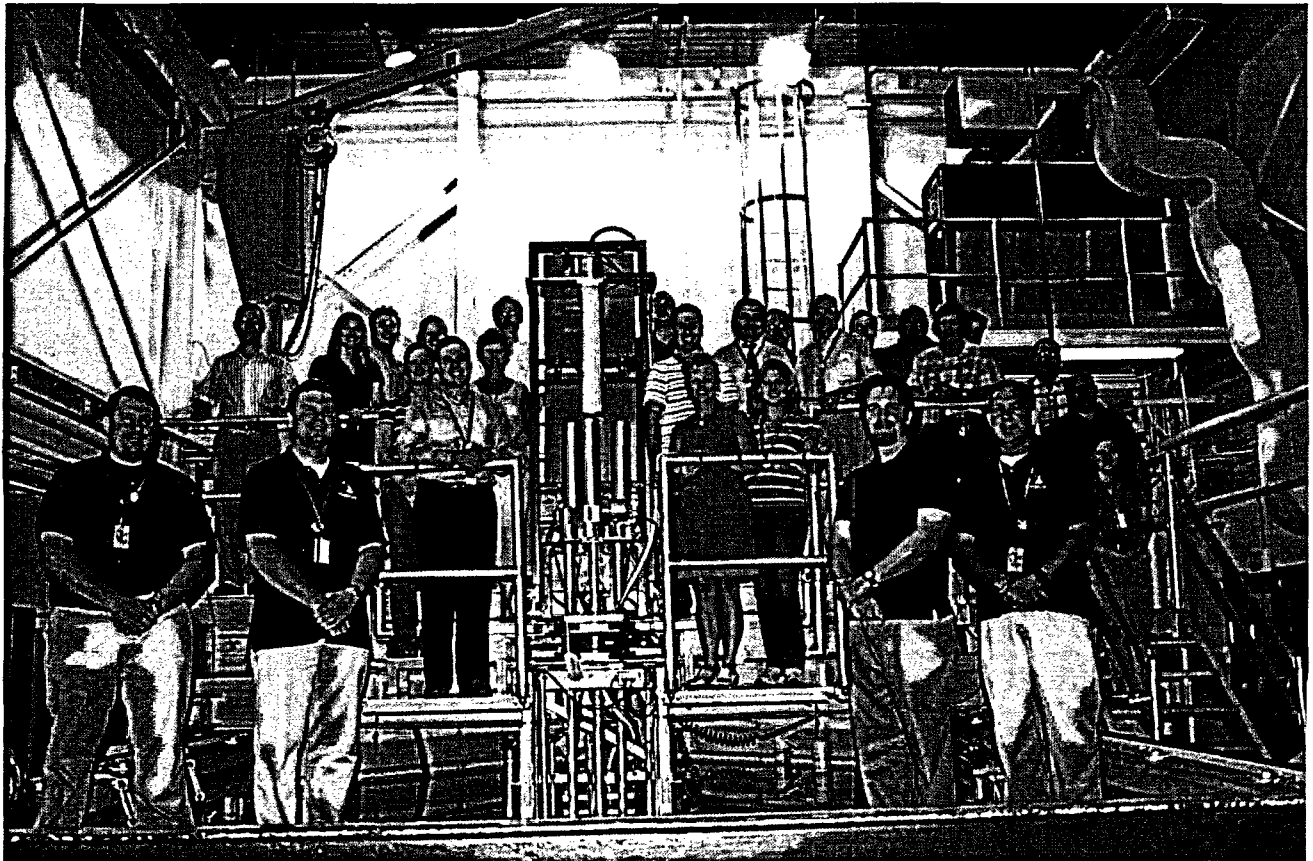
In conducting this mission in pursuit of the stated vision, the following activities are highlighted among the numerous accomplishments reported in the pages that follow:

- Architectural plans for the RSEC expansion for a new Neutron Beam Hall and Neutron Beam Ports facilities are completed. Working with a professional architectural firm, a contractor, and related personnel from various university functions, we obtained a firm estimate for the expansion cost. Internal benefactors of the new neutron beam facilities are identified. We obtained support letters or expression of interests from about 30 faculty members from four different colleges within the university. More than half of the total budget for expansion is currently available, and efforts to raise the remaining portion of the budget continue. The Penn State University responded to a US Department of Energy request for an Expression of Interest (EOI) last April for the RSEC expansion for a new Neutron Beam Hall and Neutron Beam Ports. The response for the EOI was submitted with active support and participation of the Dean of the College of Engineering and the Vice President for Research.
- Considerable faculty and staff effort was rewarded when DOE issued the INIE (Innovations in Nuclear Infrastructure and Education) grants. The INIE Big-Ten Consortium, led by Penn State and consisting of Purdue University, the University of Illinois and the University of Wisconsin received approximately \$1.97 million per year in FY02 and FY03 and \$2.1 in FY 04. The Ohio State University and the University of Michigan joined the Big-Ten Consortium during the FY 04. The consortium funding is about \$1.9 million per year currently and DOE plans to continue the grant program until the year 2010. The objective of the INIE program is to strengthen the Nation's university nuclear engineering programs through innovative use of the university research and training reactors. During the three-year period of the INIE grant the following was accomplished at Penn State:
 - A state-of-the-art Compton Suppression System was purchased and installed at the RAL Laboratory to increase our capabilities in NAA.

- The Room 2 laboratory/classroom and Room 111 classroom was totally refurbished and equipped with state of the art computer work stations and audio-visual equipment with partial funding from the INIE.
 - A refurbished GammaCell was purchased, and installed during the '02-'03 fiscal year. The upgraded Cobalt-60 loading decreased irradiation times by a factor of ten, providing much better service for campus users.
 - A slow neutron chopper system was developed with a chopper brought from the Cornell University, Ward Center for Nuclear Sciences, to characterize the neutron beam used for radiography and radioscopy. As part of the INIE grant, this system is available for loan to other research reactors. As part of neutron beam characterization efforts, a He-3 neutron spectrometer system was purchased and is being tested to determine the spectrum of high-energy neutrons.
 - Mini-grants were awarded on a competitive basis to PSU and non-PSU individuals submitting proposals to use the Penn State Radiation Science and Engineering Center facilities.
 - Efforts continue to lay the groundwork for the development of a cold neutron beam and new neutron beam port facilities. Both thermal and thermo-hydraulic behavior of two university based cold neutron sources are being evaluated in order to build a third generation mesitylene based cold neutron source at Penn State. Code development also continues to model the existing beam ports and various future designs.
 - Improvements in the neutron beam quality and the neutron imaging hardware and software are continuing.
- Dr. Kenan Ünlü, and Drs. Vijaykrishnan Narayanan, Mary Jane Irwin and Yuan Xie of the Department of Computer Science and Engineering continued testing of neutron induced soft errors in semiconductor memories and started to develop a soft error analysis toolset program. This research project has received wide recognitions within the academic and industrial circles. A major grant from NSF was awarded to this research project for the next three years.
 - Drs. Matthew Mench, Jack Brenizer, Kenan Ünlü, and Abel Chuang of the Department of Mechanical and Nuclear Engineering continue major research projects using neutron radioscopy and neutron radiography for investigation of fuel cells for several major automotive companies. Several other companies used the beam facilities for radiography and radioscopy projects, some of which were associated with NASA's space shuttle program. A DOE-NEER grant is awarded for the extension of this project for the development of neutron tomography at the RSEC for the next three years.
 - Dr. Kenan Ünlü, and Dr. Peter I. Kuniholm from Cornell University continue neutron activation analysis of absolutely dated tree rings to identify climatically significant marker events in history and prehistory. A DOE-NEER grant was awarded for this project for the next three years. Also this project received wide national and international recognition last year. The project is featured in numerous web pages worldwide including NSF web page: (http://www.nsf.gov/news/news_summ.jsp?cntn_id=104245&org=NSF&from=news). The NSF has also prepared an audio clip for the "Imagine That" program for this project. This clip was broadcasted over 500 radio stations nationwide during August/September months. The clip can be listened from the link below:

- <http://www.flpradio.com/features>, click on the Imagine That! link, click on the 8.22.05-9.16.05 dated link, and then select the 23 IT 9.5.05.mp3 link.
- The neutron irradiation of semi-conductors for commercial, military and space applications continued at a very healthy pace.
- The use of neutron radioscopy and neutron transmission as a research and service tool to industry continued at a very high level during the year with increasing interest by companies who fabricate boron containing metals used in the nuclear industry. Efforts are underway to upgrade the software and hardware associated with this work.
- Income from service work done for industrial users was used to continue the support of three PhD graduate students in the nuclear engineering department. Two students are working in the area of modeling the Penn State TRIGA reactor core and developing better computer code tools for fuel depletion tracking and core loading designs. The third student is working in the area of thermal-hydraulic modeling of the TRIGA core.
- Numerous high school, Penn State, and non-Penn State college/university groups participated in educational programs at the RSEC under the direction of Candace Davison during the year. In many cases, experiments teaching nuclear concepts were performed. The RSEC also supported educational events such as Boy Scout and Girl Scout merit badge programs. The facility hosted over 2400 visitors during the fiscal year. A complete list of groups hosted is presented in Appendix B.
- Increased reactor usage for university courses continued this year as multiple sessions were needed in the NE 451 and NE 450 laboratory courses. An increased emphasis on graduate students taking NE 497F, Nuclear Reactor Operations, resulted in more reactor usage during the year.
- In light of concern for terrorist activities that could be directed against university research reactors, continuing efforts were made in expanding the total scope of facility security. Additional attention to security issues is expected to continue, both self-directed and in response to NRC guidance. The staff is meeting the challenge of providing security without compromising the education and research mission of the reactor facility.

PERSONNEL



Several undergraduate students worked in work-study or wage payroll positions during the year. Daniel Skilone, Ashley Talley, Aaron Wilmot, Doug Yocum, and Amy Miller assisted Candace Davison in facility educational programs for high school students. Jared Hoover, Fernando Palacios, and Jung Rim assisted Dr. Kenan Ünlü on research projects.

Jeremy Myers, computer support specialist, resigned in July of 2004.

Michael Smith was hired as a computer support specialist in September of 2004. He was promoted to Information Technology Specialist I on February 11, 2005.

Angela Pope resigned as Staff Assistant V in September 2004 when she became a full time undergraduate student.



Figure 1. Reactor Operator Interns, Rachel Slaybaugh (front), Joshua LaFrance and Adina LaFrance (back).

Undergraduate Eric Schwarz was hired as a reactor operator intern in October of 2004. He received his senior reactor operator's license in June of 2005. Eric had previous nuclear navy experience.

Adam Koziol, undergraduate senior reactor operator, resigned his position on December 20, 2004.

Chanda Decker, undergraduate senior reactor operator, resigned her position on April 27, 2005.



Figure 2. Candace Davison, Senior Reactor Operator, Adam Koziol, Senior Reactor Operator Intern, and Brenden Heidrich, Senior Reactor Operator.

The following changes to the membership of the Penn State Reactor Safeguards Committee (PSRSC) were effective on Jan. 1, 2005. Richard Benson (Professor and Department Head, Mechanical and Nuclear Engineering, Penn State) completed his second term. Matthew Mench (Assistant Professor of Mechanical Engineering, Penn State) was appointed to a first term. Committee chair Tom Litzinger (Professor and Director of Leonhard Center, Penn State) and Kostadin Ivanov (Professor in Charge of Fuel Management, Penn State) were reappointed to second terms.

TABLE 1

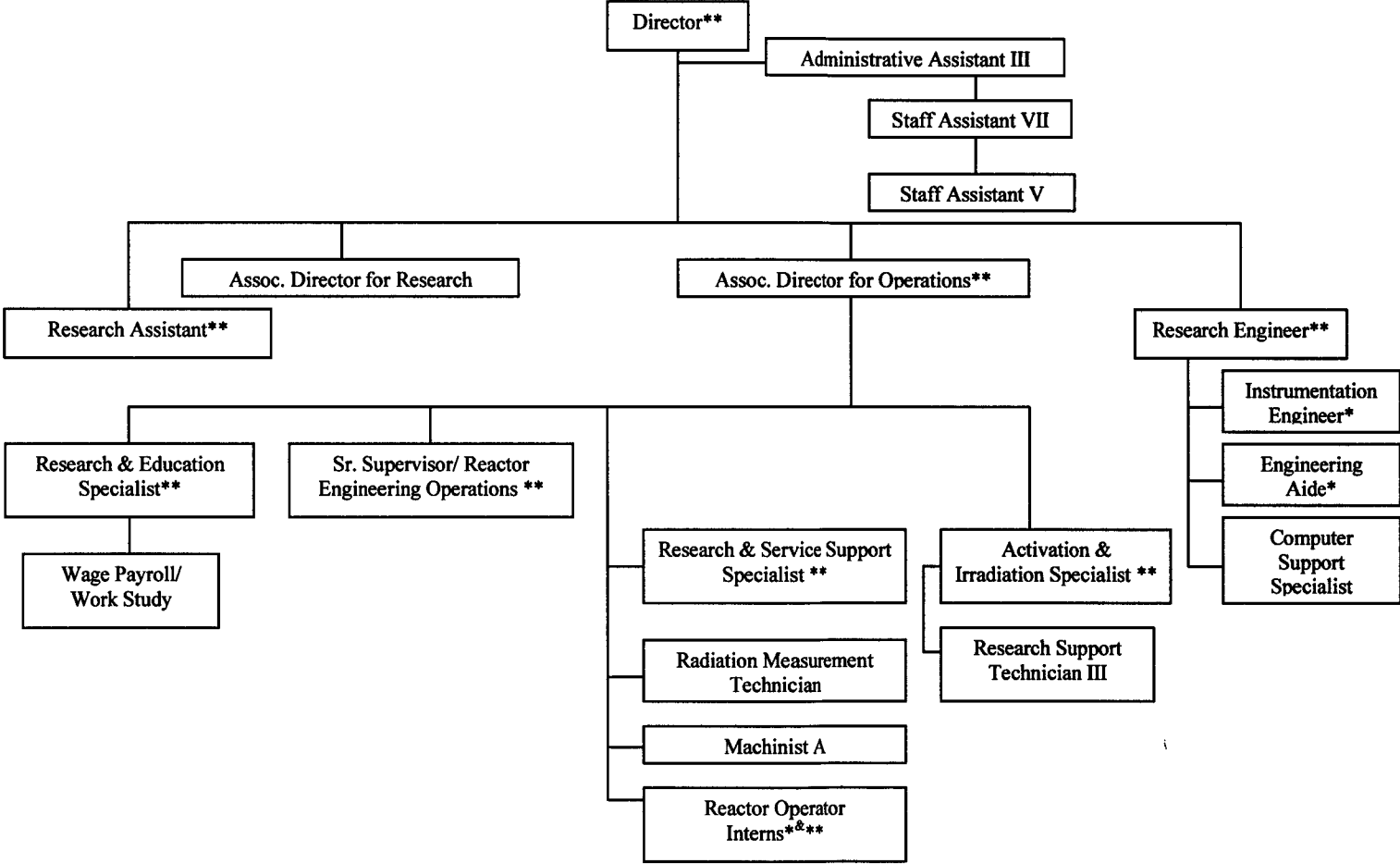
Faculty and Staff	Title
Jack S. Brenizer	Professor & Program Chair, Nuclear Engineering
** Mac E. Bryan	Research Engineer/Supervisor, Reactor Operations
Gary L. Catchen	Professor, Nuclear Engineering
** Thierry H. Daubenspeck	Activation & Irradiation Specialist/Supervisor, Reactor Operations
** Candace C. Davison	Research & Education Specialist/Supervisor, Reactor Operations
** Chanda C. Decker	Reactor Operator Intern (resigned)
Wendy R. Belinc	Staff Assistant VII
Ronald L. Eaken	Reactor Machinist
** Terry L. Flinchbaugh	Associate Director for Operations
** Brenden J. Heidrich	Research Assistant
Eric G. Knepp	Engineering Aide (resigned)
** Adam W. Kozial	Reactor Operator Intern (resigned)
** Adina K. LaFrance	Reactor Operator Intern
** Joshua A. LaFrance	Reactor Operator Intern
Jana Lebedzik	Research Support Technician III
** Gary M. Morlang	Senior Supervisor/Reactor Engineering Operations
Jeremy M. Myers	Computer Support Specialist (resigned)
Angela D. Pope	Staff Assistant V (resigned) - continued as part-time wage payroll
** Alison R. Portanova	Research & Service Support Specialist/Supervisor, Reactor Operations
Paul R. Rankin	Radiation Measurement Technician
** Bret M. Rickert	Reactor Operator Intern
Susan K. Ripka	Administrative Aide III
** C. Frederick Sears	Senior Scientist/Director, RSEC, Associate Professor, Nuclear Engineering
** Eric A. Schwarz	Reactor Operator Intern
* Rachel N. Slaybaugh	Reactor Operator Intern
Michael G. Smith	Began as wage payroll - promoted to Information Technology Specialist I
Sally Thomas	Staff Support
Kenan Ünlü	Senior Scientist/Associate Director for Research, Professor, Nuclear Engineering
* <i>Licensed Operator</i>	
** <i>Licensed Senior Operator</i>	
Wage Payroll/Work Study	
Jared Hoover	Daniel Skilone
Amy Miller	Ashley Talley
Fernando Palacios	Aaron Wilmot
Jung Rim	Doug Yocum
Graduate Students	
Jennifer Butler	A. Kevin Heller
Sacit M. Çetiner	Corey Trivelpiece
Nesrin O. Çetiner	Seth May
Danielle Hauck	

TABLE 2

Penn State Reactor Safeguards Committee

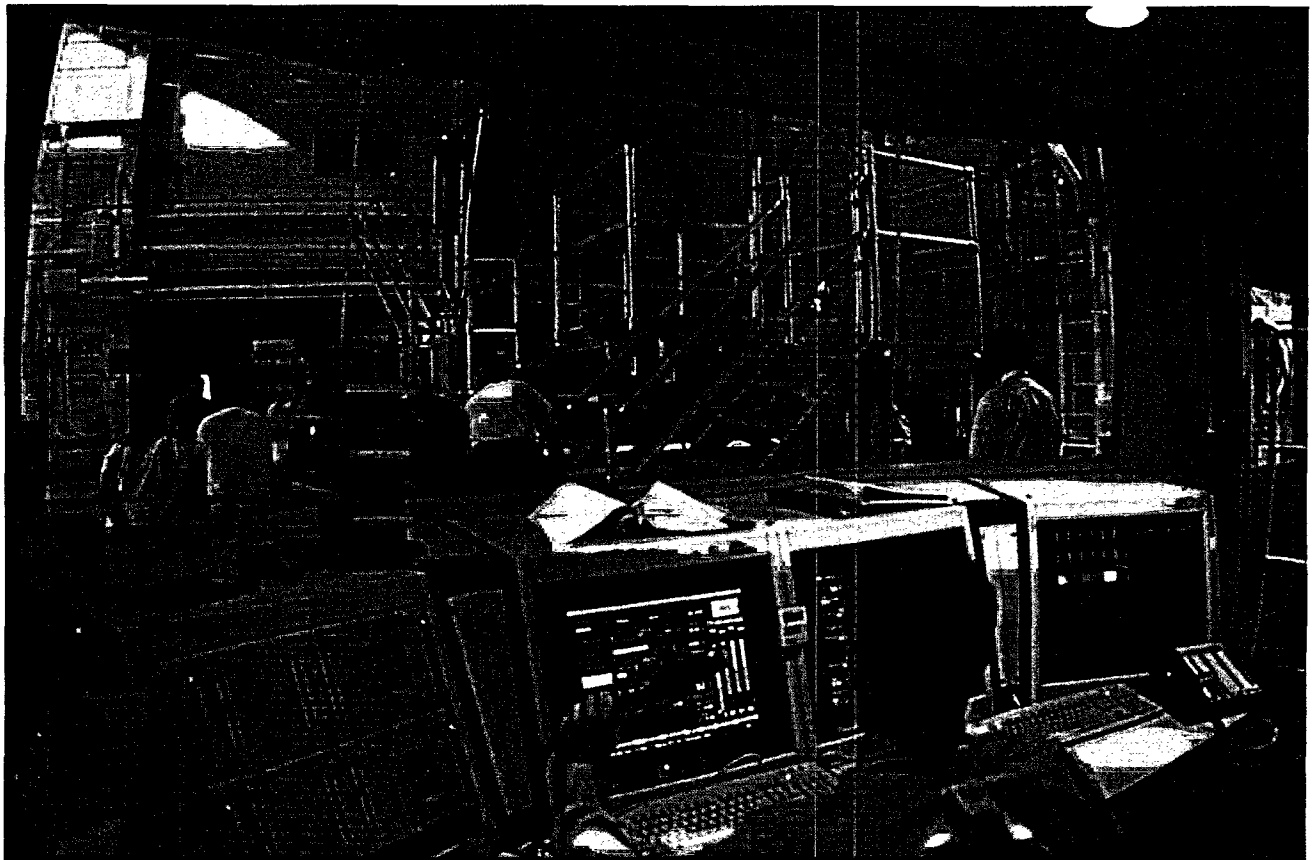
	Y. Azmy	Professor of Nuclear Engineering, Penn State
*	R. Benson	Professor & Dept. Head, Mechanical & Nuclear Engineering, Penn State
	E. Boeldt	Manager, Radiation Protection, Penn State Environmental Health & Safety
	F. Eisenhuth	Sr. Engineer, Pennsylvania Power & Light Susquehanna Steam Electric Station
***	K. Ivanov	Professor in Charge of Fuel Management, Penn State
***	T. Litzinger, Chairman	Professor & Director of Leonhard Center, Penn State
	I. McMaster	Retired Deputy Director, RSEC
**	M. Mench	Assistant Professor of Mechanical Engineering, Penn State
	G. Robinson	Professor Emeritus, Nuclear Engineering, Penn State
	C.F. Sears	Ex-Officio, Director RSEC
	R. Tropasso	Manager of Nuclear Design, Exelon
* ** ***	<i>Served through January 1, 2005</i>	
	<i>Initial Appointment January 1, 2005</i>	
	<i>Reappointed effective January 1, 2005</i>	

**FIGURE 1
RSEC Organization Chart**



* Licensed Operator
 ** Licensed Senior Operator

REACTOR OPERATIONS



Research reactor operation began at Penn State in 1955. In December 1965, the original 200 kW reactor core and control system was replaced by a more advanced General Atomics TRIGA core and analog control system. TRIGA stands for Training, Research, Isotope Production, built by General Atomic Company. The new core is capable of operation at a steady state power level of 1000 kW with pulsing capabilities to 2000 MW for short (milliseconds) periods of time.

In 1991, the reactor console system was upgraded to an AECL/Gamma-Metrics dual digital/analog control system. Further enhancements were made in 2004. This system provides for improved teaching and research capabilities and features a local area network whereby console information can be sent to laboratories and emergency support areas.

Utilization of the Penn State Breazeale Reactor (PSBR) falls into four major categories:

Education

Utilization is primarily in the form of laboratory classes conducted for graduate and undergraduate degree candidates and numerous high school science groups. These classes will vary from the irradiation and analysis of a sample, non-destructive examinations of materials using neutrons or x-rays, or transient behavior of the reactor to the calibration of a reactor control rod.

Research

Involves radionuclear applications, neutron depth profiling, neutron radiography, gamma irradiation, several research programs by faculty and graduate students throughout the University, and various applications by the industrial sector.

Training

Programs for PSBR Reactor Operations Staff.

Service

Involves radionuclear applications, neutron transmission measurements, radioscopy, semiconductor irradiations, isotope production and other applications by the industrial sector.



Figure 1. Mac Bryan operates at the reactor console.

OPERATIONS

The PSBR core, containing about 7.5 pounds of Uranium-235 in a non-weapons form, is operated at a depth of approximately 18 feet in a pool of demineralized water. The water provides the needed shielding and cooling for the operation of the reactor. It is relatively simple to expose a sample by positioning it in the vicinity of the reactor at a point where it will receive the desired radiation dose. A variety of fixtures and jigs are available for such positioning. Various containers and irradiation tubes can be used to keep samples dry. A pneumatic transfer system offers additional possibilities. A heavy water tank and neutron beam laboratory provide for neutron transmission, neutron radiography, and neutron beam activities. Core rotational, east-west and north-south movements, provide flexibility in positioning the core against experimental apparatus.

In normal steady state operation at 1000 kW, the thermal neutron flux available varies from approximately 1×10^{13} n/cm²/second at the edge of the core to approximately 3×10^{13} n/cm²/second in the central region of the core.

When using the pulse mode of operation, the peak flux for a maximum pulse is approximately 6×10^{16} n/cm²/second with a pulse width of 15 milliseconds at half maximum.

Support facilities include hot cells, a machine shop, electronic shop, darkroom, laboratory space, and fume hoods.

STATISTICAL ANALYSIS

Tables 3 and 4 list Reactor Operation Data and Reactor Utilization Data-Shift Averages, respectively, for the past three years. In Table 3, the Critical time is a summation of the hours the reactor was operating at some power level. The Subcritical time is the total hours that the reactor key and console instrumentation were on and under observation, less the Critical time.

Subcritical time reflects experiment set-up time and time spent approaching reactor criticality.

The Number of Pulses reflects demands of undergraduate labs, researchers, and reactor operator training programs. Square Waves are used primarily for demonstration purposes for public groups touring the facility, as well as researchers and reactor operator training programs.

The Number of Scrams Planned as Part of Experiments reflects experimenter needs. Unplanned Scrams from Personnel Action are due to human error. Unplanned Scrams Resulting from Abnormal System Operation are related to failure of experimental, electronic, electrical or mechanical systems.

Table 4, Part A, Reactor Usage, describes total reactor utilization on a shift basis. The summation of Hours Critical and Hours Subcritical gives the total time the reactor console key is on. Hours Shutdown includes time for instruction at the reactor console, experimental setup, calibrations or very minor maintenance that occupies the reactor console but is done with the key off. Significant maintenance or repair time spent on any reactor component or system that prohibits reactor operation is included in Reactor Usage as Reactor Not Available.

Table 4, Part B gives a breakdown of the Type of Usage in Hours. The Department of Mechanical and Nuclear Engineering and/or the reactor facility receives compensation for Industrial Research and Service. University research and service includes both funded and non-funded research, for Penn State and other universities. The Instruction and Training category includes all formal university classes involving the reactor, experiments for other University and high school groups, demonstrations for tour groups and in-house reactor operator training.

Table 4, Part C statistics, Users/Experimenters, reflects the number of users, samples and sample hours per shift.

Table 4, Part D shows the number of eight hour shifts for each year.

INSPECTIONS AND AUDITS

On February 23-27, 2004, Tom Dragoun of the NRC conducted a routine inspection of reactor operations. No issues of non-compliance were identified. (This item was omitted from last year's annual report).

On November 17, 2004, there was a NRC inspection of the Special Nuclear Material License SNM-95. No items of non-compliance were identified.

On December 2, 2004, a NRC inspection looked at the Special Nuclear Material inventory audit records and compared it against the NMSS data base. A minor error from 1995 in the Penn State accounting that had been propagated was discovered. A correction was made.

On December 4, 2004, an audit of the PSBR was conducted to fulfill a requirement of the Penn State Reactor Safeguards Committee charter as described in the PSBR Technical Specifications. The audit was conducted by Bob Agasie, Director, Nuclear Reactor Laboratory, University of Wisconsin-Madison. The reactor staff implemented changes suggested by that report, all of which exceed NRC requirements.

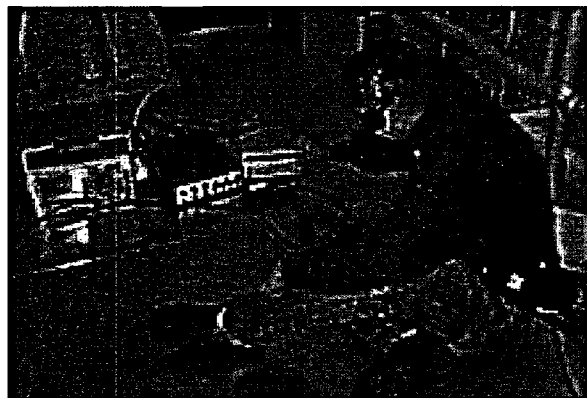


Figure 2. Thierry Daubenspeck, senior reactor operator, assists in performing a calibration procedure.

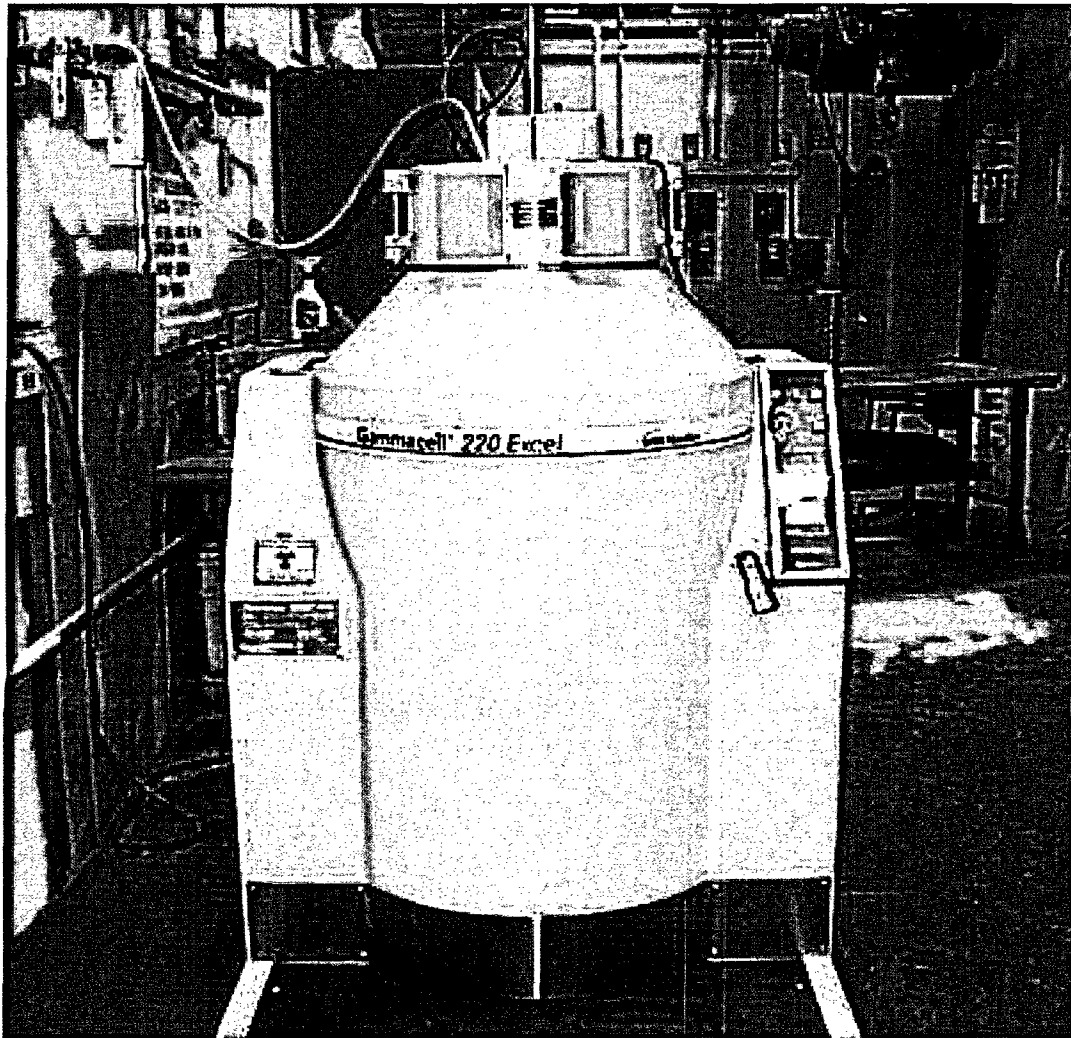
Reactor Operation Data July 2002 – June 2005

	<u>02-03</u>	<u>03-04</u>	<u>04-05</u>
A. Hours of Reactor Operation			
1. Critical	745	1070	1034
2. Subcritical	414	417	450
3. Fuel Movement	0	6	16
B. Number of Pulses	125	116	152
C. Number of Square Waves	59	62	39
D. Energy Releases (MWH)	458	736	657
E. Grams U-235 Consumed	24	38	34
F. Scrams			
1. Planned as Part of Experiments	16	1	4
2. Unplanned – Resulting From:			
a) Personnel Action	0	1	3
b) Abnormal System Operation	2	2	0

TABLE 4**Reactor Operation Data
July 2002 – June 2005**

	<u>02-03</u>	<u>03-04</u>	<u>04-05</u>
A. Reactor Usage Per Shift			
1. Hours Critical	2.9	3.9	3.7
2. Hours Subcritical	1.6	1.5	1.6
3. Hours Shutdown	2.1	2.4	2.2
4. Reactor Not Available	<u>0.2</u>	<u>0.1</u>	<u>0.2</u>
TOTAL HOURS PER SHIFT	6.8	7.9	7.7
B. Type of Usage – Hours Per Shift			
1. Industrial Research and Service	3.0	3.5	3.0
2. University Research and Service	0.8	1.4	2.0
3. Instruction and Training	1.6	1.9	1.1
4. Calibration and Maintenance	1.4	1.1	1.6
5. Fuel Handling	0	0	0.1
C. Users/Experiments Per Shift			
1. Number of Users	2.9	3.2	2.9
2. Pneumatic Transfer Samples	0.2	0.1	1.3
3. Total Number of Samples	3.2	3.5	4.8
4. Sample Hours	2.5	3.5	3.8
D. Number of 8 Hour Shifts	255	273	282

GAMMA IRRADIATION FACILITY



The Gamma Irradiation Facility includes in-pool irradiators and a dry-shielded GammaCell 220 Excel irradiator. This provides a great deal of flexibility for dose rates and irradiation configurations.

IN-POOL IRRADIATORS

For the in-pool irradiators, the source rods are stored and used in a pool that is 16 feet by 10 feet, filled with 16 feet of demineralized water. The water provides a shield that is readily worked through and allows great flexibility in using the sources. Due to the number of sources and the size of the pool, it is possible to set up several irradiators at a time to vary the size of the sample that can be irradiated, or to vary the dose rate. Experiments in a dry environment are possible by use of either a vertical tube or by a diving bell type apparatus. Four different irradiation configurations have been used depending on the size of the sample and the dose rate required. The advantage of the in-pool irradiators is that the dose rate can be varied in a manner which is optimal for agricultural and life science research.

In March 1965, the University purchased 23,600 curies of Cobalt-60 in the form of stainless steel clad source rods to provide a pure source of gamma rays. In November 1971, the University obtained from the Natick Laboratories 63,537 curies of Cobalt-60 in the form of aluminum clad source rods. These source rods have decayed through several half-lives, and the dose rates available are summarized in Table 5. In June of 2003 more sources were moved around the six-inch diameter tube to increase the dose rate. The sources around the three-inch diameter tube were moved to change the dose rate and is currently being re-configured.

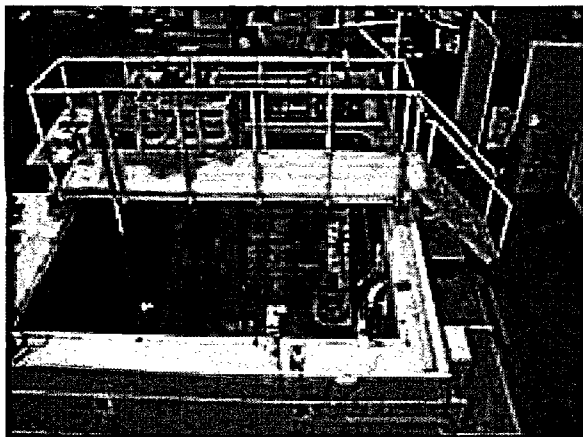


Figure 1. In-Pool Irradiation Facility

GAMMACELL 220 EXCEL DRY IRRADIATOR

The GammaCell 220 Excel dry irradiator was acquired in July 2003 through funding from the U.S. Department of Energy INIE grant. The new irradiator is located in the back area of the Hot Cell Laboratory. This irradiator replaced the old GammaCell 220 Irradiator which was housed in the same room as the pool irradiator. The new irradiator has a dose rate that is considerably higher (by a factor of 10) than the old Gammacell 220 irradiator. Other advantages of the GammaCell 220 Excel include a large irradiation chamber (approximately 6 inches in diameter and 7.5 inches high), an automatic timer to move the sample chamber away from the source and the ability to conduct in-situ testing of components during irradiation. The only disadvantage is the decay heat from the higher dose rate, which increased the temperature of the irradiation chamber. The maximum dose rate is summarized in Table 5.

USE OF GAMMA IRRADIATION SERVICES

There are many different applications utilizing gamma radiation from sanitization and sterilization, crosslinking and polymerization, F-center formation in crystals and cryogenic reduction of proteins. Figure 2 shows some of the variety of samples and purpose for irradiations this past year. The total number of irradiations had been increasing steadily over the last few years, however the number of sample hours (irradiation) is slightly lower this year, well over 100 hours per month. The sample irradiations could not have been conducted using the old Gammacell as the number of hours would have exceeded that available in a year! Other University and pre-college educational institutions utilized the gamma irradiation facility for research projects, INIE minigrant projects or the Reactor Sharing program. Several departments on campus utilized the services of the Gamma Irradiation facility. This information is outlined in the Research and Service utilization section and in Appendix A. Table 6 compares the past three years' utilization of the Cobalt-60 Irradiation Facility

TABLE 5

Summary of Current Gamma Irradiation Facilities as of 7/1/2005		
Facility	Maximum Dose Rate in KRads/hour*	Sample Limitations
North Tube 6-inch	28.5	Must be less than 6 inches in diameter
South Tube 3-inch	depends on source array	Must be less than 3 inches in diameter
10-inch Chamber	depends on source array	Cylinder approx. 10 inches in diameter by 12 inches in height
GammaCell 220 Excel Dry Cell Irradiator	1511	Cylinder approx. 6 inches in Diameter by 7.5 inches in height

TABLE 6

Cobalt-60 Utilization Data						
July 1, 2002 - June 30, 2005						
	02-03	02-03	03-04	03-04	04-05	04-05
	Pool Irradiator	Gamma Cell 220	Pool Irradiator	Gamma Cell 220	Pool Irradiator	Gamma Cell 220
A Time Involved (Hours)						
1. Set-Up/Admin. Time	16	71	19	85	5	73
2. Total Sample Hours	1835	7352	1086.5	1423 ²	121	1267 ³
B Numbers Involved						
1. Total Irradiations	84	223	50	249	64	290
2. Samples Containers Run ¹	958	959	294	1379	638	1178
3. Different Experimenters	11	25	11	39	14	32
4. Configurations Used	4	N/A	4	N/A	4	N/A

¹ Note that each sample container may contain multiple samples and that multiple samples may be run in one batch.

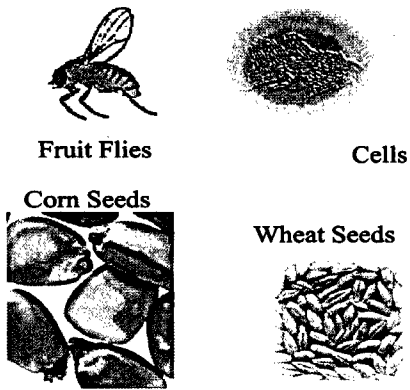
² Note the sample hours for the GammaCell 220 Excel would be equivalent to over 14,000 sample hours in the old GammaCell 220

³ Note the sample hours for the GammaCell 220 Excel would be equivalent to over 12,000 sample hours in the old GammaCell 220

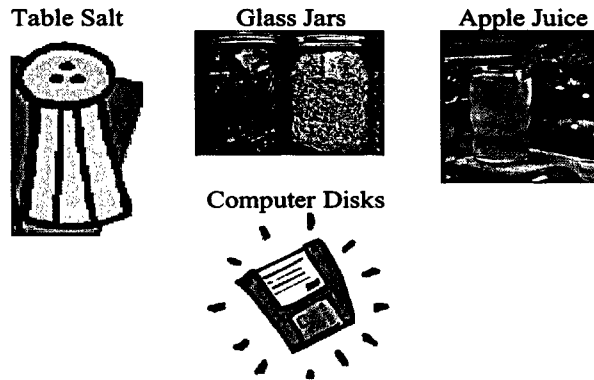
Figure 2

Gamma Irradiation Uses and Examples

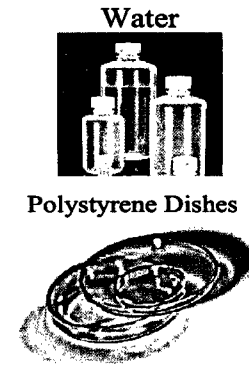
Genetic Changes



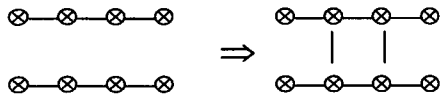
Class Projects and Demonstrations:



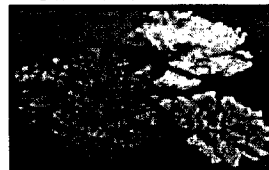
**Sterilization
Medical & Laboratory Products**



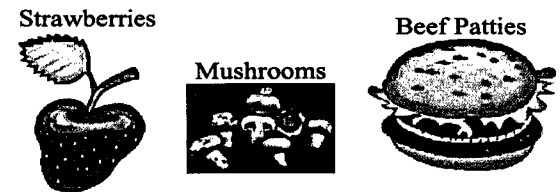
Cross-Linking of Polymers



**Soil & Leaves for
Environmental Research**
Carnation Leaves



Food Irradiation



EDUCATION AND TRAINING



The RSEC staff utilized the facilities and equipment to provide educational opportunities and tours for student and teacher workshops, many of which were conducted as part of other programs on campus. These programs are typically conducted through the Penn State College of Engineering, the Women in Science and Engineering (WISE) Institute, the Continuing and Distance Education Program, Campus Admissions and the University Relations Offices. The student programs included: VIEW (Vision in Engineering Week), Nittany Science Camp for Girls, GUTS (Girls Utilizing Technology and Science), the Upward Bound program, Pennsylvania Junior Academy of Sciences and other programs associated with campus activities.

RSEC STAFF ASSIST WITH BOY SCOUT MERIT BADGE

The Radiation Science and Engineering Center provided the setting for many of the photographs utilized in the new Boy Scout Nuclear Science Merit Badge Booklet which was published in early 2005. Candace Davison was one of several ANS members who provided input into the new requirements. Once the badge was drafted and requirements finalized, she worked with the photographer to set up demonstration photos. RSEC staff worked with scout troupes to assist them in conducting activities for the Atomic Energy Merit Badge. The Penn State ANS student chapter conducted several one-day workshops where scouts earned their Nuclear Science Merit badge. Weather affected the January 2005 workshop with about 14 scouts attending. The new Nuclear Science Merit Badge was utilized for the April 2005 workshop where 54 scouts and adults attended. Students and staff also provided suggestions for the requirements of a nuclear science interest patch for Girl Scouts.

Job shadowing was another means by which some pre-college students learned about nuclear applications. The students spent from half a day to several days shadowing staff and faculty at the facility to enhance their understanding of nuclear technology and careers.

U.S. DOE – INIE MINIGRANT

Several educational institutions participated in mini-grant projects at the RSEC facility through the INIE minigrant process. The following is a synopsis of the institutions that participated in educational outreach and educational research projects utilizing the Penn State Reactor Facility. All of the participants traveled to the reactor facility to learn about nuclear applications and understand some of the procedures and equipment utilized in the projects. The Central Virginia Governor's School conducted a half-life experiment and reactor demonstration.

Neutron activation analysis, neutron irradiation and neutron radiography were demonstrated, but this

presented a problem in conducting projects due to the production of radioactive materials. Therefore most of the projects involved gamma irradiation so the students could test the samples afterward. Forty-four students from Park View HS in South Hills, Virginia spent a full day conducting experiments and activities. They conducted a neutron radiography project to compare lawn mower blade wear.

Guy Anderson, a chemistry teacher from Bald Eagle Area High School and his students conducted projects utilizing the facility.

NUCLEAR SCIENCE & TECHNOLOGY COURSE

A one-week course on Nuclear Science and Technology was conducted from July 12-16, 2004. John Vincenti was the coordinator of the course, which was held again based upon the success of the previous course. Twelve teachers and four High School Students attended the workshop. The teachers received free Geiger Counters through a grant from the American Nuclear Society and U.S. Department of Energy. Candace Davison provided instruction on radiation, reactor basics, nuclear applications and conducted experiments at the facility for the participants.

TOURS

Over 2,800 people toured the reactor facility during this reporting period. In addition to the full or half-day programs with experiments, educational tours were conducted for students, teachers, and the general public. All groups, including those detailed in the above sections, which toured the facility are listed in Appendix B. The RSEC operating staff along with the Mechanical and Nuclear Engineering Department conducted several open house events for the Parent and Family Weekend, the general public and potential undergraduate or graduate students. Over 450 people participated in Open House and "Spend a Day" experiences.



Figure 1. A school tour group looks over displays in the Reactor Bay.

ACADEMIC INSTRUCTION

The RSEC supports academic instruction by providing information and expertise on nuclear technology topics, tours and experiments conducted at the facility and through the availability of specialized equipment and classroom/laboratory space.

The joint instructional experience for students in the IE 408W (Human Factors) course was continued this academic year. The students were instructed on reactor basics so that they could understand the control signals and input along with an overview of the control console in the classroom. The students then went into the control room where they observed a start-up and the operator's actions. They also observed the reactor while at power. Feedback from the students was very positive concerning their real-world experience.

The reactor classroom was utilized as the base of instruction for several courses including; Freshman Seminar (Fall 2004 and Spring 2005), NucE 497, NucE 450, and NucE 451. The TRIGA reactor and Cobalt-60 irradiation facilities were used by several nuclear engineering courses and courses in other departments of the university as outlined in the table below.

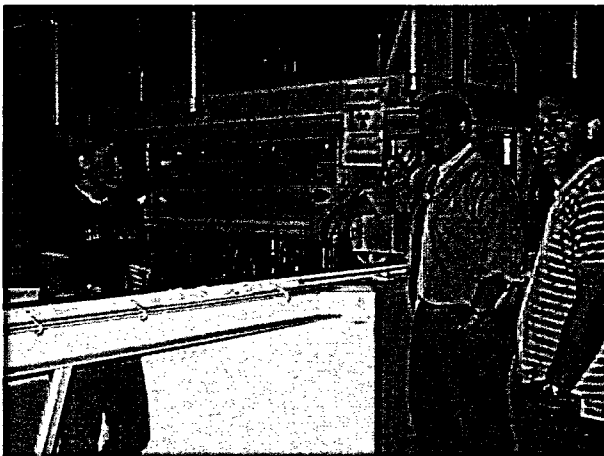


Figure 2. Brenden Heidrich, research assistant, giving reactor tour to Freshman Seminar.

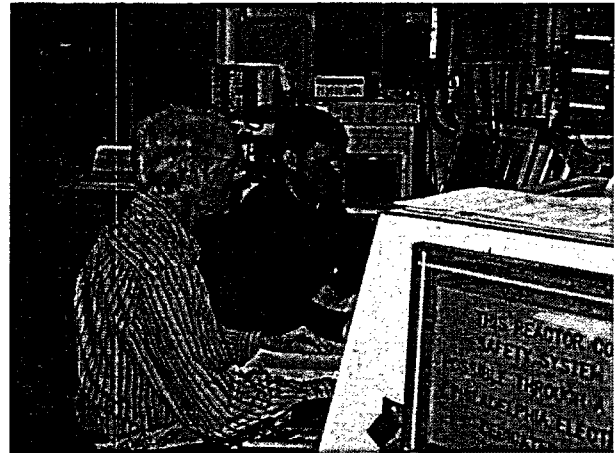


Figure 3. Terry Flinchbaugh, teaches the Reactor Operations course, NucE 497.



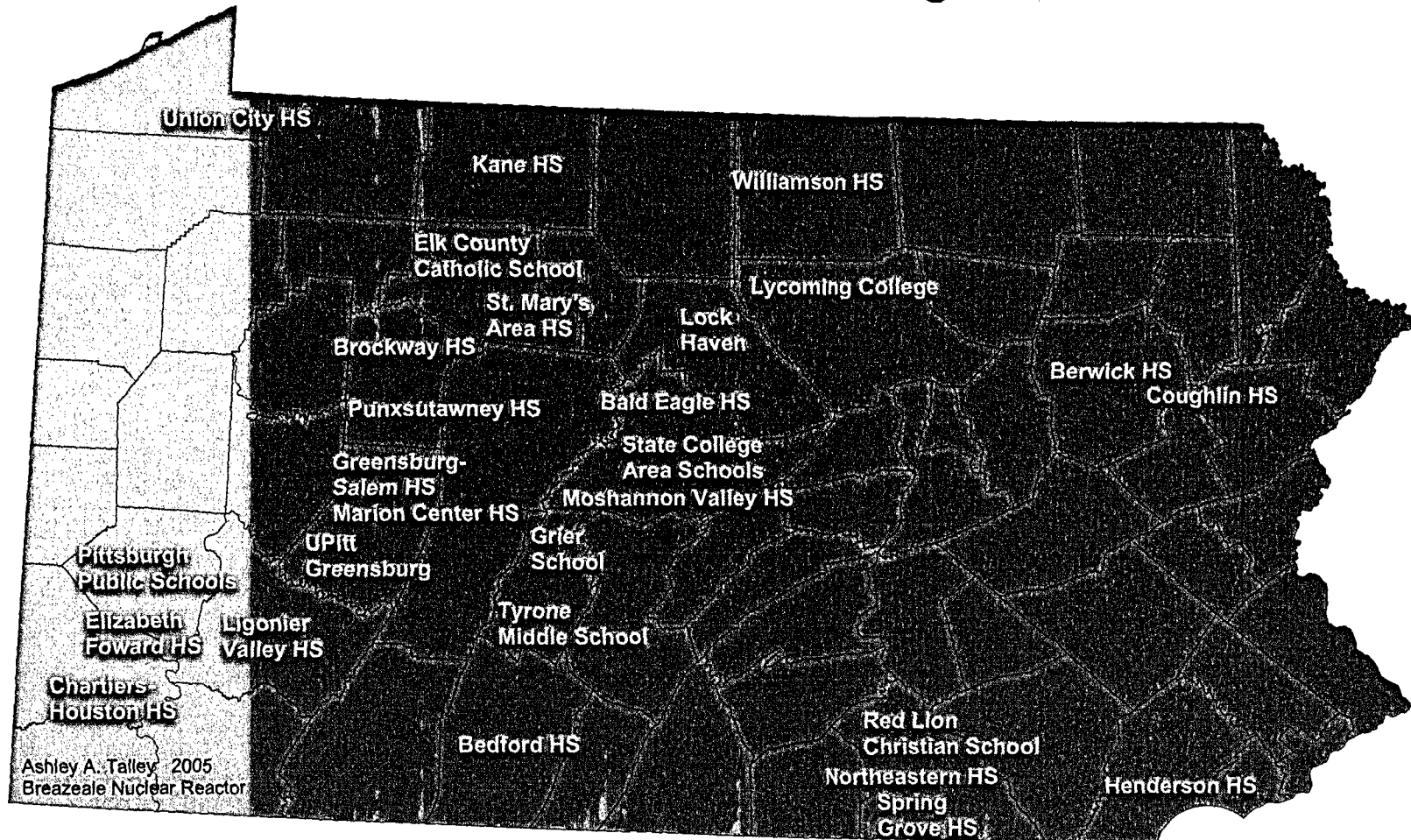
Figure 4. NucE 451 students participate in a laboratory session utilizing the Breazeale Reactor Facility.

TABLE 7

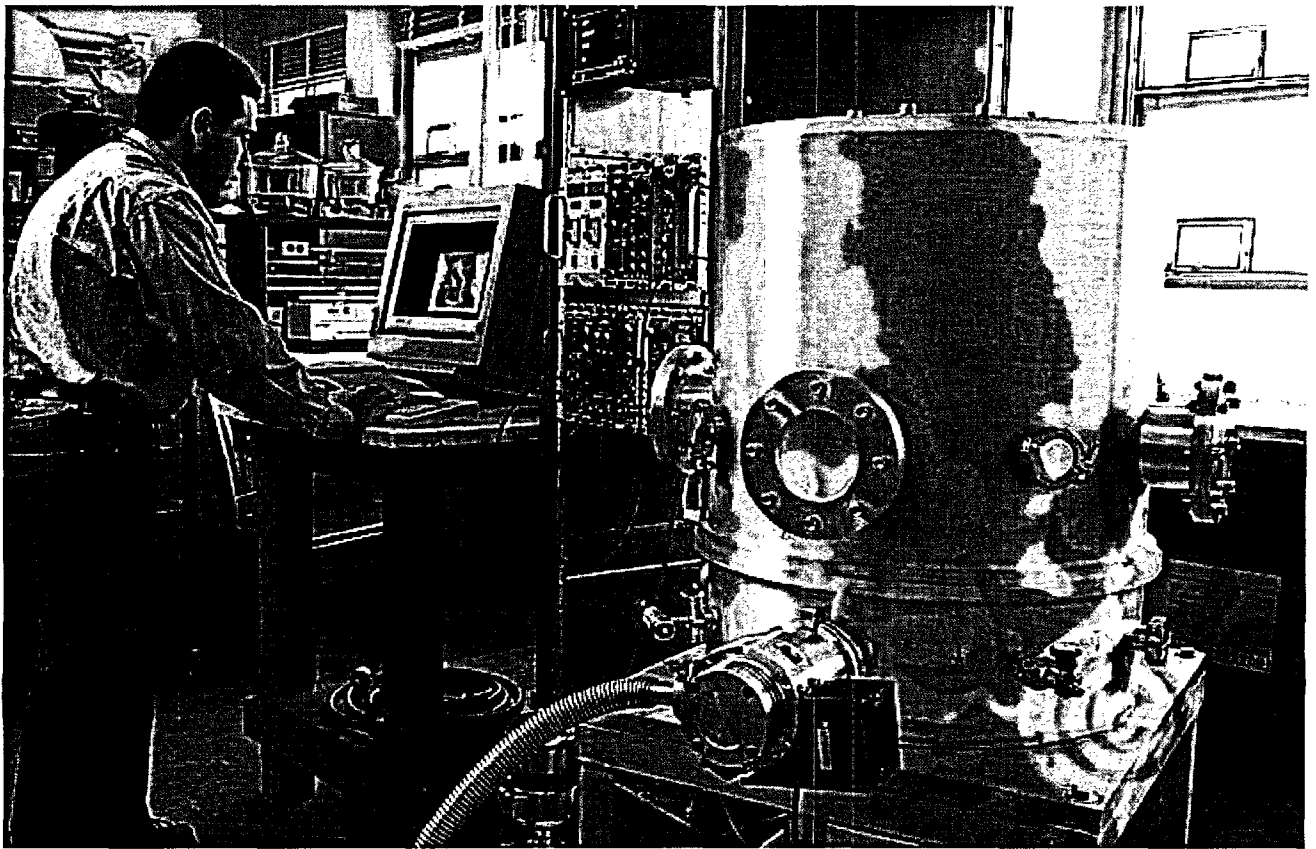
Semester	Course	Instructor	Students	Hours
Summer 2004	SCIED 498B – Nuclear Science and Technology Workshop	J. R. Vincenti C. C. Davison	12	6
Fall 2004	NucE 001S – Freshman Seminar	J. S. Brenizer	37	4
Fall 2004	NucE 301 – Fundamentals of Reactor Physics	R. M. Edwards	34	2
Fall 2004	NucE 401 – Introduction to Nuclear Engineering	K. Ünlü	13	1
Fall 2004	NucE 451 – Experimental Reactor Physics	R.M. Edwards	29	30
Fall 2004	NucE 497F – Nuclear Reactor Operations	C. F. Sears	3	51
Fall 2004	Food Science 413 – Science & Technology of Plant Food	R. B. Beelman	20	3
Fall 2004	IE 408 W-Human Factors	L. Newman	67	4
Spring 2005	NucE 001S – Freshman Seminar	J. S. Brenizer	16	2
Spring 2005	NucE 497F – Nuclear Reactor Operations	C. F. Sears	1	30
Spring 2005	Nuc E 450 – Radiation Detection and Measurement	K. Ünlü	30	6
Spring 2005	CHEM 036 (Penn State Altoona)	C.S. Reed	8	1

FIGURE 3

Educational Institutions Visiting the RSEC



NEUTRON BEAM LABORATORY



NEUTRON BEAM LABORATORY

The Neutron Beam Laboratory (NBL) is one of the experimental facilities at the RSEC. Well-collimated beams of neutrons, thermalized by D₂O, are passed into the NBL for use in various neutron beam techniques. When the reactor core is placed next to a D₂O tank and graphite reflector assembly near the beam port locations, thermal neutron beams become available for neutron transmission and neutron radiography measurements from two of the seven existing beam ports. In steady state operation at 1-MW, the thermal neutron flux is 1×10^{13} n/cm²sec at the edge of the core and 3×10^{13} n/cm²sec in the central thimble. The Penn State Breazeale Reactor (PSBR) can also pulse with the peak flux for maximum pulse $\sim 6 \times 10^{16}$ n/cm²sec with a pulse width of 15 msec at half maximum.

Current Status of PSBR Beam Ports:

The PSBR has seven beam ports. The internal diameter of the beam ports are four inches for BP #3 and BP #5; five inches for BP #1 and BP #7; and six inches for BP #2, BP #4 and BP #6. The center of BP #4 is sixty five inches from the pool floor while BP #1, BP #3, BP #5 and BP #7 sixty inches and BP #2 and BP #6 are fifty four inches from the pool floor. With the current setup of reactor-core-moderator assembly only BP #4 is at the centerline of the TRIGA core. (Active length of TRIGA fuel is 15"). BP #1, 3, 5 and 7 are five inches below the centerline of the core and BP #2 and 6 are eleven inches below the centerline of the core. The core grid assembly does not permit lowering the core more than the current arrangement. When the PSBR reactor was built MTR type fuel elements with active length of 24" were used. With the MTR fuel the beam port arrangement did not limit the maximum neutron output. In the mid 60's the PSBR was converted from MTR type to TRIGA type fuel. Because of these inherited limitations only two beam ports are currently being used. BP #4 with 3×10^7 n/cm²sec flux at the aperture is used for research, primarily neutron radiography and radioscopy, and BP #7 with $\sim 10^5$ n/cm²sec neutron flux is used for service activities involving neutron transmission measurements. Since the BP #4 collimators are primarily designed and optimized for neutron radiography and radioscopy measurements, it is not possible to obtain desired results for other measurements. We are currently trying to use BP #4 for all of our research projects. Due to space limitations, we must shuffle delicate research equipment around. More importantly, each project or experimental techniques require a special or dedicated neutron beam with different collimations and neutron flux.

New Beam Ports and Beam Hall Expansion:

Due to inherited design issues with the current arrangement of beam ports and reactor core-moderator assembly, the development of innovative experimental facilities utilizing neutron beams is extremely limited. Therefore, a new core-moderator location in the PSBR pool and beam port geometry needs to be determined in order to build useful neutron beam facilities. A study is continuing with the support of DOE-INIE funds to examine the existing beam ports for neutron output and to investigate new core and moderator designs that would be accessible by new additional beam ports. We envision a location in the pool where the reactor core would be "parked" and surrounded by a moderator (D₂O or graphite). New beam ports would be geometrically aligned with the core-moderator assembly for optimum neutron output.

The new core-moderator and beam port arrangement requires expansion of the existing beam laboratory in order to place instrumentation, neutron guides, and beam catcher, etc. The new beam hall will have a total of 3,700 sq ft of experimental area (the existing area of $\sim 1,000$ sq ft plus a new additional area of $\sim 2,700$ sq ft). Also, about 3,100 sq ft of new office and meeting/classroom space will be added in the second floor of the expanded beam hall to support students and faculty working in this area.

Architectural plans for the RSEC expansion for a new Neutron Beam Hall and Neutron Beam Ports facilities are completed. Working with a professional architectural firm, a contractor, and related personnel from various university functions, we obtained a firm estimate for the expansion cost. Internal benefactors

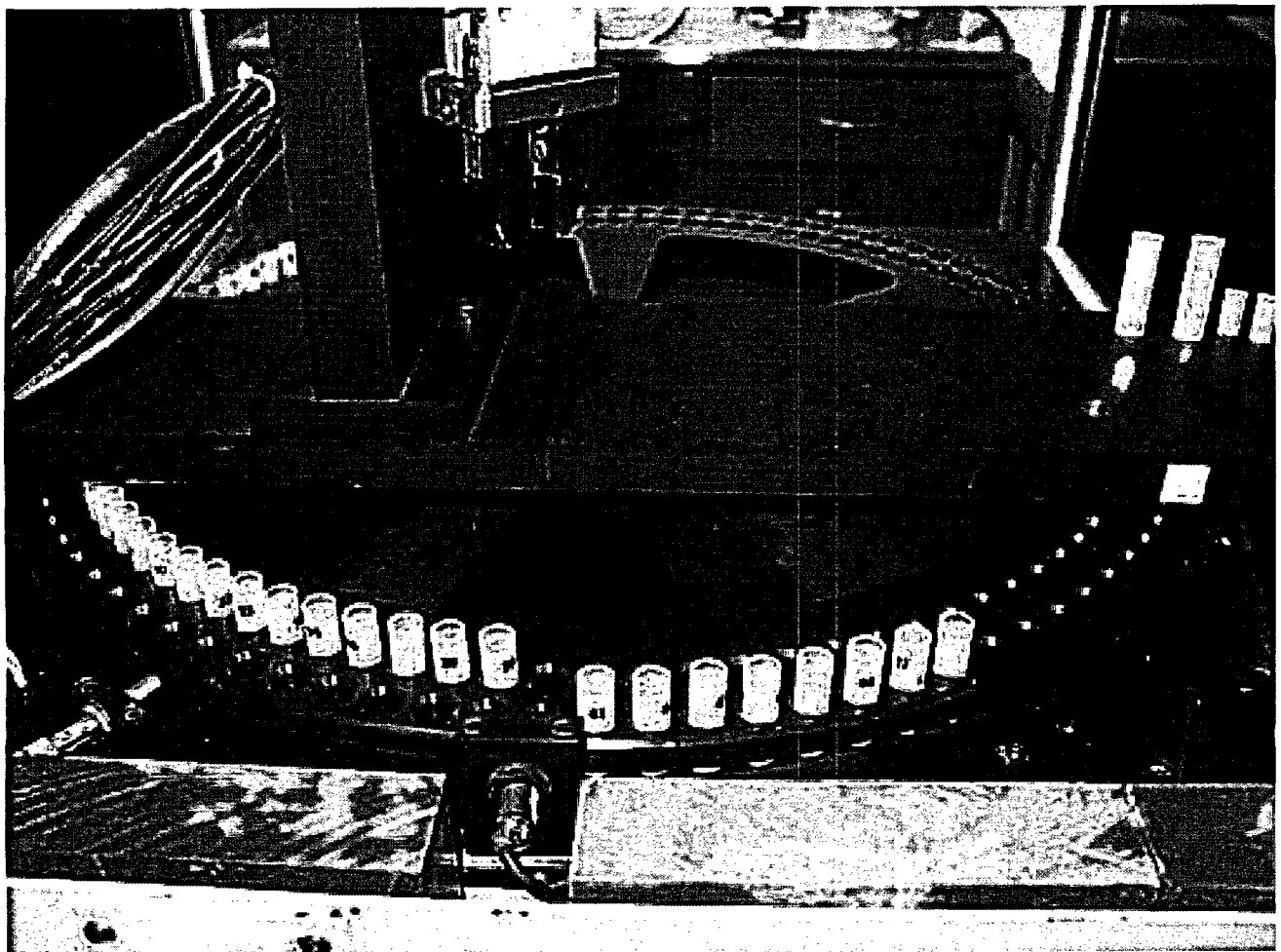
of the new neutron beam facilities are identified. We obtained support letters or expression of interests from about 30 faculty members from four different colleges within the university. More than half of the total budget for expansion is currently available, and efforts to raise the remaining portion of the budget continue. The Penn State University has responded to US Department Energy's request for an Expression of Interest (EOI) last April for the RSEC expansion for a new Neutron Beam Hall and Neutron Beam Ports. The response for the EOI was submitted with the active support and participation of the Dean of the College of Engineering and the Vice President for Research.

Research areas envisioned for RSEC's new beam port/beam hall design are as follows. Neutron Depth Profiling facility for depth vs. concentration measurements, impurity determination of He-3 and B-10 in semiconductors, metal and alloys; Cold Neutron Source and Cold Neutron Prompt Gamma Activation Analysis for neutron focusing research, materials characterization and determination of impurities in historically or technologically important material; Neutron Powder Diffraction for structural determination of materials, and a Triple Axis Diffractometer to train students on neutron diffraction and perform preliminary structural determinations of materials.

Projects utilizing the NBL during the year included the following:

- Compton Suppression System (see Research and Service Utilization Section, page 30)
- Time-of-Flight Neutron Depth Profiling at the Penn State University Breazeale Nuclear Reactor (see Research and Service Utilization Section, page 34)
- Neutron Activation Analysis of Absolutely Dated Tree Rings (see Research and Service Utilization Section, page 39)
- Neutron Imaging System Improvements (see Research and Service Utilization Section, page 43)
- Study of Water Distribution and Transport in a Polymer Electrolyte Fuel Cell Using Neutron Imaging (see Research and Service Utilization Section, page 48 and page 53)
- Soft Error Analysis Toolset (SEAT) Development (see Research and Service Utilization Section, page 56)
- Testing Neutron-Induced Soft Errors in Semiconductor Memories (see Research and Service Utilization Section, page 61)
- Neutron Beam Characterization of the Breazeale Nuclear Reactor at the Pennsylvania State University, Radiation Science and Engineering Center (see Research and Service Utilization Section, page 66)
- Thermal-Hydraulic Analysis of Neutron Cooling System (see Research and Service Utilization Section, page 71)
- Modelling of existing beam-port facility at Penn State University Breazeale Nuclear Reactor by using MCNP (see Research and Service Utilization Section, page 75)
- Neutron transmission measurements and neutron radioscopy were conducted for borated metals and other borated materials for Northeast Technology Corporation, Eagle-Picher Industries, Transnuclear, NY, and Cogema, France.
- Radiographic and radioscopy techniques were demonstrated as part of several student projects; including demonstration of neutron and x-ray imaging for the Governor's School students and students enrolled in the freshman seminar (NucE 001S). The students assembled plaques containing a variety of objects and predicted their neutron & x-ray attenuation characteristics. Experiments with neutron & x-ray radiography confirmed their predictions.

RADIONUCLEAR APPLICATIONS LABORATORY



**A. Service
B. Research**

A: SERVICE

The Radionuclear Applications Laboratory (RAL) provides consulting and technical assistance to personnel wishing to use radionuclear techniques in their research projects. The majority of these projects involve neutron activation; however, the staff is also able to provide services in radioactive tracer techniques, radiation gauging, and isotope production for laboratory, radionuclear medicine or industrial use. RAL personnel support daily RSEC operations by performing analyses of water, air monitor filters, and other samples as needed to meet regulatory requirements.

During the past fiscal year, a total of 463 semiconductor irradiations were performed for five different companies. The devices were prepared for irradiation in accordance with accepted procedures. Afterwards, the 1-MeV Silicon Equivalent fluence was calculated from the flux monitors irradiated with the devices. The irradiated devices were analyzed to determine the radioisotopes present for shipping and licensing requirements. RAL personnel returned irradiated devices in accordance with NRC and DOT regulations.

RAL personnel performed a total of 40 isotope production runs of Sodium-24, Bromine-82 and Argon-41 for industrial use during the past fiscal year. If necessary, personnel are able to analyze and test chemicals not currently on our approved list.

Penn State students and faculty members continue to use the services offered by the RAL. Sample irradiations and analytical work were performed for graduate and undergraduate students in various programs including Geosciences and Geo-Environmental Engineering. Nuclear engineering students use the RAL for various projects being performed at the RSEC. In addition to Penn State students, students from the University of Pittsburg used the reactor to perform NAA for projects required for graduation.



Figure 1. Thierry Daubenspeck, activation and utilization specialist/senior reactor operator explains Pneumatic Transfer system to students from the University of Pittsburgh.

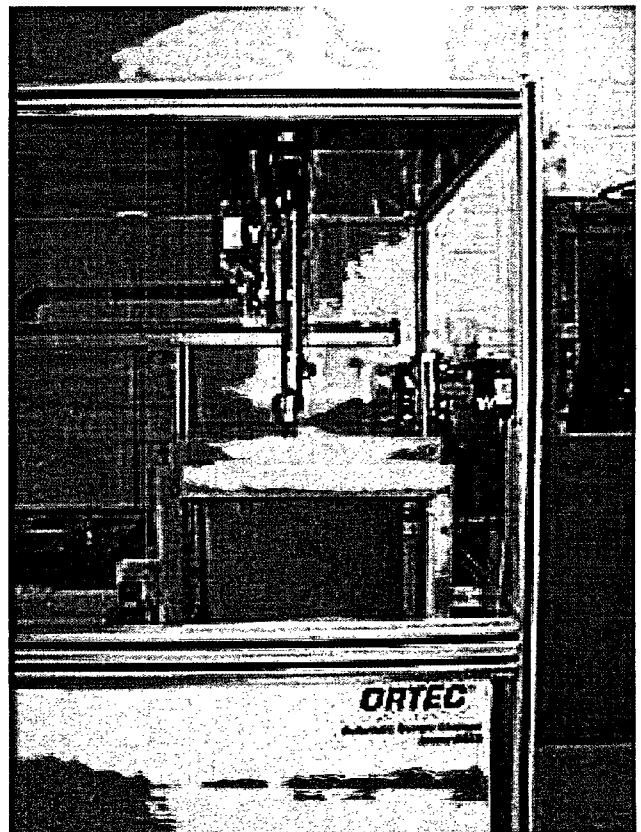


Figure 2. Ortec Automatic Sample Changer used for long-lived isotopes.

B: RESEARCH

In the past year, a Compton Suppression System (CSS) was purchased with INIE funds in order to make more in-depth analysis of some samples using NAA. Some pictures of new CSS are shown below and the description of the PSU-CSS and some more pictures and a preliminary measurement results are given on page 30. The Instrumental Neutron Activation Analysis (INAA) facility was completed last year at the Breazeale Nuclear Reactor. The INAA facility consisted of two Dry Irradiation Tubes (DT) in the reactor core, an Automatic Sample Handling System (ASHS), a High-Purity Germanium (HpGe) Detector, a Digital Spectrum Analyzer and Genie-2000 software. The characterizations of the Dry Irradiation Tubes were completed after the new core loading. The flux measurements were necessary to identify flux peak area for sample irradiation positions in the Dry Irradiation Tubes. The CSS was placed in Room 2 and the characterization of the CSS is completed. Also, Room 4 is being converted to a NAA sample preparation facility.

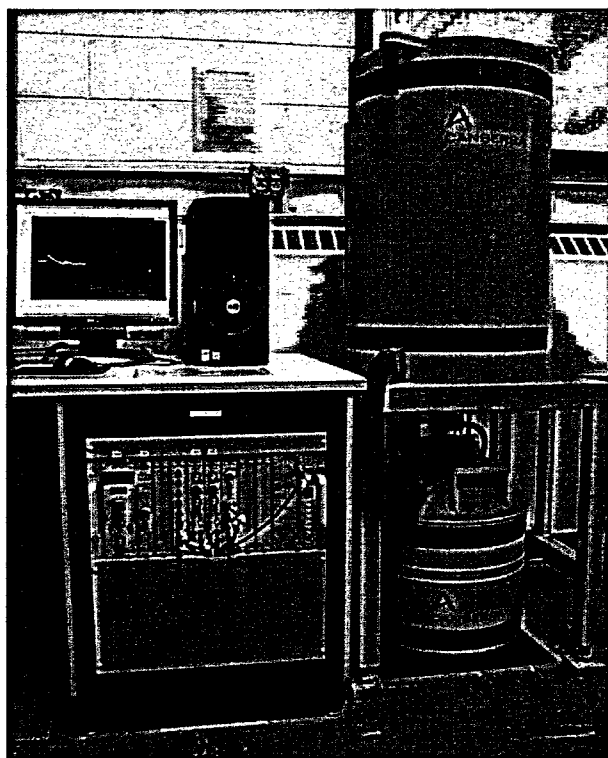


Figure 3. Recently acquired Compton Suppression System.

The current main activity at RAL is a dendrochronology project. The objective of this study is to determine experimentally periods of global environmental stress during the past six thousand years using tree samples already collected and dated and neutron activation analysis (NAA). The result of this study will provide climate modelers with a much needed extended timeline.

This study is the first coordinated dendrochemical study of a period longer than one hundred years, and the first study in the archaeologically important eastern Mediterranean. The Malcolm and Carolyn Wiener Laboratory for Aegean and Near Eastern Dendrochronology at Cornell University archives of 40,000 individually-dated tree samples with 4.5 million rings from one hundred nine forests in the eastern Mediterranean and former Soviet Union. These samples span most of the period from 7000 BC to the present. All dendrochronologically dated samples at the Wiener Laboratory are available for this study.

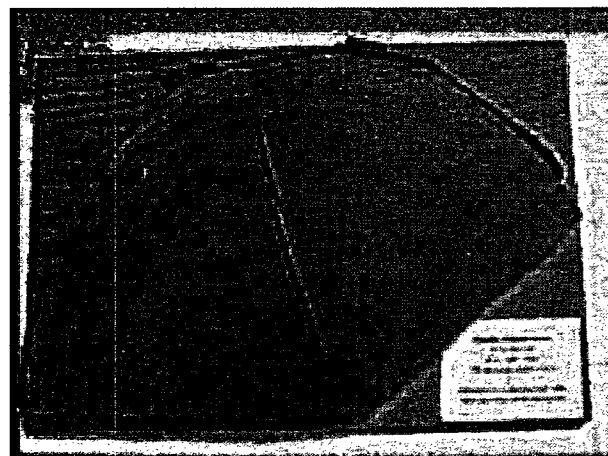
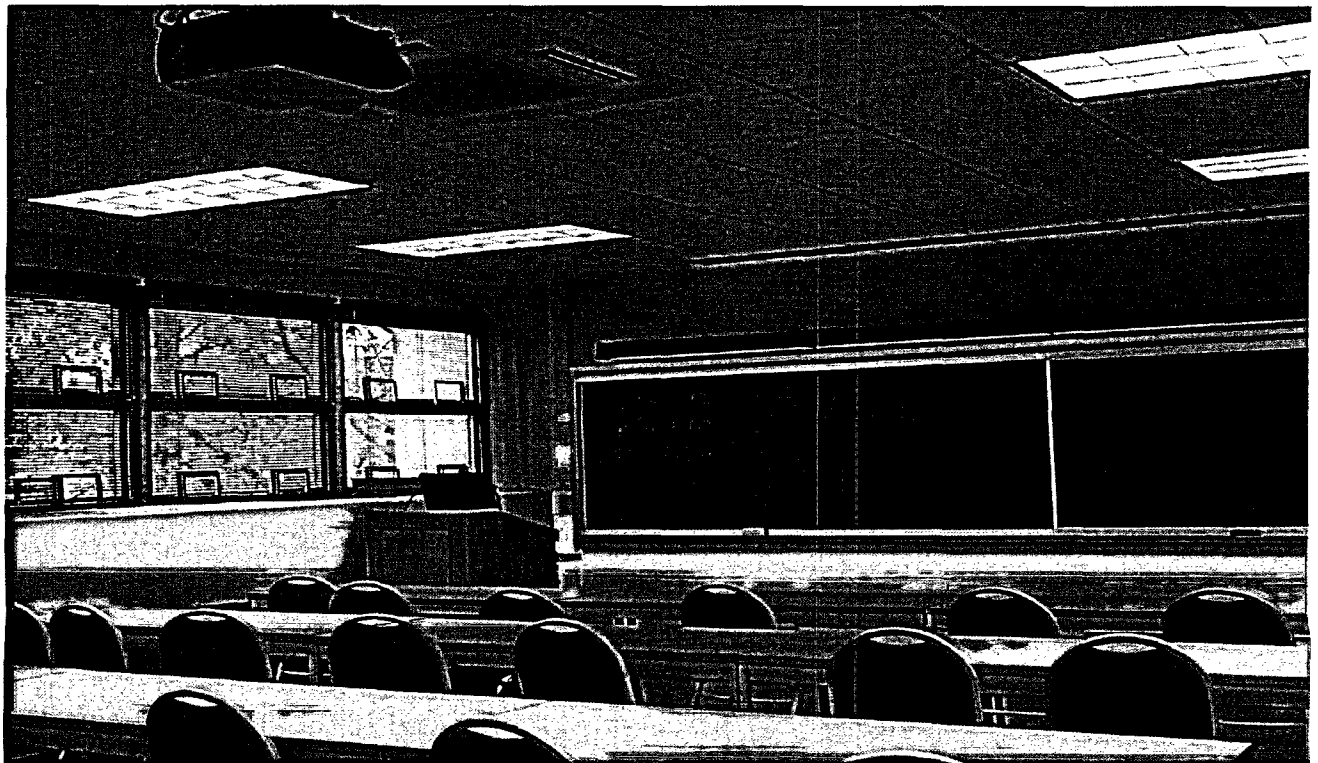


Figure 4. A tree sample from Istanbul, Belgrade Forest. The innermost pin is placed at 1800 A.D., other pins follow at 50-year intervals.

Staff and students of the Wiener Laboratory have already prepared approximately three thousand samples of wood for this study. A dedicated NAA system was built at Cornell's Ward Center for Nuclear Sciences, the prepared samples, gamma spectroscopy system, and sample changer were transferred to Penn State, Radiation Science and Engineering Center. Measurements will continue using the 1-MW Breazeale Nuclear Reactor. Please see details of this project in page 39 of this report. Another research activity has been started in collaboration with the Chemistry Department to identify the trace elements in carbon nanotubes.

NEW CLASSROOM



CLASSROOM RENOVATIONS ROOM 111

In July and August, the main classroom at the Radiation Science and Engineering Center (RSEC) was given a facelift. The work was done by the Office of the Physical Plant Renovation Crew, on an extremely tight schedule to accommodate the first day of fall semester classes.

The major construction portion of the project required the relocation of plumbing and electrical services. A drop ceiling was added which housed a state of the art motor controlled projection screen and computer driven projector. A public address system and air conditioning were installed out of sight in a new suspended ceiling.

Additionally, two storage closets were added to the room. Teaching and tour supplies as well as material needed for numerous committee meetings and open houses were placed in these areas. Finally, new furnishings including desks, chairs, and podium were placed in the room.

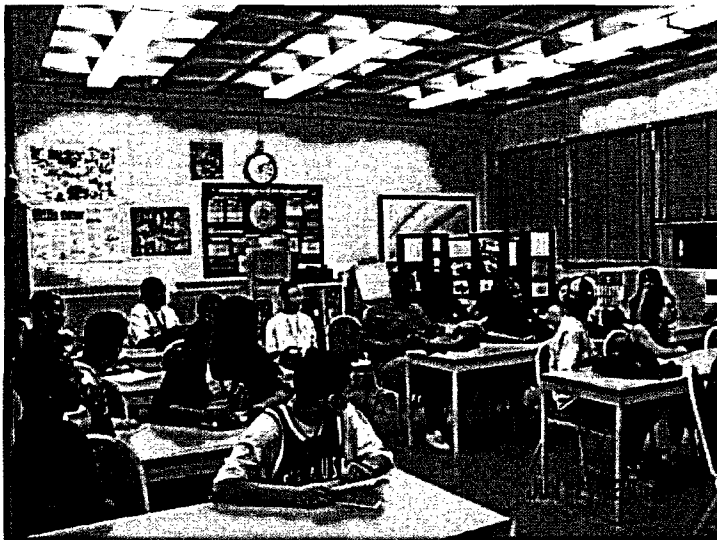


Figure 1. Classroom before the renovations

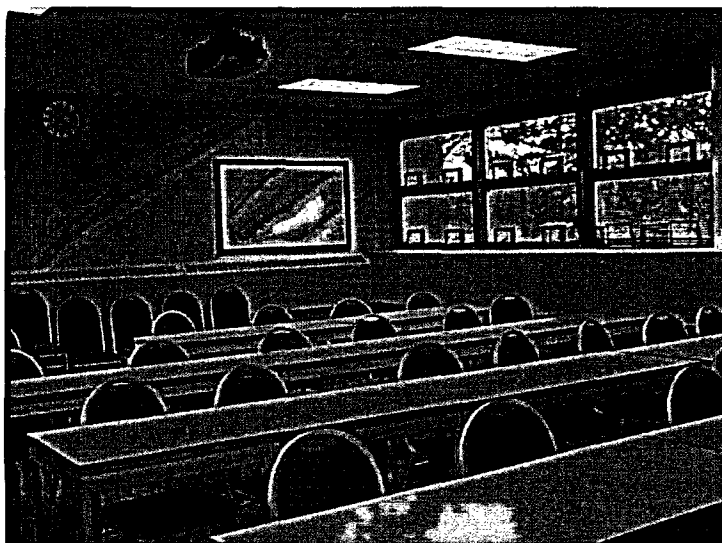
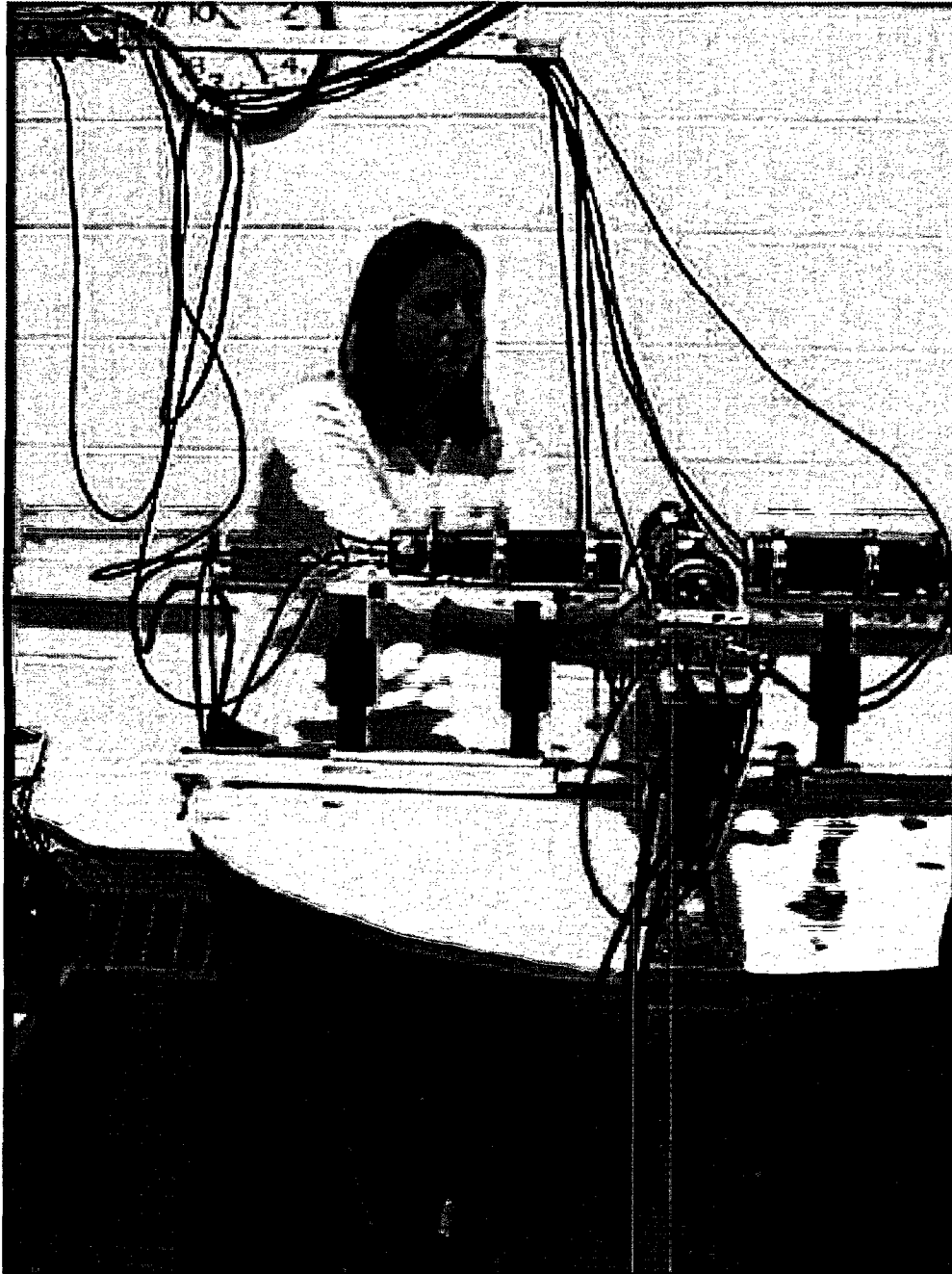


Figure 2. Classroom after the renovations

ANGULAR CORRELATIONS LABORATORY



ANGULAR CORRELATIONS LABORATORY

The Angular Correlations Laboratory has been in operation for approximately 16 years. The laboratory, which is located in Room 116 and Room 6 of the RSEC, is under the direction of Professor Gary L. Catchen. The laboratory contains three spectrometers for making Perturbed Angular Correlation (PAC) measurements. One apparatus, which has been in operation for 16 years, measures four coincidences concurrently using cesium fluoride detectors. A second spectrometer was acquired 14 years ago, and it measures four coincidences concurrently using barium fluoride detectors. A third spectrometer was set up eight years ago to accommodate the increased demand for measurement capability, but currently it is in storage. The detectors and electronics provide a nominal time resolution of 1 nsec FWHM, which places the measurements at the state-of-the-art in the field of Perturbed Angular Correlation Spectroscopy.

Penn State has a unique research program that uses PAC Spectroscopy to characterize technologically important electrical and optical materials. This program represents the synthesis of ideas from two traditionally very different branches of chemistry; materials chemistry and nuclear chemistry. Although the scientific questions are germane to the field of materials chemistry, the PAC technique and its associated theoretical basis have been part of the fields of nuclear chemistry and radiochemistry for several decades. The National Science Foundation and the Office of Naval Research have sponsored this program in the past.

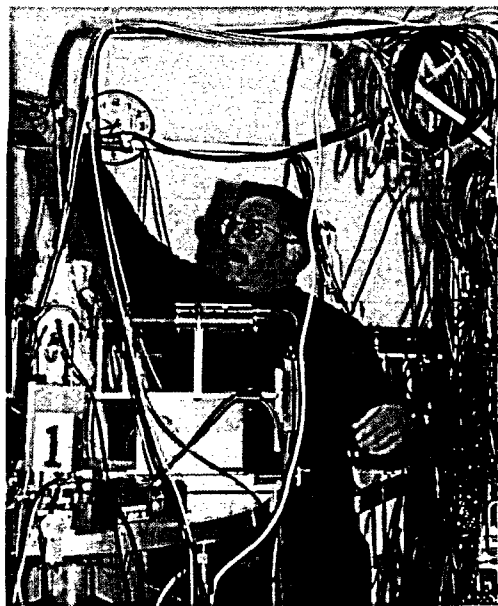


Figure 1. Prof. Catchen inserts a sample into a high-temperature sample furnace, which is mounted in the center of the four-detector array of the perturbed-angular-correlation spectrometer.

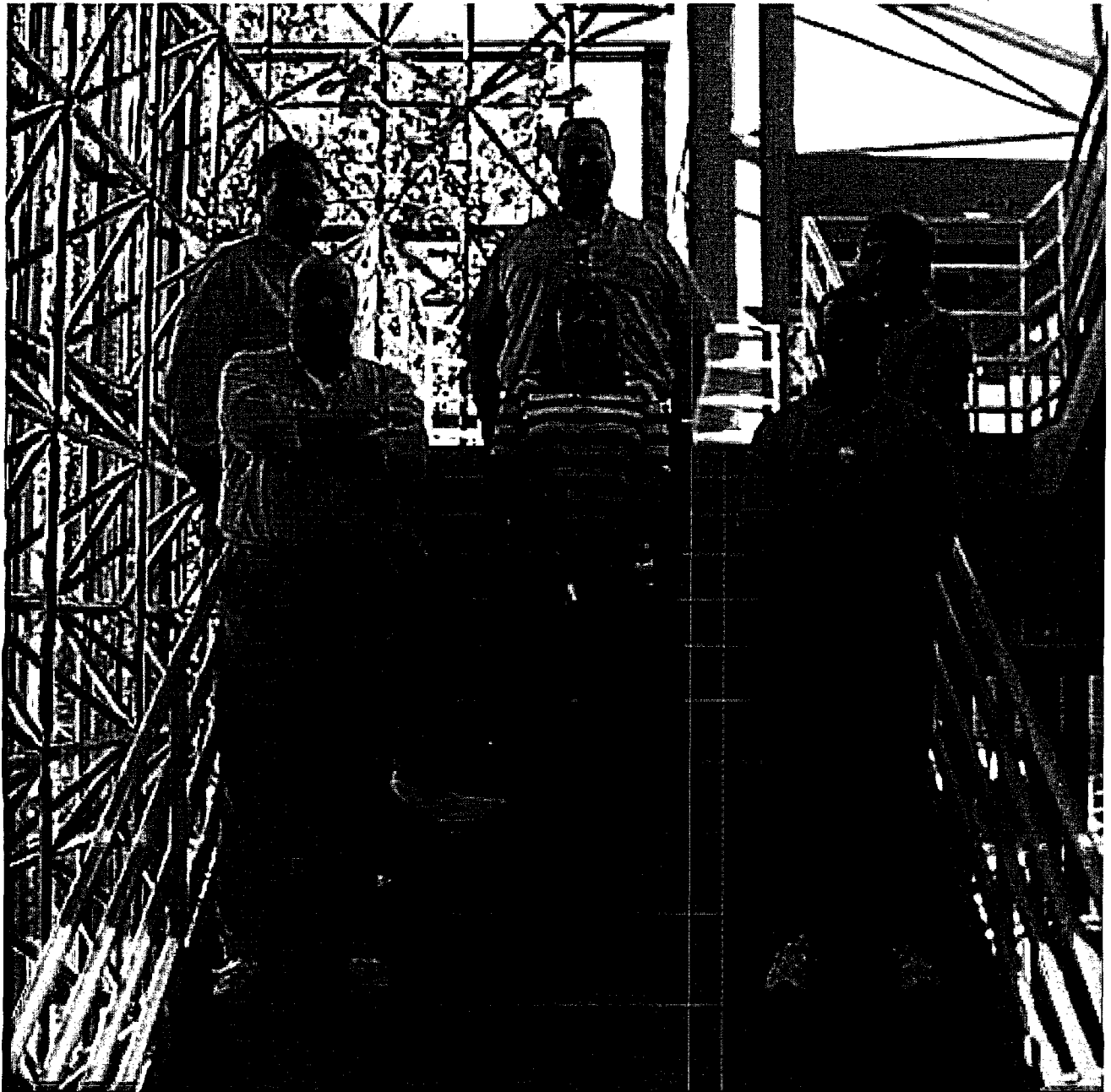
Professor Catchen completed a research program funded by the Petroleum Research Fund of the American Chemical Society. It is titled: "Drag Reduction in Turbulent Flows: Direct Observation of Very Rapid Fluctuations in Polymer-Solvent Interactions." Low concentrations of linear polymers can greatly reduce drag in various types of fluid transport. Although scientists have identified many drag-reducing polymers, investigators have not been able to observe directly the polymer-solvent interactions causing drag reduction. For this purpose, Professor Catchen explored this possibility using PAC spectroscopy.

The PAC technique is based on substituting a radioactive probe atom such as ^{111}In or ^{181}Hf into a specific site in a chemical system. Because these atoms have special nuclear properties, the nuclear (electric-quadrupole and magnetic-dipole) moments of these atoms can interact with the electric field gradients (efgs) and hyperfine magnetic fields produced by the extranuclear environment.

Static nuclear electric-quadrupole interactions can provide a measure of the strength and symmetry of the crystal field in the vicinity of the probe nucleus. In the case of static interactions, the vibrational motion of the atoms in the lattice is very rapid relative to the PAC timescale, i.e., 0.1-500 nsec. As a result, the measured efg appears to arise from the time-averaged positions of the atoms, and the sharpness of the spectral lines reflects this "motional narrowing" effect. In contrast to static interactions, time-varying interactions arise when the efg fluctuates during the intermediate-state lifetime. In solids, these interactions can provide information about defect and ionic transport. In liquids these interactions can provide information about, for example, the conformations of macromolecules such as polymers. The effect of the efg fluctuating in either strength or direction, which can be caused, for example, by ions "hopping" in and out of lattice sites or by molecules tumbling in a solution, is to destroy the orientation of the intermediate state. Experimentally, this loss of orientation appears as the attenuation or "smearing-out" of the angular correlation. And, often a correspondence can be made between the rate of attenuation and frequency of the motion that produced the attenuation.

Magnetic hyperfine interactions, which can be measured in ferromagnetic and antiferromagnetic bulk and thin-film materials, are used to study the mechanisms that cause the transition between the magnetically-ordered phase and the disordered phase. Current laboratory research is detailed in Section X of this report.

ENVIRONMENTAL HEALTH & SAFETY



ENVIRONMENTAL HEALTH AND SAFETY

Environmental Health and Safety (EHS) is an active participant in ensuring the overall safety of the Radiation Science and Engineering Center (RSEC) operations. The RSEC and EHS are committed to the health and safety of the environment, public, students and employees. EHS is responsible for the overall administration of the radiation safety program for The Pennsylvania State University. The University is licensed by the U.S. Nuclear Regulatory Commission (NRC) to receive, acquire, possess, and transfer byproduct material (radioactive material produced by a nuclear reactor), source material (naturally occurring radioactive material, uranium compounds), and special nuclear material (radioactive material that has the potential to undergo nuclear fission) and to operate the Breazeale Nuclear Reactor at the Radiation Science and Engineering Center. The College of Engineering has administration responsibility for the reactor operations license (R-2 licence).

The ALARA radiation protection philosophy, keeping the radiation exposure as low as reasonably achievable, is the basis for the RSEC and EHS radiation protection and safety programs. Both groups collaborate to maintain the highest level of health and safety programs necessary for the administration of nuclear programs and compliance with federal and state regulations.



Figure 1. Mark Linsley of radiation protection surveys samples in a laboratory.

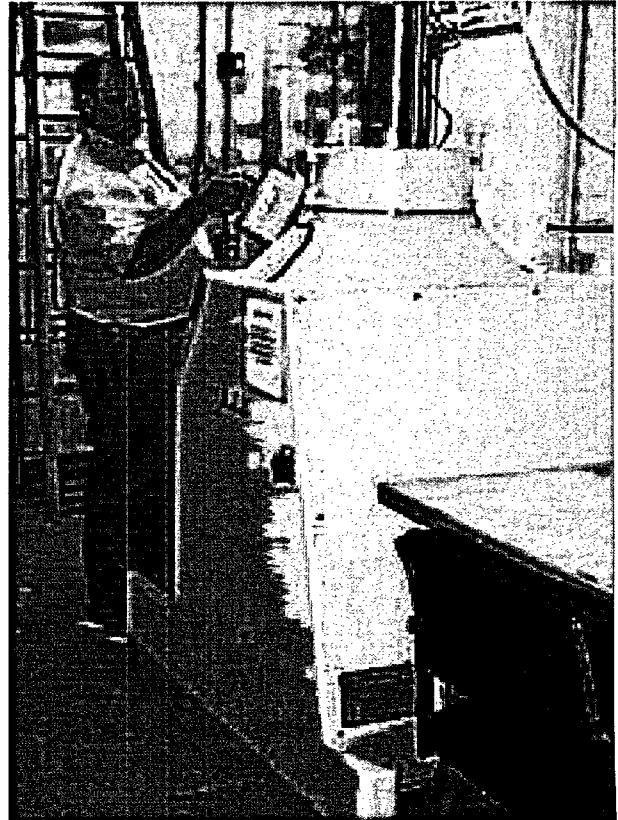


Figure 2. Greg Herman of radiation protection surveys around the GammaCell 220 Excel Irradiator.

ALARA PROGRAMS

This year EHS performed over 138 radiation surveys at the RSEC. Survey results showed that all radioactive material was being handled in a safe and controlled manner. The surveys were conducted to detect possible transferable contamination from radioactive materials work or to survey radiation sources such as activation products, sealed sources, equipment, and reactor operations. The radioactive contamination surveys are performed in laboratories where radioactive materials are used and in the balance of the RSEC's public areas to ensure that no radioactive material has been transferred to these areas. Both the contamination surveys and the radiation surveys are redundant to the surveys performed routinely by the RSEC staff. The redundancy of the contamination and radiation surveys is fundamental to the University's ALARA program.

EHS staff regularly attend scheduled RSEC operation meetings. The meetings provide a forum for participants to review the current reactor operations and experiments. This active participation has established an open line of communication between the RSEC and EHS. Input by the radiation protection staff has contributed to the facility's safety and ALARA programs.

SERVICE

EHS is responsible for the shipping and transfer of radioactive materials (RAM) to customers of the RSEC. The U.S. Nuclear Regulatory Commission and U.S. Department of Transportation mandate complex requirements for the packaging, shipping and transfer of radioactive materials. EHS shipped 39 RAM shipments to RSEC customers. Customer support included packaging and shipping Ar-41 and Na-24 for Tru-Tec Inc., Ar-41 for Syntex Inc. and Na-24 for NWT Inc. The shipping and transfer of radioactive materials includes the disposal of reactor radioactive waste materials.



Figure 3. Dave Bertocchi of radiation protection and Thierry Daubenspeck, senior reactor operator, load a shipment of RAM.

LICENSING AND REGULATORY REQUIREMENTS

Dosimetry requirements are administered by EHS and dosimetry is issued to RSEC personnel to measure staff, student, and worker radiation exposures. This year EHS issued a total of 596 dosimeters to RSEC personnel, all were below established limits. Administration of the dosimeter program includes issuing dosimeters, processing dosimeters and maintaining all dosimetry records. EHS has administered a thermal neutron dosimeter program to check exposures more accurately for those working around the neutron radiography laboratory. One neutron dosimeter is a permanent fixture in the laboratory, and individuals wear the others as they work in the lab. A total of sixty thermal neutron dosimeters were monitored with no indication of any measurable thermal neutron exposures to personnel. Self-reading dosimeters are issued to transient persons and visitors to the RSEC. The information for the temporary dosimetry is documented in logbooks maintained by the administrative staff at the facility.

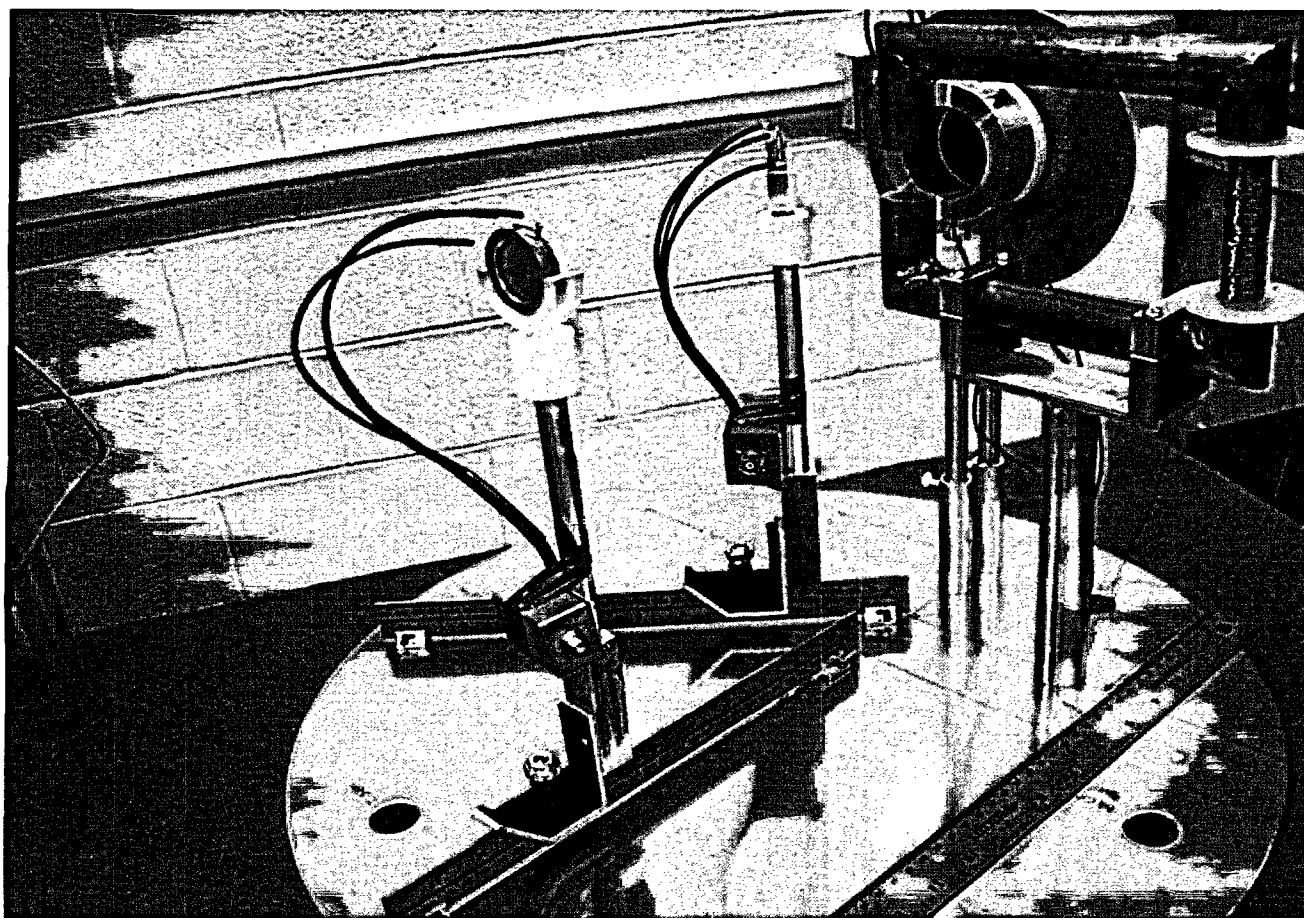
The RSO is a member of the Reactor Safeguards Committee. Eric Boeldt, the RSO, has taken an active role in the Safeguards Committee and has provided input regarding many reactor safety issues brought to the committee's floor this year.

TRAINING

Training programs provided by EHS to the RSEC are license and regulatory driven. Training covering the requirement of shipping limited quantities of radioactive material was given to three reactor personnel this year. Also, forty one new reactor personnel and students attended the radiation safety orientation. Required retraining for all radiation workers was provided to the RSEC by means of a newsletter distributed to all laboratory supervisors. All RSEC personnel also completed the annual Chemical & Chemical Waste Refresher Training. In October EHS provided Preparedness, Prevention, and Contingency (PPC) plan training to RSEC personnel. The RSEC has a history of being in compliance with Penn State's Chemical & Chemical Waste Handling programs.

RADIATION SCIENCE AND ENGINEERING CENTER

RESEARCH AND SERVICE UTILIZATION



Research and service continues to be the major focus of the RSEC. A variety of research and service projects are currently in progress as indicated on the following pages. The University-oriented projects are arranged by department in Section A. Theses, publications, papers and technical presentations follow the research description to which they pertain. In addition, Section B lists users from industry and other universities.

The reporting of research and service information to the editor of this report is the option of the user and therefore the projects in Sections A and B are only representative of the activities at the facility. The examples cited are not to be construed as publications or announcements of research. The publication of research utilizing the RSEC is the prerogative of the researcher.

Appendix A lists all university, industrial, and other user of RSEC facilities, including those listed in Sections A and B. Names of personnel are arranged under their department and college or under their company of other affiliation. During the past year, 40 faculty and staff members, 38 graduate students, and 15 undergraduate students have used the facility for research. This represents a usage by 14 departments or sections in 5 colleges of the University. In addition, 69 individuals from 27 industries, research organizations, or other universities used the RSEC facilities.

SECTION A. PENN STATE RESEARCH UTILIZING THE FACILITIES OF THE RSEC

MECHANICAL AND NUCLEAR ENGINEERING DEPARTMENT

NE 497F, REACTOR OPERATIONS LABORATORY

Participants: C.F. Sears, Professor and Director, RSEC

NE 497F is a threecredit laboratory course which provides students the opportunity to individually operate the Penn State TRIGA Reactor and perform selected reactor experiments including checkout, approach to critical, numerous startups, power operations in manual and automatic control, power coefficient measurements, rod worth measurements both manually and with a reactor computer, square wave operations and pulse operations. This brings a hands on application to their analytical and theoretical class work.

NE 450, UNDERGRADUATE LABORATORY--RADIATION DETECTION AND MEASUREMENT

Participants: K. Unlu, Professor and Associate Director for Research, RSEC

Services Provided: Laboratory Space, Machine Shop, Electronics Shop, Reactor Instrumentation and Support Staff

The Nuclear Engineering 450 course is the first of two 3-credit laboratory courses required of all Penn State nuclear engineering undergraduates and is typically taken during the Spring of the junior year. Each weekly laboratory exercise consists of two lectures and one laboratory session. NucE 450 introduces the student to many of the types of radiation measurement systems and associated electronics used in the nuclear industry as well as many of the mathematical techniques used to process and interpret the meaning of measured data. The radiation instruments studied in this course include GM detectors, gas flow proportional counters, NaI (TI) detectors, BF₃ counters, ion chambers, wide range GM detectors, high-purity Germanium detector and gamma spectroscopy, and surface barrier detectors. The data collection and analysis techniques studied include radiation counting statistics, gamma ray and charged particle spectroscopy, and the interfacing of computers with nuclear instrumentation.

The wide range GM detector and BF₃ detector are studied in the Cobalt Irradiation Facility. Ion chambers are studied with the reactor.

NE 451, UNDERGRADUATE LABORATORY OF REACTOR EXPERIMENTS

Participants: R.M. Edwards, Professor of Mechanical and Nuclear Engineering

Services Provided: Laboratory Space, Machine Shop, Electronics Shop, Neutron Irradiation Using Subcritical Pile, Reactor Instrumentation and Support Staff

The Nuclear Engineering 451 course is the second of two 3-credit laboratory courses required of all Penn State nuclear engineering undergraduates and is typically taken during the Fall of the senior year. Each weekly laboratory exercise consists of two lectures and one laboratory session. By the beginning of the senior year, the students have already covered the LaMarsh Introduction to Nuclear Engineering text including reactor point kinetics. The 451 course emphasizes experiments using the instrumentation that was covered in NucE 450 and is divided into two "tracks". These tracks can be coarsely described as TRIGA and non-TRIGA experiments. The non-TRIGA track includes three graphite pile experiments.

In 2003, the TRIGA track included:

1. Digital Simulation of TRIGA Reactor Dynamics
2. Large Reactivity Insertion (Pulsing)
3. Control Rod Calibration
4. Reactor Frequency Response
5. Neutron Noise
6. Reactor Control
7. Source Affects and Feedback

The laboratory utilizes Macintosh computers with GW Electronics MacAdios Jr. data acquisition hardware and Superscope II software. The Superscope II software was a major software upgrade for 1993, and with its new point-by-point seamless mode enabled effective reactivity calculations and control experiments. The Mathworks SIMULINK simulation software was used for the digital simulation exercise for the first time in 1992. Reactor control is offered as a graduate course in our department but our undergraduates do not receive a complete introduction to feedback control. The reactor control experiment interfaces a general purpose PC computer to an Experimental Changeable Reactivity Device (ECRD). Control experiments make use of one of two ERCDD's implemented as a moveable experiment where an aluminum tube containing an absorber material is positioned within the central thimble of the reactor. The first ERCDD with a worth of approximately \$0.35 has a maximum insertion rate of about \$0.12/s while the second with a worth of about \$0.94 may be inserted up to \$0.35/s. ERCDD #1 is used for experiments of up to 65 percent where temperature changes produce significant reactivity changes. ERCDD #2, added in 2000, is for use at low power (less than 0.1 percent) where temperature change and its reactivity effect are negligible. The SIMULINK Real Time Workshop is used to implement an experimental control algorithm. The SIMULINK automatic C code generation process produces and downloads the necessary real-time program for execution in a microprocessor-based controller with an ETHERNET network interface to the host workstation.

The 1994 version of the control experiment thus unified all of the MATLAB/ SIMULINK instruction earlier in the course into a demonstration of state-of-the-art CASE-based control system design and implementation.

COMPTON SUPPRESSION SYSTEM

Participants: K. Ünlü, Prof. of Mechanical and Nuclear Engineering Department
J. S. Brenizer, Prof. of Mechanical and Nuclear Engineering Department
N. O. Çetiner, M.S. student, Mechanical and Nuclear Engineering Dept.

Services Provided: Radionuclear Application Laboratory

Sponsors: DOE-INIE, DOE-NEER, RSEC

INTRODUCTION

The three major interaction mechanisms of gamma-rays with matter are photo-electric absorption, Compton scattering and pair production. In all these interactions, gamma-ray photon energy is partially or completely transferred to electron energy. In the photoelectric absorption, a photon interacts with an atom and the photon completely disappears. In the Compton scattering the gamma ray interacts with an electron, causing an increase in the electron's energy. A new gamma ray with a smaller energy is then emitted. The new gamma ray can escape from the matter or can be absorbed through the photoelectric effect. In the pair production high-energy gamma rays are absorbed and two particles are created (an electron and a positron) and share the energy of the gamma ray. The positron loses its energy through ionization or excitation. If it is stationary, the positron interacts with an electron creating two gamma rays with energies of 511 keV each (annihilation radiation). These two gamma rays can escape or interact with matter through the Compton scattering or Photoelectric effect. Pair production does not occur below 1.022 MeV. The Compton effect is the predominant effect at intermediate gamma energies (200 keV to several MeV).

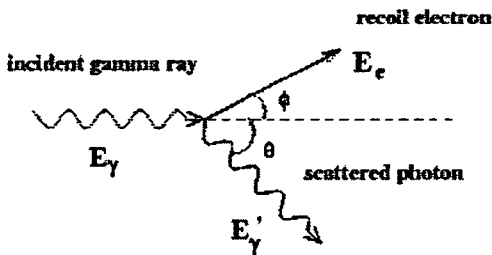


Figure 1. Compton scattering diagram

The vast majority of the scattered photons in Compton Scattering escape the detector by causing background counts in the gamma spectrum. If all of the energy of the incident photon is not absorbed in the detector, then there is a continuous background in the energy spectrum, known as the Compton continuum. This continuum extends up to an energy corresponding to the maximum energy transfer, where there is a sharp cut-off point, known as Compton edge. In order to reduce the contribution of scattered gamma-rays the detector can be surrounded by a guard detector. The two detectors are operated in anti-coincidence, which means that if an event occurs at the same time in both detectors, then the event is rejected. The guard detector catches the escape photons and the effect of those photons is subtracted from the background. Compton suppressors provide a tool to suppress the unwanted background. The combination of a 9"-diameter annulus NaI(Tl) detector and a central germanium detector is called a Compton suppression spectrometer.

COINCIDENCE/ANTI-COINCIDENCE

Coincidence and anti-coincidence are detection modes used to produce a simplified spectrum from certain types of detector systems. In a system of two detectors, each detector produces separate signals. In coincidence mode those signals are counted. In anti-coincidence the signals produced at the detectors cancel or veto each other, leaving the non coincident signals to be counted. The advantage of coincidence or anti-coincidence techniques is achieving greater accuracy in the determination of full energy peaks in the spectrum.

COMPTON SUPPRESSION SYSTEM AT PSU FACILITY



Compton Suppression System at the facility includes

- HPGe detector
- NaI guard detector in a lead shield.
- NIM Bin /Power supply(Canberra Model 2100)
- PC desktop
- Genie 2000 software

Figure 2. Compton Suppression System at PSU

Canberra Model 3106D NIM high voltage power supply is used for operation with HPGe detector.
The HPGe detector properties:

Reverse electrode closed-end coaxial Ge detector	
Relative efficiency	50%
Resolution	2.2 keV(FWHM) at 1.33 MeV
Peak/Compton	58:1
Diameter	64mm
Length	71mm
Cryostat description	vertical slimline dipstick cryostat having 2.5" endcap, 4" long remotedetector chamber, and ultra low background cryostat hardware.

The suppression of Compton events can only be as good as the ability of the guard detector to detect the scattered photons. A Canberra Model 3002D high voltage power supply is used with a NaI(Tl) guard detector. NaI(Tl) detector consists of an annulus and a plug detector. Addition of a plug above the sample greatly reduces the Compton edges.

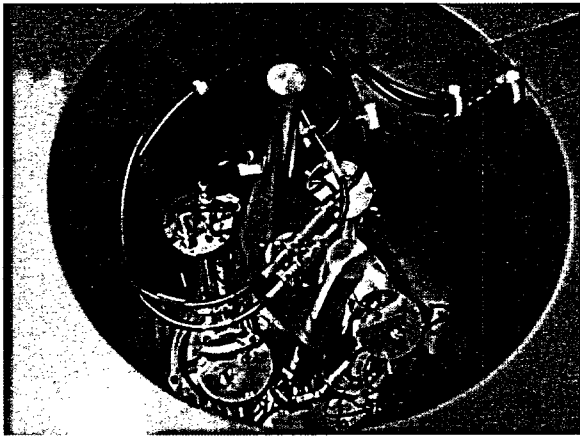


Figure 3. Inside view of the shield where plug detector and PM tubes can be seen

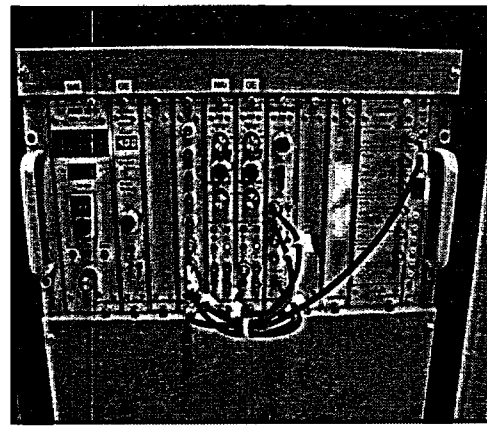


Figure 4. NIM Bin

- Canberra High Voltage Power Supply (Model 3002D)
- Canberra High Voltage Power Supply (Model 3106D)
- Canberra Spectroscopy Amplifier (Model 2026)
- Canberra Coincidence Gate (Model 2040)
- Canberra Multipart II MCA

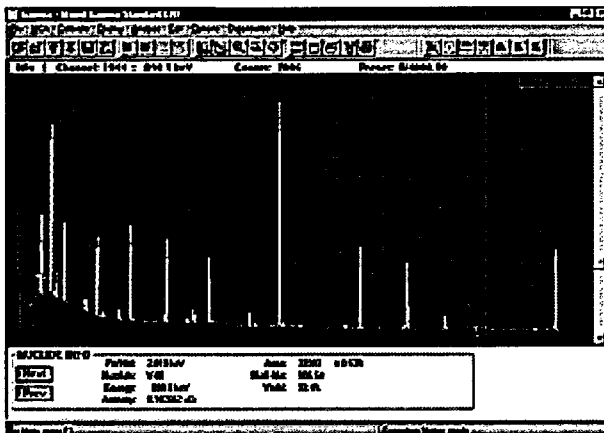


Figure 5. Genie 2000 Basic Spectroscopy Software

Genie 2000 Basic Spectroscopy Software is a comprehensive environment for data acquisition, display and analysis in personal computers. It provides independent support for multiple detectors, extensive networking capabilities, windowing interactive human interface and comprehensive batch procedure capabilities.

TESTING RESULTS

The ^{137}Cs source is counted in Compton Suppression System. Peak/Compton ratio, which is the ratio of the full energy peak to the Compton continuum, is calculated in order to see the performance of the system. Figure 6 shows the comparison of counting when suppression (SUP) is on with Pile Up Rejection (PUR) and when suppression is off (NOSUP) with Pile Up Rejection (PUR).

$$\text{Peak / Compton} = \frac{\text{Number of counts in highest channel of } 662.2 \text{ keV peak}}{\text{Average counts per channel (396 keV and 422 keV)}}$$

$$\text{Peak / Compton} = 1001.00$$

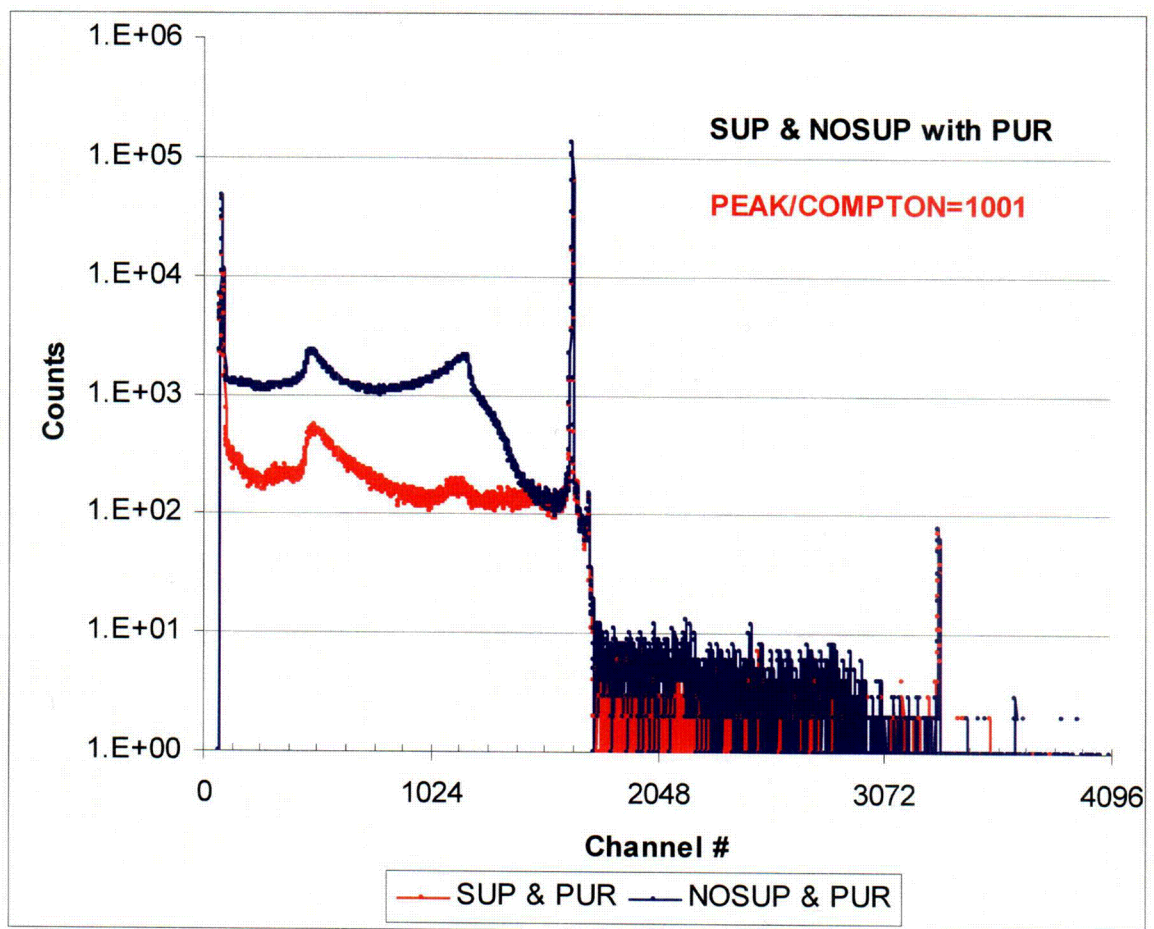


Figure 6. Spectra of ^{137}Cs counted with the Compton Suppression System with suppression enabled (red) and disabled (blue)

TIME-OF-FLIGHT NEUTRON DEPTH PROFILING (TOF-NDP) AT PENN STATE RADIATION SCIENCE AND ENGINEERING CENTER

Participants: K. Ünlü, Prof. of Mechanical and Nuclear Engineering Dept.
S. M. Çetiner, Ph.D. Candidate, Mechanical and Nuclear Eng. Dept.

Services Provided: Neutron Beam Laboratory

Sponsor: U.S. Department of Energy, under
Nuclear Engineering Education Research (NEER) grant

INTRODUCTION

Neutron depth profiling (NDP) is a near-surface analysis technique to measure the spatial distribution of certain light isotopes of technological importance in substrates with low neutron affinity. Ziegler [1, 2] first reported the use of neutron depth profiling as a nuclear reaction analysis (NRA) technique to obtain boron profiles in semiconductors. Biersack et al [3] later thoroughly investigated and improved the technique to almost present capabilities.

Upon neutron absorption, certain light isotopes emit a charged particle, either a proton or alpha depending on the isotope, and a recoil nucleus. The particle emission is monoenergetic and isotropic. As the charged particle and the recoil move in the substrate they lose kinetic energy through nuclear and coulombic interactions with host atoms. The amount of energy loss can then be correlated to the distance traveled by the particles, which is an indication of the depth at which the particles are created.

Conventional NDP is based on the direct measurement of particle energies by charged particle detectors, mostly by silicon semiconductor detectors. This technique is called conventional because almost all of the NDP measurements to date have been done through direct measurements of particle energies. Charged particle semiconductor detectors can be one of surface barrier detectors (SBD), passivated implanted planar silicon (PIPS) detectors or PIN photodiodes.

Conventional NDP has been used extensively for obtaining the depth profile of light elements in various fields. However, proportional to the advances in scientific and technological applications, depth profiling with higher resolutions has become a necessity. It can be shown that neutron depth profiling has reached the limits of resolution that can be attained by the conventional techniques. Time-of-flight neutron depth profiling (TOF-NDP) is proposed as an alternative approach to overcome the restraints that keep the conventional technique from achieving higher resolution.

CONVENTIONAL NEUTRON DEPTH PROFILING

There is multitude of mechanisms that result in limited measurement resolution, including the uncertainties due to the stochastic nature of the charged particle transport in the substrate, and if used, in the semiconductor detector, and uncertainties introduced because of limited capabilities of measurement electronics. One should also take into account the inevitable noise contamination from environmental factors such as the noise created by nearby high-frequency electronics and RF broadcasters.

In order to make the analysis more coherent, we intend to classify the uncertainty components into two major categories: (1) uncertainties created by the analyzed sample, (2) uncertainties introduced by the measurement system.

Uncertainties Introduced by the Substrate

Since the charged particle transport is a stochastic process, the substrate becomes the first source of uncertainty in revealing the true structure of the material. One source of uncertainty is a process called *straggling*. Straggling can be perceived as the degree of deviation from an expected trajectory of a particle as a result of randomness. Straggling can be evidenced in the form of both longitudinal and lateral deviations.

Multiple small-angle scattering is yet another mechanism that contributes to total uncertainty created by the substrate. Figure 1 (a) shows the plot of uncertainty for alpha particles in various depths for a 1- μm silicon substrate. It can be observed that straggling is the major uncertainty factor.

Uncertainties Introduced by the Measurement System

Since the measurement system has multiple components including the detector and pulse-processing electronics, it would be easier to approach each component separately.

Uncertainties introduced by the silicon semiconductor detector

The uncertainty mechanisms that are involved in silicon semiconductor detectors are similar to the mechanisms in the analyzed substrate. Since the principle of operation of a semiconductor detector is based on the ionization due to moving ions and subsequent creation of electron/hole pairs in the crystal, the number of electron/hole pairs created and hence the pulse output of the detector is determined by the energy of the ion. However, the path of charged particles in *detector window*, or *dead layer*, is not unique and suffers from the straggling effect as in the substrate. Therefore, variations in particle trajectories result in different levels of ionization and a slight change in registered energy by the detector.

The uncertainty mechanism explained above refers to the measurement uncertainty for two identical charged particles striking the detector at the same energy and angle of incidence. The uncertainty due to straggling in the detector is created by the set of all possible trajectories the particles can follow. However, there is another uncertainty involved for particles that conform to the aforementioned criterion and additionally followed the same trajectory within the semiconductor detector. Even if the particles assume the same trajectories, the ionization and the resulting electron/hole pair creation need not necessarily be identical due to *charge carrier statistics*. Figure 1 (b) demonstrates the uncertainties created within the detector.

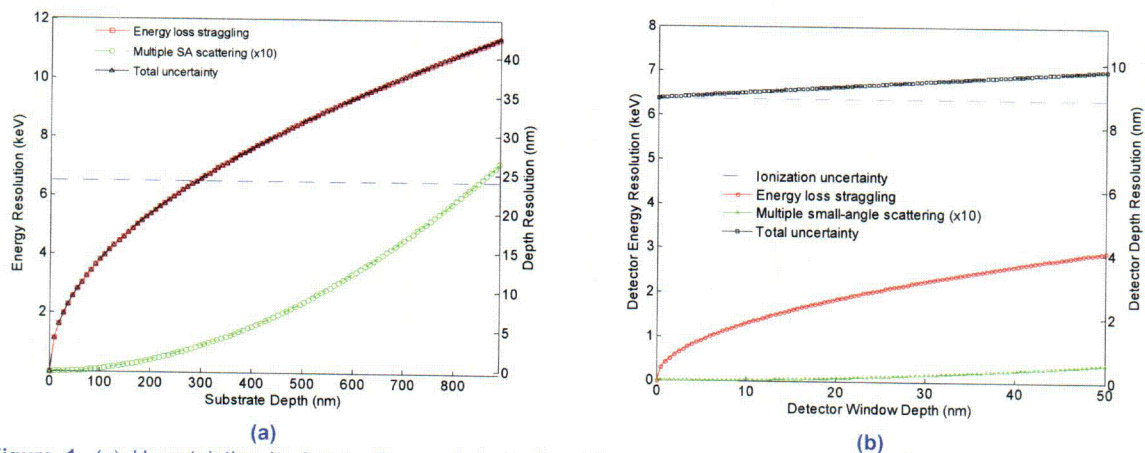


Figure 1. (a) Uncertainties in 1-mm silicon substrate for alpha particles emitted from the $^{10}\text{B} (n, \alpha)^7\text{Li}$ reaction; (b) components of uncertainties introduced in the detector during the particle detection

The uncertainties caused by the substrate and the detector are also given in TABLE for a particular case of alpha particles moving in silicon. The semiconductor detector amounts to about 60% of the total uncertainty. It can be concluded that, at least for the particular case of alphas with 1.5-MeV initial energy in silicon, the use of silicon semiconductor detectors for direct measurement of particle energy becomes bottleneck of resolution.

Table 1. Uncertainties for alpha particles with 1.5-MeV initial energy moving in silicon having traveled 200 nm

	UNCERTAINTY FROM SUBSTRATE (keV)	UNCERTAINTY FROM DETECTION SYSTEM (keV)		TOTAL UNCERTAINTY Actual (Detector %)
		Detector	Electronics	
Energy Loss Straggling	5.4	2.9	N/A	8.3 (35 %)
Multiple Scattering	< 0.5	0.04	N/A	0.59 (9 %)
Geo. Acceptance	N/A	0.01	N/A	0.01 (N/A)
Ionization Uncertainty	N/A	~ 5	N/A	~ 5 (100 %)
Others	-	-	(~ 10 %)	~ 10 % (N/A)
TOTAL	~ 6	~ 8	(~ 10 %)	13.9 ±10% (58 %)

TIME-OF-FLIGHT NEUTRON DEPTH PROFILING

The limitation of conventional NDP due to the use of charged particle semiconductor detectors can be reduced through a proposed technique called time-of-flight neutron depth profiling (TOF-NDP). TOF-NDP eliminates the semiconductor detector and employs microchannel plates for particle detection in time-of-flight configuration. Figure 2 shows the experimental setup used in TOF-NDP measurements.

The virtue of incorporating an experimental in time-of-flight configuration is twofold: (1) time measurement can be done much precisely than the energy measurement, (2) since microchannel plate output is not proportional to particle energy, the energy can be deduced from the flight time.

Microchannel plates (MCP) are millions of electron multipliers each with 4-12- μm channel diameter operating independently. When a particle strikes the inner wall of a channel, it causes the first particle-induced electron emission. Those electrons are accelerated under the high electric field into the opposite wall subsequently creating cascade secondary electrons along the channel resulting in electron multiplication of about 10^4 in a single stage. In two stages, a multiplication of 10^6 can be obtained under normal operating conditions. The MCP's used in our experimental setup employ two-stage multiplication in chevron configuration.

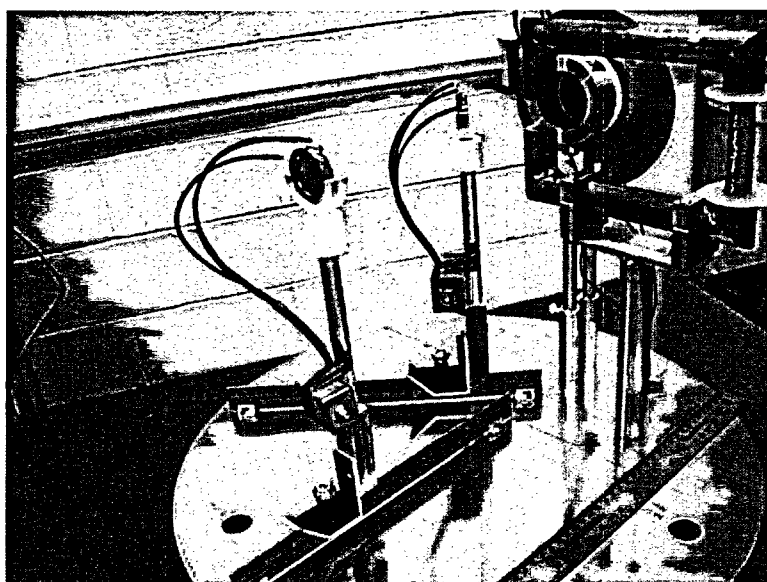


Figure 2. Penn State TOF-NDP spectroemeter

In order to create a time basis, a start and a stop trigger are needed to detect the onset of an event. Those triggers must be stimulated by two events that take place simultaneously enough for experimental purposes. Welsh [5] et al proposed using the electron emission created by the moving ion in the substrate. As the ion leaves the surface of the test material, almost simultaneously, the electrons created are also ejected with the ion. Those electrons, however, do not carry adequate kinetic energy to reach the microchannel plate, and would most likely fall back onto the surface of the material. Therefore, an electric field is introduced to create a forced motion in the vicinity of the surface by using a finely-meshed transmission grid. Either the sample is negatively biased and the grid is held at ground potential, or vice versa. The potential difference between the sample and the grid is usually kept between 500 V to 2000 V, where microchannel plate detection efficiency for electrons tends to be higher. Another factor to keep the potential difference within that range is to refrain from creating *spontaneous desorption* on material surface. The potential introduces insignificant change in kinetic energies of charged particles or recoils.

Once the electrons and particles pass the *acceleration zone*, they enter into a *magnetic field zone*. The magnitude of the field is just enough to steer electrons but make no significant change in charged particle trajectory. In other words, magnetic field acts as a particle separator where electron trajectories are bent onto the start MCP—since electron velocity is larger compared to other particles' velocities—and charged particles and recoils follow their straight paths onto the stop MCP. From the two signals, it is possible to find the flight time of particles from the sample to the microchannel plates.

Uncertainties Introduced by the TOF Measurement System

Replacing the semiconductor detectors with microchannel plates reduces the uncertainty component introduced by the detector, though not completely eliminates it. The time that it takes from the creation of the first electron until all the electrons leave the channel is called *transit time*. Transit time also varies depending on various factors such as the location where the charged particle first hits the channel wall. One other factor that needs to be kept in mind is that secondary electron multiplication is a stochastic process and therefore, by nature, is associated with uncertainty. The uncertainty in transit time is called *transit time spread (TTS)*. Common transit time and transit time spread figures for a single-stage microchannel plate are 100 ps and 30-40 ps, respectively. We should specify that for TOF-NDP, two microchannel plates detectors are used, which makes four microchannel plates total.

Other factors that contribute to the overall uncertainty by the measurement system are time spread from electronics and noise. Those figures can be pulled from the manufacturer's data of the instrumentation.

When all these figure are taken into account, and the time uncertainty is converted to energy uncertainty for particles from $^{10}\text{B}(n, \alpha)^7\text{Li}$ reaction moving in silicon matrix, we get an uncertainty value of about 4 keV for alpha particles, and about 800 eV for lithium recoil. Compared to the uncertainties plotted in Figure 1 (b), theoretically this corresponds to a ten-time improvement when lithium is used for the stop signal. The improvement is more substantial for heavier and less energetic recoils.

PRELIMINARY MEASUREMENTS

Preliminary measurements have been done by using a radioactive source. ^{210}Po , an alpha emitter, was chosen as the source in order to simulate the neutron-induced charged particle emission. ^{210}Po is a convenient source to mimic a neutron depth profiling experiment because it has a single emission branch, hence emits monoenergetic charged particles. ^{210}Po disintegrates according to the following reaction

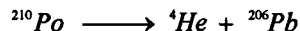


Figure 3 (a) and (b) show the energy spectra of alpha particles from ^{210}Po taken by direct energy measurement (a) and by time-of-flight technique (b). The sensitivity of the measurement technique can be seen from the increase in the number of points representing the energy distribution. However, this does not need to represent actual resolution of the measurement system. The resolution improvement can be assessed based on the observation that Figure 3 (b) includes artifacts that (a) does not show. The asymmetry of the distribution, for instance, and the humps showing in the trailing edge of the peak in

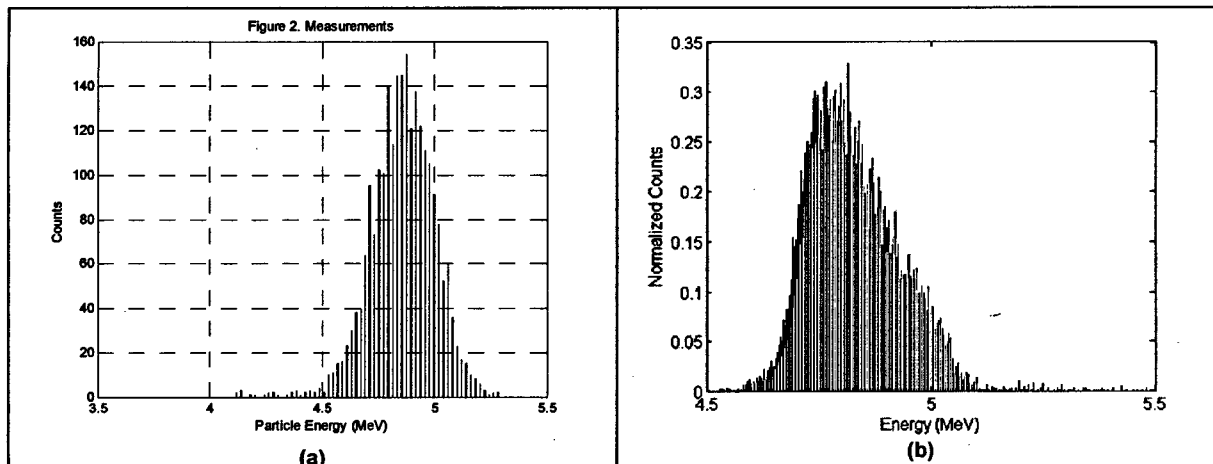


Figure 3. (a) Alpha energy spectrum taken by direct energy measurement; (b) same spectrum taken with TOF spectrometer

The time-of-flight measurement shown in Figure 3 (b) was taken using a microchannel plates that are known to be not of high quality. In the final stage of the development, the measurements will be performed using microchannel plates that were designed for precision time signals. Those microchannel plates are expected to have lower transit time spread, which must further improve the measurement resolution.

CONCLUSION AND FUTURE WORK

The ultimate objective of this study will be the demonstration of the depth profiling of ultrashallow junction devices using the time-of-flight neutron depth profiling technique. Ultrashallow junctions are defined as the junctions with implantation depths below 100 nm. The resolution that can be obtained by the conventional neutron depth profiling is usually no better than 20 nm for on-angle measurements. Off-angle measurements can improve the resolution to 15 nm, but that requires excessive measurement time, which is still not adequate for representing a less than 100-nm distribution. The theoretical calculations show that the depth resolution must be around 5 nm with the time-of-flight technique.

ACKNOWLEDGEMENTS

This project is sponsored by U.S. Department of Energy under Nuclear Engineering Education Research (NEER) grant.

REFERENCES

1. J. F. ZIEGLER, G. W. COLE, J. E. E. BAGLIN, *J. Appl. Phys.*, v. 43 (1972), p. 3809.
2. W. K. CHU, V. L. MORUZZI, J. F. ZIEGLER, *J. Appl. Phys.*, v. 46, No. 7 (1975), pp. 2817-2820.
3. J. P. BIRSACK, D. FINK, R. HENKELMANN, K. MÜLLER, *Nuc. Inst. Meth.*, v. 149 (1978), pp. 93-97.
4. S. M. CETINER, K. ÜNLÜ, R. G. DOWNING, 11th Int. Conf. on Modern Trends in Activation Analysis, University of Surrey, Gilford, UK, 2004 (Proceeding will be published in *Journal of Radioanalytical and Nuclear Chemistry*).
5. J. F. WELSH, *The Development and Evaluation of Recoil-Nucleus Time-of-Flight Neutron Depth Profiling*, Ph.D. thesis, Texas A&M University, August 1996.

NEUTRON ACTIVATION ANALYSIS OF ABSOLUTELY DATED TREE RINGS

Participants: K. Ünlü, Prof. of Mechanical and Nuclear Engineering Dept.
T. H. Daubenspeck, Activation & Irradiation Specialist, RSEC
D. K. Hauck, Ph.D. student at Mechanical and Nuclear Engineering Dept.

Services Provided: Neutron Beam Laboratory

Sponsors: DOE-NEER, Cornell University, NSF and RSEC

INTRODUCTION

The dendroanalysis project is a search for heightened gold concentration in tree rings with Instrumental Neutron Activation Analysis (INAA). Large amounts of stratospheric sulfur from volcanic eruptions, forest fires, or industrial pollution produce acid rain, which stresses trees and results in increased nutrient uptake. We are concentrating on gold because of its suitability to INAA and its chemical similarities to copper, a plant micronutrient which is taken up during times of stress. Tree rings with increased gold concentration can be used to pinpoint years of volcanic eruptions. This information can be used to determine the climatic effect of aerosols and volcanic ash injected into the atmosphere during an eruption by correlating it with historical draught and crop records, or ash layers in bedrock and ice cores. Historians use eruption timelines to date associated historical events, such as plaque, crop extinction, wars, and the end of civilizations, which are sometimes precipitated by volcanic events.

The Dendroanalysis project has been progressing at the Radiation Science and Engineering Center since January of 2003. Within the last year, a third tree sample named CGRPPG4 was analyzed for its trace constituents. Tree Sample CGRPPG4 grew in Greece between 1411 and 1988 AD. Tree samples CTUKLK10B and CTUCAT14C, which both grew in Turkey, were analyzed in 2003 and 2004, respectively. All three trees have been analyzed for their concentrations of gold, sodium, potassium, zinc and bromine. The correlations coefficients for isotope concentration between tree samples indicate that the two Turkish samples provide the most correlated data set. This suggests that the uptake mechanisms for certain elements are regionally dependent. In addition, Icelandic eruptions are correlated with peaks in tree ring gold concentration more consistently than eruptions in any other geographic area. This observation is consistent with the fact that due to their latitude and magma type, Icelandic eruptions are climatically more significant than similar sized volcanic eruptions which happen elsewhere.

EXPERIMENTAL FACILITY

The INAA facility was completed at the Radiation Science and Engineering Center in the previous year (2004). According, descriptions of the Dry Irradiation Tubes (DITs), the Automatic Sample Handling System (ASHS), and the High Purity Germanium (HPGe) detector are available in the Radiation Science and Engineering Center 49th Annual Progress Report. Only a summary of the facility and gamma acquisition equipment is offered here.

Dry Irradiation Tubes

An irradiation facility was built for the purpose of analyzing tree ring samples with NAA. The facility consists of two closed bottom aluminum "dry" tubes which are placed in empty holes in the grid plate. The positions of the dry tubes correspond to grid plate locations E4 and E13 in the core. Since the dry tubes were put into place in 2003, there has been one core reloading done in late 2004. The original loading was altered by placing additional fuel elements in close proximity to the dry tubes, thus increasing the flux.

Automatic Sample Handling System

For handling multiple samples quickly and easily, an Automatic Sample Handling System (ASHS) was built for transferring samples one at a time to the detector for counting. It is capable of holding up to 90 samples at a time and has programmable logic control.

High Purity Germanium Detector

For gamma radiation detection a co-axial High Purity Germanium (HpGe) semiconductor detector was used. The detector purchased for this project has a relative efficiency of 36% and energy resolution of 1.8 keV at an energy of 1173 keV. The crystal is kept in thermal contact with a tank of liquid nitrogen to stabilize temperature and reduce noise. Pre-war lead bricks surround the detector, providing 4" of protection from background radiation.

Gamma Acquisition and Analysis

Gamma acquisition was completed with the use of a PC running Genie-2000 software, a DSA-2000 and a HpGe detector, described above. The DSA-2000 works as the multi-channel analyzer (MCA), amplifier and high voltage power source to the detector. The Genie-2000 software controls the count settings and allows for automated nuclide identification for qualitative or quantitative NAA.

Sample Description and Preparation

Tree samples were gathered and dated by the Malcolm and Carolyn Weiner Laboratory for Aegean and Near Eastern Dendrochronology at Cornell University. Members of the laboratory travel to Turkey and Greece to obtain tree samples for dendrochronology and dendroanalysis during last 30 years. Tree samples chosen for further analysis through INAA are systematically cut into rings to produce samples which range from .1 to .25 grams in size. The rings are placed into polyethylene heat sealed bags, labeled with a permanent marker and set aside for irradiation.

Samples are irradiated for 4 Megawatt-hours and allowed to decay for 15 hours before counting. This allows for adequate activation of the gold without producing excessive amounts of radioactivity. Tree rings are irradiated in groups of 40. Therefore, counting samples for 1 hour each insures that they will all be counted before the gold has decayed by 1 half-life.

RESULTS

Three tree samples covering approximately the last 400 years were analyzed for their trace constituents. Six elements were consistently identified in the wood samples including sodium, potassium, bromine, zinc, lanthanum and gold. It is possible to define a cross correlation coefficient for each of these isotopes as

$$r = \frac{\sum_i ([M_1] - \overline{[M_1]})([M_2] - \overline{[M_2]})}{\left[\sum_i ([M_1] - \overline{[M_1]})^2 \sum_i ([M_2] - \overline{[M_2]})^2 \right]^{1/2}}$$

where $[M_i]$ is the concentration of isotope M in the i th tree sample. The cross correlation coefficient, r , indicates a perfect correlation for two time series when it is equal to one, and a perfect anti-correlation when it is equal to negative one. Figure 1 shows the cross correlation coefficients for element concentrations between two trees. The element with the highest correlation is potassium for all three comparisons. Zinc and Bromine follow, and are consistent with relation to each other for each comparison. Gold is either slightly negative or slightly positive, indicating that the correlation is very close to zero. The tree samples CTUKLK10B and CTUCAT14C, which both grew in Turkey, are the best correlated. The low correlation coefficients for gold indicate that individual tree samples do not show a complete record of environmental events that may be indicated by gold. Therefore, several tree samples may be needed to identify significant events in history.

The size of an eruption is often designated by the Volcanic Explosivity Index (VEI) which is an order of magnitude estimate of the amount of tephra released into the atmosphere. Generally speaking, the larger the VEI for the eruption, the greater its effect on the environment will be. Eruptions with a VEI of 4 or greater may inject aerosols into the stratosphere and have widespread effects as a result. Figure 2 lists the volcanoes that have a VEI of 4 or greater that had correlated gold peaks in any one of the three trees.

The largest volcanic eruption in recent history was the eruption of Tambora in 1815 with a VEI of 7. Tambora released over 8 cubic kilometers of ash and has substantial signals in both the arctic and Antarctic ice cores. However, the only tree in which a visible gold concentration peak appears in 1815 is CTUKLK10B. The peak in 1815 appears at the end of an active gold region which begins in approximately 1809. There has been evidence from other sources of an eruption of unknown origin in 1809. Along with Tambora, its signal is evident in both the northern and southern ice cores, and sometimes the two peaks are referred to as the "Tambora doublet".

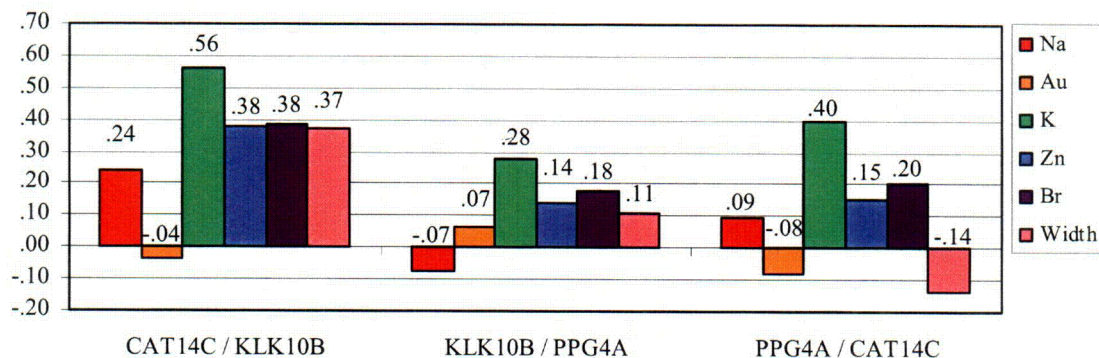


Figure 1. Cross Correlation Coefficients for Isotope Concentrations

Many of the eruptions which had correlated peaks in gold concentration occurred in Iceland. Katla, Hekla and Grimsvotn are currently the most active volcanoes in the region and have been identified multiples times in the data. The fact that Icelandic eruptions are well correlated with gold concentration is consistent with the fact that the characteristics of Icelandic eruptions make them climatically significant.

The volcanoes that have the largest atmospheric effect are those which have basaltic magma, which contains large concentrations of sulfur. The composition of magma is characteristic of the tectonic plate which it originates from in the volcanic rift or hotspot. Icelandic magma is very basaltic in nature and eruptions in that area often make large contributions to the global sulfur budget. Also important is the ability to inject aerosols into the stratosphere. Since the tropopause is lower at high latitudes, a smaller plume height is required to reach the stratosphere. Near Iceland, the tropopause is at a height of 8-10 km, and even relatively small explosions can break through it.

CONCLUSIONS

The volcanoes which were most consistently identified in the gold peak data occurred on Iceland. This is consistent with the fact that Icelandic magma is very basaltic in nature and the island is at low latitudes. However, some Icelandic eruptions which are known to have a large atmospheric effect, such as Grimsvotn in 1783, do not show up in the data.

There are several variables at play which effect the correlation between volcanic eruptions and gold concentration in tree rings. In order for a tree to be stressed by acidic fallout from an eruption, volcanic aerosols must pass over the sample site and be correlated with abundant rainfall. The complexity of Earth's dynamic system makes it impossible to predict on a theoretical basis which regions will experience acid aerosol washout. Contrarily, it is hoped that a statistical analysis of the eruptions that did stress trees in the Near-East can help quantify the effects of climate dynamics from an empirical stand point.

Dendrochemistry has the possibility of supplying an independent dating scheme for volcanic eruptions, with use to both environmentalists and historians. However, more research is needed which is aimed at understanding the mechanisms behind growth patterns and heavy metal ion uptake. Studying multiple trees over the past 20-30 years would allow for a better statistical analysis of the correlations between them. During this period detailed atmospheric data is available from research satellites. The effects from climatically important eruptions may then be mapped and compared to satellite data of the volcanic sulfur clouds produced by recent eruptions.

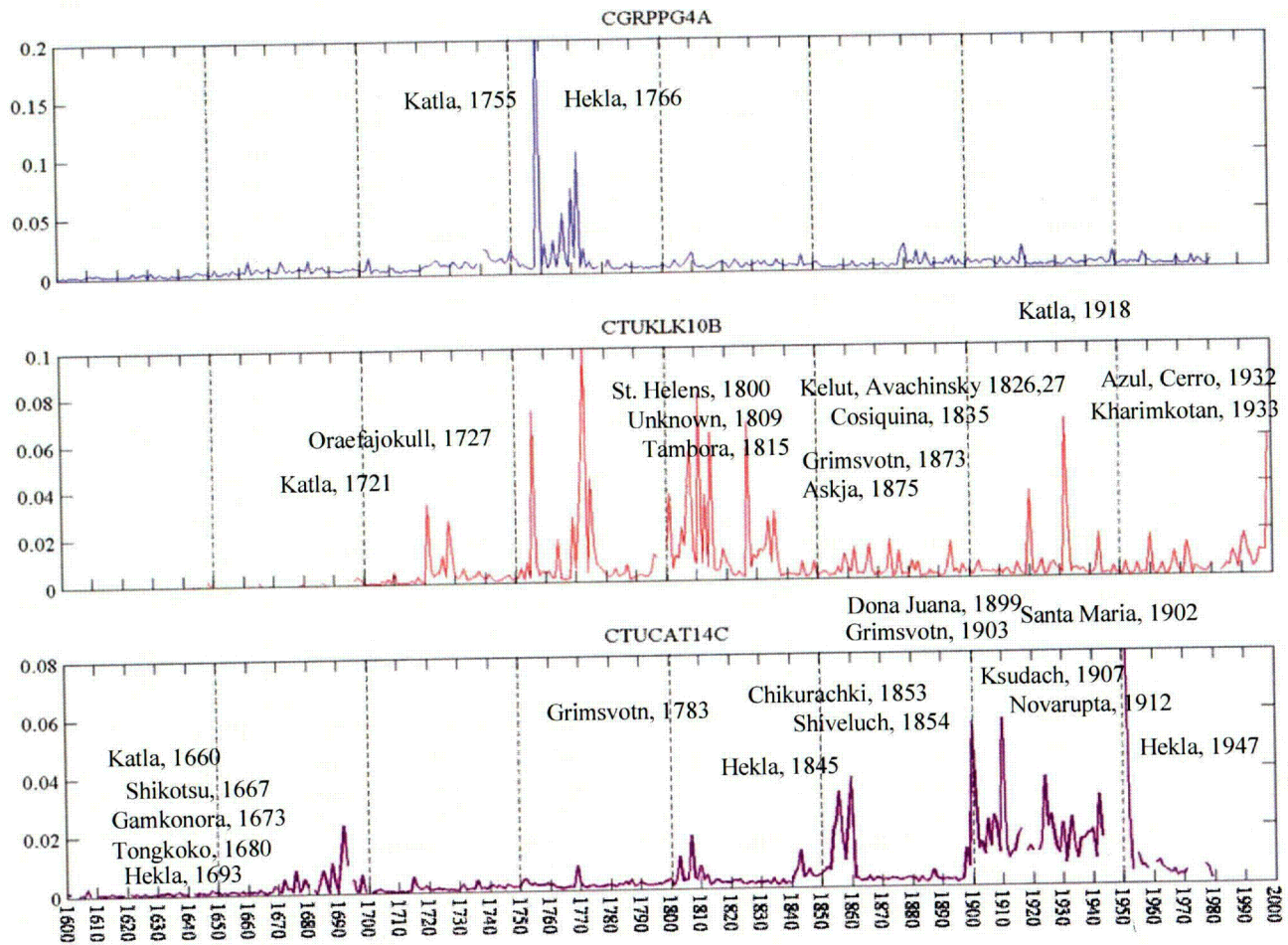


Figure 2. Gold concentration in three tree samples

NEUTRON IMAGING SYSTEM IMPROVEMENTS

Participants: J. Brenizer, Prof. of Mechanical and Nuclear Engineering Dept.
M. M. Mench, Assistant Prof. of Mechanical Engineering Dept.
K. Ünlü, Prof. of Mechanical and Nuclear Engineering Dept.

K. Heller, PhD student at Mechanical and Nuclear Engineering Dept.
A. Turhan, PhD student at Mechanical and Nuclear Engineering Dept.
J. J. Kowal, PhD student at Mechanical and Nuclear Engineering Dept.

Services Provided: Neutron Beam Laboratory

Sponsors: DOE- INIE, RSEC, MNE, and Automotive Manufacturer

INTRODUCTION

The growing demand for dynamic neutron imaging (radioscopy), especially for fuel cell research, has placed new requirements on our existing neutron imaging capabilities. These included developing a more efficient means of data acquisition and storage, better post processing techniques, and a more accurate quantification of water present in the radioscopic images. To this end, the neutron imaging team at the Radiation Science and Engineering Center (RSEC) has made several fundamental and very advantageous changes to its equipment and software resources. The following sections describe the recent upgrades to our imaging and post-collection image processing systems.

EQUIPMENT UPGRADES

For many years our dynamic imaging system consisted of an analog camera connected to a computer through an analog-to-digital interface card that allowed the capture of 30 fps images at 640x480 and 8-bit grayscale depth. This system provided a stable foundation to support the development of data capturing and post processing procedures. To meet the requirements for our recent fuel cell research, a "turn-key," completely digital, image acquisition system was added.

Purchased through the company "I-Cubed," the complete system is comprised of a Pentium IV computer system with camera interface card, a Cohu CCD Camera and image capture software. The computer system is exceptional for both storage of the large volumes of digital image data being captured during radioscopy experiments and the running of the in-house developed, post processing and water quantification software. The digital CCD Cohu camera supplied with the system has a 1004x1004 pixel resolution and a 10-bit deep grayscale range. When connected to the computer's interface card, frame rates as high as 30 fps are possible. The unique driver set and onboard buffers of the Epix interface card make this possible.

Norpix's Streampix image acquisition software was included with the computer. Image capturing and storage is done in the form of proprietary image stacks called "sequence files," which can then be exported to a variety of formats, most notably TIFF and AVI. All post processing is done in the TIFF format since it is a lossless image format and can be read on PC, Macintosh or Unix computers. AVI files are convenient when a qualitative, "real-time" inspection of an object is desired. The saved image sequence file can be converted to the AVI movie format and played back on Quicktime or Windows media player without the need for secondary movie conversion software.

The Streampix software also includes the ability to run user-written plug-ins. This feature allows the synchronization of image capture with external devices through the serial port or external data acquisition cards. Capturing an image along with a pressure or temperature reading is now possible, as well as capturing an image at the request of an external device, such as a rotation table signaling proper test subject alignment.

The decision to use a “turn-key” system was based on the desire to avoid incompatibilities between the various hardware components. An added advantage of the “turn-key” system is the accompanying tech-support, which can troubleshoot problems and provide quick solutions.

POST PROCESSING SOFTWARE UPGRADES

The Penn State neutron imaging team has focused on developing in-house software for data analysis. PSUMagic is the latest incarnation of the PSU Frame Grabber software originally designed for use with the older analog imaging system. With high-speed digital image capture now accomplished through Norpix’s Streampix, an earlier version of PSUMagic was modified to enhance its post-processing and water quantification algorithms.

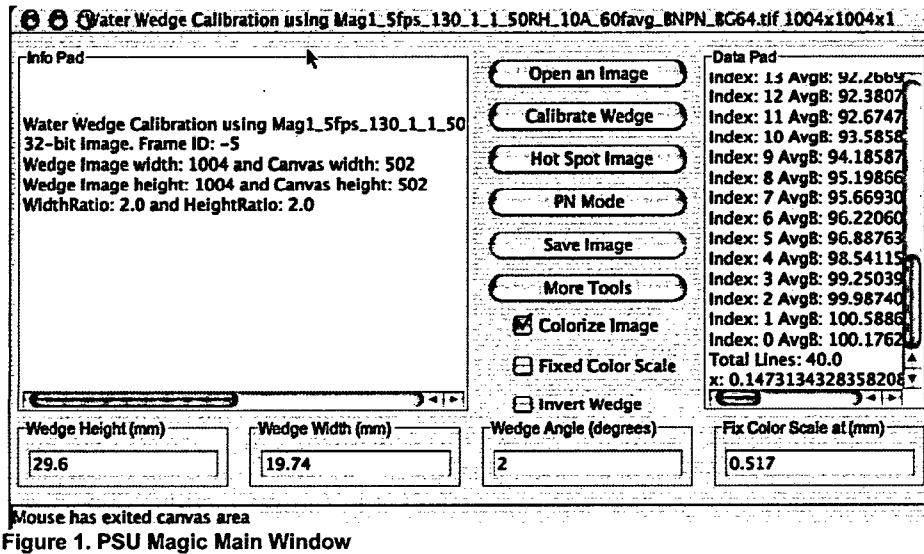


Figure 1. PSU Magic Main Window

Several post-process image enhancement techniques were incorporated to increase the overall image quality and accuracy of the water quantification process. To account for the random noise in sequential images, the luminance value of corresponding pixels within sequential images can be averaged. To correct for minor fluctuations (typically $\ll 1\%$) in the reactor power level, which result in changes in the neutron beam flux and consequently the pixel luminance values in a captured image, the beam intensity between each frame is determined and the entire image is normalized accordingly. The PSU Magic software can correct for variations in the intensity of the neutron beam across the image plane using a beam normalization technique (sometimes called “flat-fielding”). Image enhancement techniques to improve qualitative analysis include highlighting water levels in presentations of single images or video clips such as false colorization of liquid water in the fuel cell and a technique that produces an image of only liquid water in the cell.

Many of the aforementioned post processing procedures are used when isolating and quantifying the water present in neutron images. In addition to calculating a water mass, the latest version of PSUMagic can, at the user’s discretion, track the statistical fluctuation in grayscale of the pixels in the recorded images throughout post processing. This is used to provide a measure of the error involved in the calculation of a water mass. By using this latest feature while analyzing a water-filled test block of known dimensions, an average error of approximately 6.5% was found to be associated with a quantified water mass value.

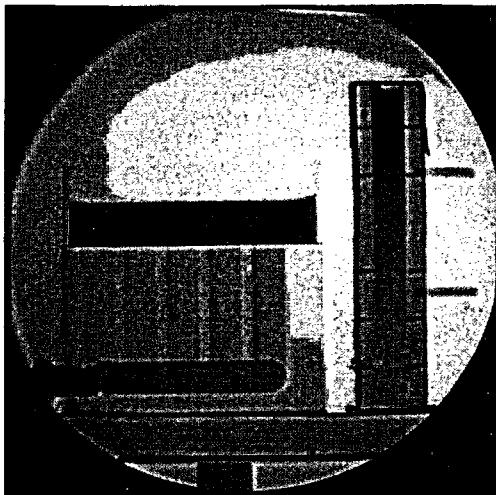


Figure 2. Raw test block image

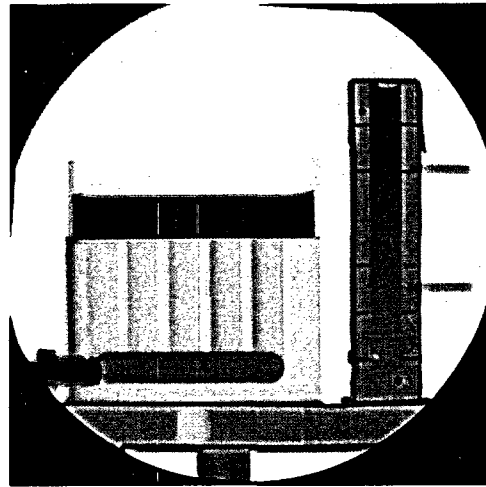


Figure 3. Test block image after post processing

To reduce the users effort when analyzing large numbers of images, a user friendly GUI was included to automate Power Normalization, Flat-Fielding, Water Attenuation Map Isolation and Water Analysis and Colorization.

The screenshot shows a software window titled "PSU Magic Automation Menu". At the top is a menu bar with four items: "1) Normalize", "2) Prep", "3) Analyze", and "Micron Slicing". Below the menu bar are several sections:

- Water Wedge:**
 - Water Wedge Image: A text box containing ".5fps_130_1_1_50RH_10A_60favg_BNPN_BC64.tif" and a "Browse" button.
 - Water Wedge ROI: A section with four input fields: "Start X: 50", "Start Y: 360", "Width: 134", and "Height: 200".
- Hot Spot:**
 - Hot Spot Image: A text box containing ".5fps_130_1_1_50RH_10A_60favg_BNPN_BC64.tif" and a "Browse" button.
 - Hot Spot ROI: A section with a dropdown menu and a "Browse" button.
 - ROI Coordinates: A section with four input fields: "Start X: 432", "Start Y: 232", "Width: 504", and "Height: 504".
- Create A New Directory and save data in:**
 - A text box containing "r/Desktop/FuelCellPics/10-28-04/S_1_1/10-27-04" and a "Browse" button.
- At the bottom, there is a checked checkbox labeled "This Step Only" and a "Slice It!" button.

Figure 4. PSU Magic Automation Menu

The ability to store individual images digitally allows for easy post-process analysis including ascertaining pixel luminance values of features in the image, such as water within a fuel cell. Consequently, the determination of water content within a cell as a function of time is attainable by referencing a pre-generated calibration look-up table that correlates water thickness to pixel luminance. This table is generated using a water-filled calibration wedge that duplicates the neutron attenuation and scattering effect of the fuel cell. The wedge is the exact distance from the beam port aperture as the fuel cell to ensure the equal beam intensity and hence measured attenuation as the fuel cell.

The wedge contains a water-filled channel of continuously varying thickness. The steady and gradual decrease in pixel luminance from the bottom to top of the wedge is representative of the increasing water thickness level within the wedge. This luminance data can then be referenced to assign water thickness values to individual areas within the cell or the entire cell as a whole. The mass and volume of water in the cell can then be computed for finite instances or as a varying function of time. This method works well in this application because the water thickness are at most 1 mm, and typically less than 250 μm . Thus, there are essentially no multiple neutron scatters.

The water quantification procedure was confirmed using an aluminum block milled with channels of known width, height and thickness, filled with water and exposed to the neutron beam where radioscopic images were captured. The post processing and water quantification procedures were applied and the measured values showed good agreement with the theoretical values. The error due to fluctuation of pixel grayscale values was also calculated and plotted.

Aluminum Block Measured Channel Values vs. Calculated

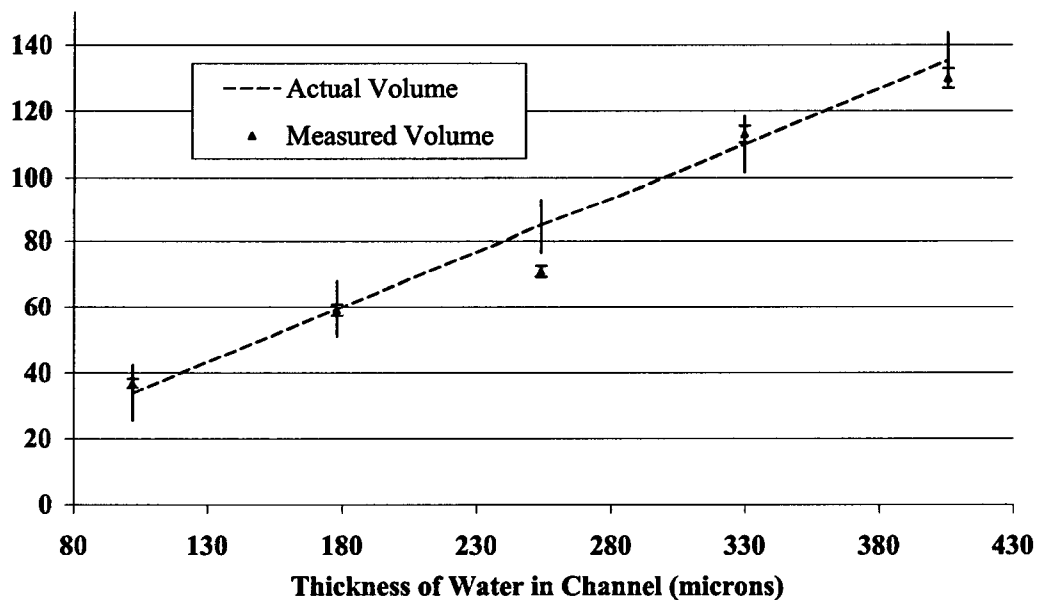


Figure 5. Theoretical and measured water values vs. channel thickness. The (|) bars indicate the machining error of the aluminum block while the ($\bar{\Delta}$) bars indicate the error associated with the quantified water mass values due to grayscale fluctuation.

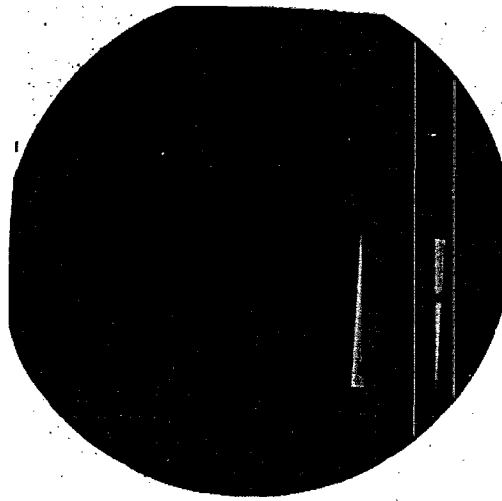


Figure 6. Test block water attenuation image

FUTURE INNOVATIONS

Refinement of water quantification in neutron imaging is ongoing. The look-up table method of analysis will be replaced with a fitted equation providing more accuracy.

A Neutron Computed Tomography (CT) system is being developed to compliment our neutron imaging capabilities. The CT system will make use of recent software developments such as the cross sectional reconstruction software, Octopus, and the volume 3-D image generation software, VGStudio Max. A software plugin for Streampix to synchronize turntable movement and image capture has been implemented and is now undergoing rigorous testing. This plugin is undergoing final testing

Further enhancements and upgrades to the imaging system equipment are being explored, including the use of a fiber optic image pipe. This image pipe will provide quick and easy swapping of one camera for another, thus allowing the use of a high temporal resolution camera in a fuel cell experiment and the use of a camera resistant to long periods of radiation exposure in a tomography experiment.

STUDY OF THE NATURE OF FLOODING AND DRYING THE NATURE OF FLOODING AND DRYING IN POLYMER ELECTROLYTE FUEL CELLS

Participants: M. M. Mench, Assistant Prof. of Mechanical and Nuclear Engineering Dept.
 J. Brenizer, Prof. of Mechanical and Nuclear Engineering Dept.
 K. Üniü, Prof. of Mechanical and Nuclear Engineering Dept.

K. Heller, PhD student at Mechanical and Nuclear Engineering Dept.
 A. Turhan, PhD student at Mechanical and Nuclear Engineering Dept.
 J. J. Kowal, PhD student at Mechanical and Nuclear Engineering Dept.

Services Provided: Neutron Beam Laboratory

Sponsor: General Motors Corporation, RSEC

INTRODUCTION

Due to its high efficiency, low operating temperature (~30-80°C), and rapid evolution since over the past decade, the polymer electrolyte fuel cell (PEFC) is currently under intense research and development. Compared to present power systems, such as the internal-combustion engine, fuel cells are advantageous for several reasons and present a promising future. The operating efficiencies can reach as high as 50-90% for units and also pollutants such as nitrous oxides and particulate matter are eliminated, while carbon dioxide and carbon monoxide are reduced to near zero.

Figure 1 shows the basic operation of a hydrogen PEFC. Hydrogen is supplied to the anode of the fuel cell while oxygen, usually taken from the air, is supplied to the cathode. The electrochemical oxidation reaction at the anode produces hydrogen ions and electrons.

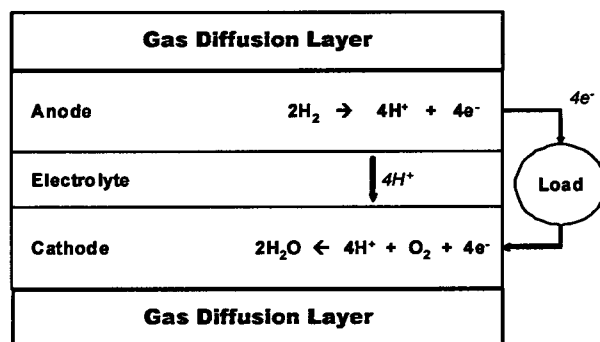


Figure 1. Simplified Schematic of PEFC

The flow of the electrons through an external circuit powers a load. The ions produced at the anode are transported through an ionically conductive polymer electrolyte to the cathode, where water is produced. A ~10-20 μm platinum catalyst layer is typically employed at both electrodes to reduce the activation energy for the electrochemical reactions. Covering each electrode is a 200-400 μm porous carbon fiber gas diffusion layer (GDL). The GDL functions to enable reactant transport to, and product from the catalyst layer, while providing conductivity for electron transport.

In a PEFC, the level of water must be precisely balanced. Adequate water vapor must be available to maintain high electrolyte ionic conductivity and ensure suitable performance. However, if excessive water is present in the liquid phase, it can block pores in the catalyst and GDLs, hindering the transport of reactants to the catalyst. This phenomenon is known as "flooding", and greatly diminishes cell performance. Due to the delicate balance between the benefit of saturated flow and the deleterious effects of flooding concomitant with liquid water accumulation, there is extensive ongoing research to more

fundamentally understand two-phase water transport in PEFCs, to enable performance and design optimization.

Although there have been numerous models presented in literature that predict the water production and transport phenomenon in fuel cells, there has been little research in experimental visualization and quantification of the liquid water distribution and transport. Neutron radiography and radioscopy are excellent non-intrusive techniques for visualization and quantification of the two-phase flow within the fuel cell in real time or steady-state.

EXPERIMENTAL SETUP

The neutron radioscopy system and thermal neutron beam from the Breazeale Nuclear Reactor at the Penn State Radiation Science and Engineering Center was utilized in this study. Specialized image processing hardware was developed for the analysis, storage and presentation of the collected images.

An integrated test station at the Neutron Beam Lab (NBL) was built to control and monitor the fuel cell operating parameters. The NBL Test Station (NBLTS) is isolated from the neutron beam source, as illustrated in Figure 2. The station can accommodate various sized fuel cells (up to 22.8 cm diameter in a single frame) for neutron imaging processes while the following conditions are controlled by the operator on the station's control panel:

- Gas flow rates
- Inlet gas temperature and humidity
- Cell temperature
- Current/Voltage draw
- Operating pressure
- Nitrogen purge

The visualization and quantification of the water distribution in the fuel cell is performed by neutron radiography and radiography techniques.

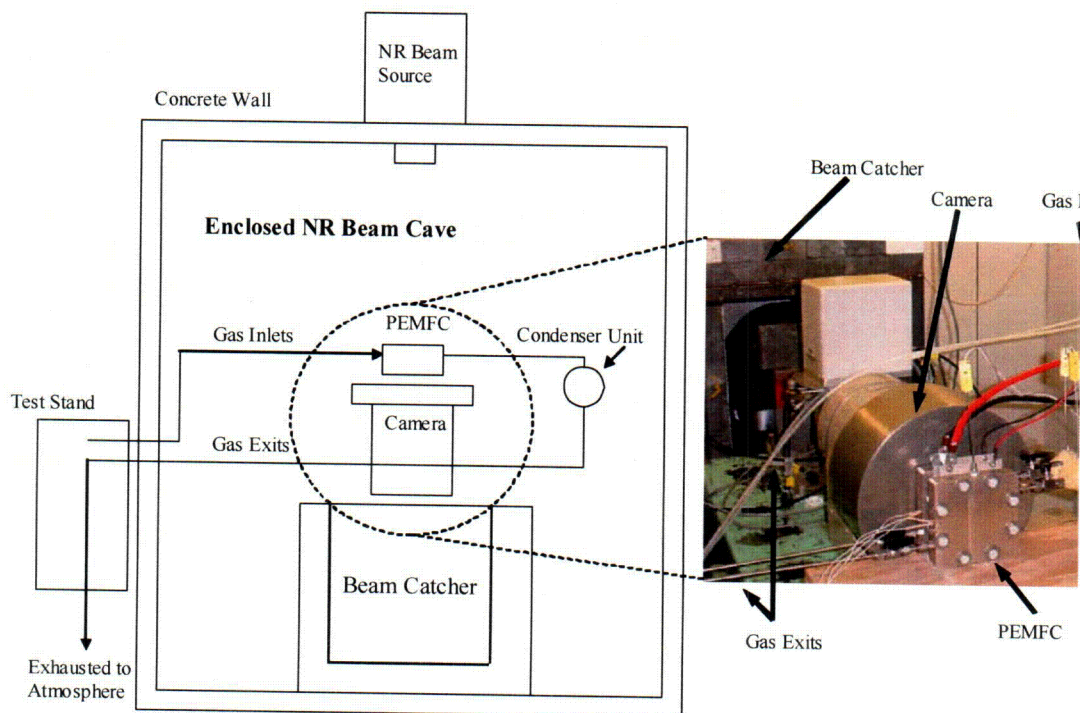
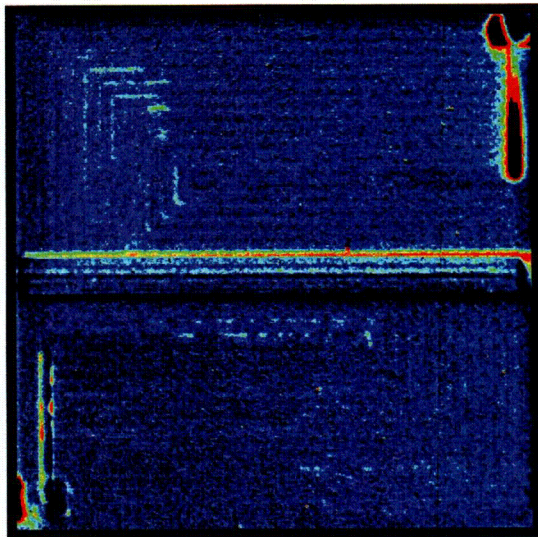


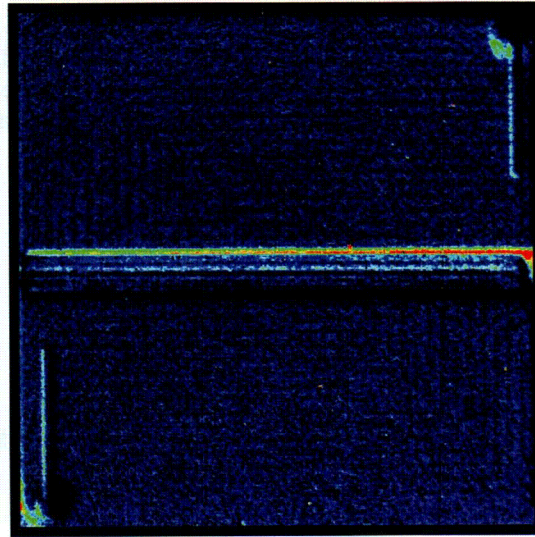
Figure 2. Test station for fuel cell imaging at the NBL

NEUTRON RADIOGRAPHY RESULTS ^[1,2]

A series of neutron images were collected using the fuel cell and imaging setup. The cell temperature (80°C) and gas flow back pressure (7.35 psig) were maintained constant throughout the experiments whereas the relative humidity of the anode and cathode were maintained at 100% at 80°C for all tests. Figure 3 shows images of two conditions with the same current density but different cell temperature. With the same water production (same current) and relatively similar water mass in the diffusion media, the fuel cell with couple of degrees lower temperature has severe flooding losses. The cell performance curve for each condition is shown in Figure 4. The polarization region for low temperature cell is clearly seen from this figure. Therefore, it is seen that the flooding behavior in the fuel cell is highly dependent on water distribution in the flow channels and diffusion media. Furthermore, the effective porosity change for both conditions was calculated and it was found that the flooding loss is due to a small difference between the porosity values.



a) $T_{\text{cell}}=80^{\circ}\text{C}$; Operating conditions: 1.50 A/cm^2 and 0.509 V ; Water content: 381mg



b) $T_{\text{cell}}=85^{\circ}\text{C}$; Operating conditions: 1.50 A/cm^2 and 0.624V ; Water content: 206 mg

Figure 3. Neutron Radiography Image Comparisons for Conditions of Flooding (a) and Not Flooding (b) for 1.0 mm by 1.0 mm Channel/Land Fuel Cell.

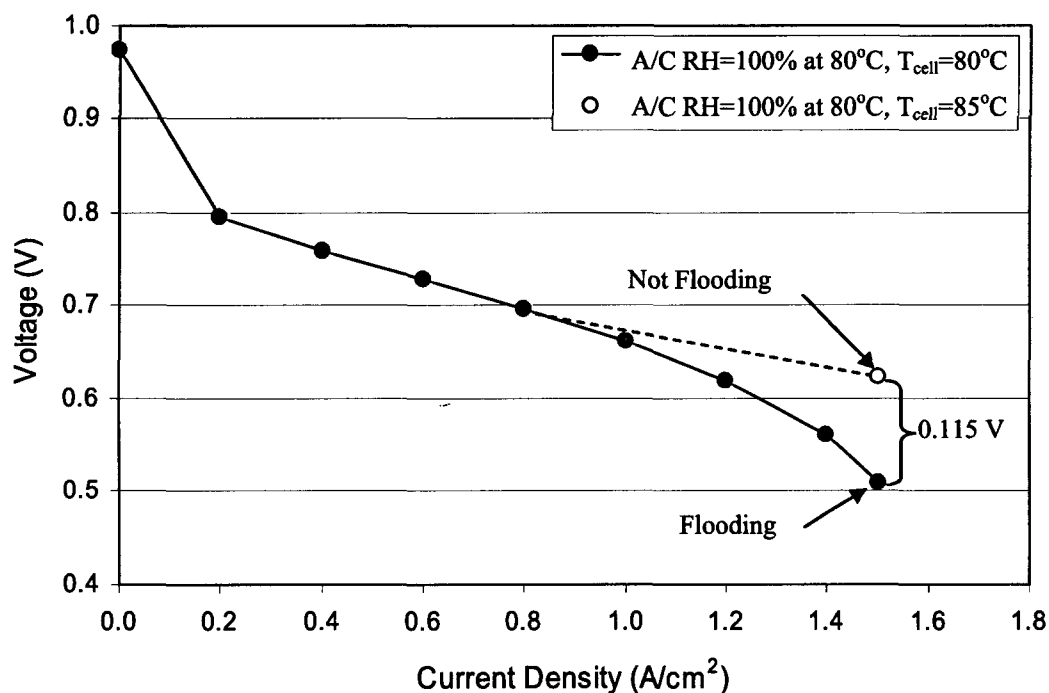


Figure 4. Polarization Curves for Conditions of Flooding and Not Flooding for 1.0 mm by 1.0 mm Channel/Land Fuel Cell.

CONCLUSIONS

Neutron radiography and radioscopy yield excellent spatial and temporal resolution for the investigation of water transport phenomenon and the measurement of liquid water inside an operating polymer electrolyte fuel cell. Results indicate that, for high current density operation with the catalyst and diffusion media utilized, flooding is a highly localized phenomenon controlled by a small volume of liquid water in the DM. The change in effective porosity is lower than predicted by a Bruggeman segregated phase filled pore model, and greater than that predicted by a thin film transport resistance model. Thus, a new combined film resistance, pore filling physical model of flooding is needed to explain the experimentally observed results.

RELATED REFERENCES AND PRESENTATIONS

- [1] Pekula, N., Heller, K., Chuang, P.A., Turhan, A., Mench, M. M., Brenizer, J. S., and Ünlü, K., "Study of water distribution and transport in a polymer electrolyte fuel cell using neutron imaging," *Nuclear Instruments and Methods in Physics Research Section A: Accelerators, Spectrometers, Detectors and Associated Equipment*, Volume 542, Issues 1-3, 21, pp 134-141, 2005.
- [2] Turhan, A., Chuang, P.A., Heller, K., Brenizer, J. S., and Mench, M. M., "The nature of flooding and drying in polymer electrolyte fuel cells," *Journal of Electrochemical Soc.* (submitted) 2005.
- [3] Chuang, P. A., Turhan, A., Heller, A. K., Brenizer, J. S., Trabold, T. A., and Mench, M. M., "The nature of flooding and drying in polymer electrolyte fuel cells," *Proceedings of the Third International Conference on Fuel Cell Science, Engineering and Technology, symposium*, paper #74051, Ypsilanti, MI, May 2005.
- [4] Pekula, N., Heller, K., Chuang, P. A., Turhan, A., Mench, M. M., Brenizer, J. S., and Ünlü, K., "Study of water distribution and transport in a polymer electrolyte fuel cell using neutron imaging," *Proceedings of the 5th International Topical Meeting on Neutron Radiography (ITNMR-5)*, Munich, Germany, September 2004.

- [5] Mench, M. M., Turhan, A., Keller, K., Ünlü, K., and Brenizer, J. S., "INIE Big-10 consortium enabled research: a new physical model of two-phase transport in polymer electrolyte fuel cells using neutron imaging at Penn State," *Accepted for presentation in the Fall ANS meeting and publication in Trans. American Nuclear Society*, November, 2005.
- [6] Pekula, N., Mench, M. M., Heller, K., Ünlü, K., and Brenizer, J. S., "Neutron imaging of two-phase transport in a polymer electrolyte fuel cell," *Trans. American Nuclear Society*, Vol. 90, pp. 309-310, 2004.
- [7] Turhan, A., Chuang, P.A., Heller, K., Brenizer, J. S., Ünlü, K., Mench, M. M., and Trabold, T., "Liquid water distribution and flooding as a function of flowfield design in a PEFC," *Abstract 1014 Presented at the 208th Electrochemical Society Meeting*, Los Angeles, California, 2005.
- [8] Brenizer, J. S., Mench, M. M., Heller, A. K., and Ünlü, K., K., "Neutron imaging at Penn State: past, present and future," (invited) *Presented at the Joint Meeting of the National Organization of Test, Research, and Training Reactors and the International Group on Research Reactors, Special session honoring the Pennsylvania State University Breazeale Reactor 50th Anniversary*, September 12-16, 2005.
- [9] Chuang, P. A., Turhan, A., Heller, A. K., Brenizer, J. S., Mench, M. M., and Trabold, T. A., "The nature of flooding and drying in polymer electrolyte fuel cells," *Presented at the Third International Conference on Fuel Cell Science, Engineering and Technology*, Ypsilanti, MI, 2005.
- [10] Turhan, A., Chuang, P. A., Heller, A. K., Brenizer, J. S., Mench, M. M., and Trabold, T. A., "Water distribution at onset of flooding and dry-out in PEFCs," *Presented at the 207th Electrochemical Society Meeting*, Quebec, Canada, 2005.
- [11] Mench, M. M., "Advanced Diagnostics for PEFCs" (Invited) *Gordon Research Conference on Fuel Cells*, Bristol, RI., July 2004.

RESIDUAL WATER DISTRIBUTION AND REMOVAL FROM PEFCs

Participants: M. M. Mench, Assistant Prof. of Mechanical and Nuclear Engineering Dept.
J. Brenizer, Prof. of Mechanical and Nuclear Engineering Dept.
K. Ünlü, Prof. of Mechanical and Nuclear Engineering Dept.
K. Heller, PhD student at Mechanical and Nuclear Engineering Dept.
A. Turhan, PhD student at Mechanical and Nuclear Engineering Dept.
J. J. Kowal, PhD student at Mechanical and Nuclear Engineering Dept.

Services Provided: Neutron Beam Laboratory

Sponsor: Automotive Manufacturer

INTRODUCTION

Polymer electrolyte fuel cells (PEFCs) are a promising energy source due to their high efficiency and low emissions. However, there are still many components and processes associated with PEFCs that need to be optimized. One major concern with PEFCs is the water distribution in the components. Water is required to conduct ions in the membrane but too much water can cover part or all of the catalyst layer, decrease reactant availability, and cause performance loss. Another concern with PEFCs is that in cold temperatures there can be degradation due to water freezing and expanding in the membrane, catalyst layers, diffusion media (DM), or the interfaces between these components. Therefore, the cell must be built to withstand this degradation and as much water as possible must be removed, or purged, before shutdown.

Unfortunately, non-intrusive water visualization within a fuel cell is difficult to achieve. Neutron radiography uses a neutron beam that is attenuated significantly by the water in the fuel cell and shows an image of the water distribution. It produces excellent resolution and remains non-intrusive. This is helpful in performance tests and model validation efforts.

EXPERIMENTAL SETUP

The tests in this study were done in the Neutron Beam Lab at the Penn State Radiation Science and Engineering Center and the Breazeale Nuclear Reactor provided the thermal neutron beam. The water in the fuel cell attenuates the neutron beam and a CCD camera is used to capture both steady state images and transient videos. Custom software developed by PSU quantifies the liquid water in the cell and produces water mass versus cell location images. The water in the channels and in the DM under the channels is also differentiated from the water under the landings of the flow field using a masking technique.

The fuel cell in this study, seen in Figure 1, has a parallel design with seven channels and the anode and cathode flows were setup in a counter flow arrangement.

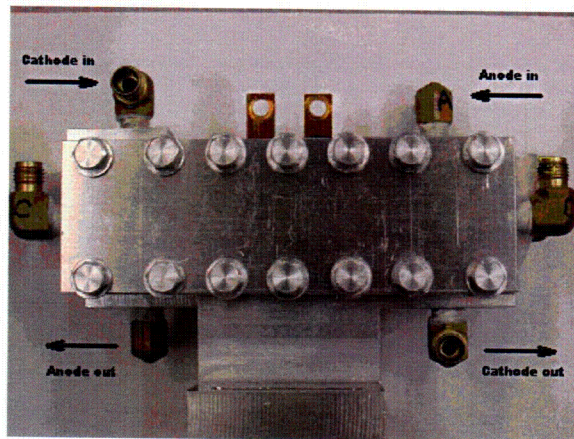


Figure 1: Fuel cell used in this study

The tests in this study were conducted at four different current densities, two flow rates, two humidity conditions, and with two different DM materials. Carbon fiber paper, with a thickness of 180 μm , and carbon fiber cloth, with a thickness of 250 μm , were the two DM materials used. The cell was kept at constant temperature (80 $^{\circ}\text{C}$) and pressure (100 kPag) for all tests.

RESULTS

The low flow rate in the test was 174 sccm at the anode and 417 sccm at the cathode. The higher flow rate was 2.5 times the low flow rate. In all the pairs of tests comparing flow rate only, the water mass in the cell decreased significantly. Figure 2 shows false-color radiographs of two such tests. The high flow rate test (Figure 2b) contains 27.2% less water than the low flow rate test (Figure 2a). The water mass decrease in the channel region was 30.7% and in the landing region it was 24.0%. The water mass decreased more in the channel region in all similar cases because the water could be convectively removed from the channels, while the water under the landings had to diffuse out to the channels and then be removed. These results also suggest that the water in the channel is in a droplet form and not in a film on the wall because a droplet has a higher frontal area and will be convectively removed more easily.

When comparing the two DM materials, it was found that the water in the paper DM tends to be under the lands more than the cloth DM. Both DM's have approximately the same total water mass in the cell. In Figure 3, the average water mass values of all ten tests conducted were normalized to account for the different thickness values of the DMs and the different areas of the three regions (total, channel and landing regions). The paper DM is shown to have much more water mass under the lands than the cloth DM, again averaging the water mass values of all ten tests. The cloth DM only has slightly more water in the landing region than in the channel region.

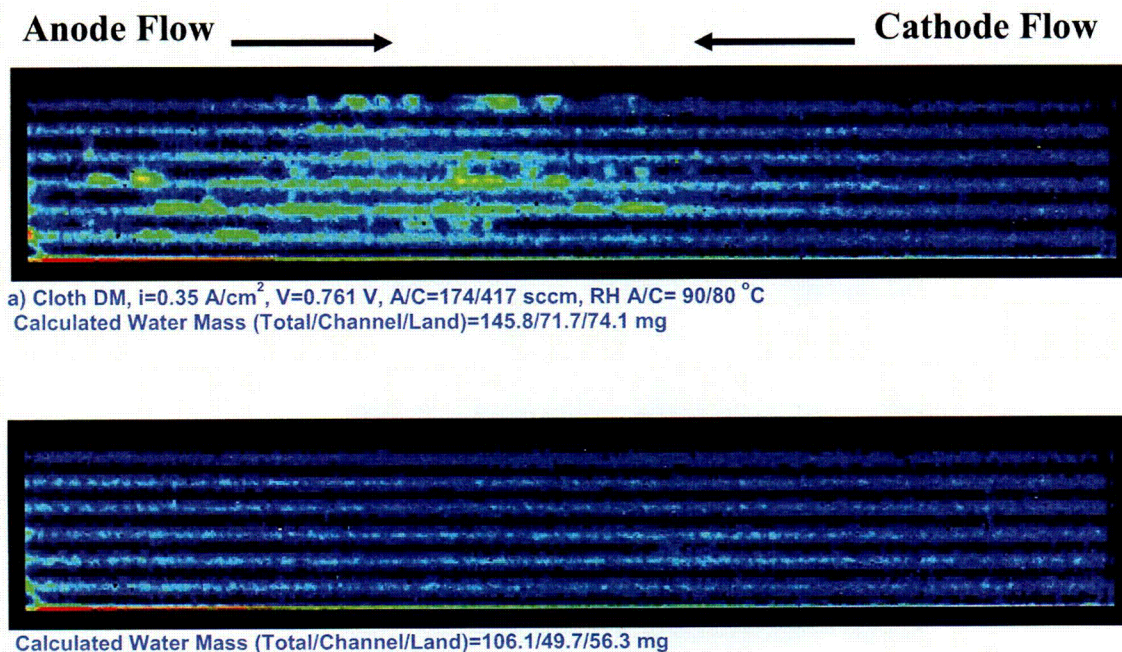


Figure 2. Neutron Radiography Images at low flow rate (a) and high flow rate (b)

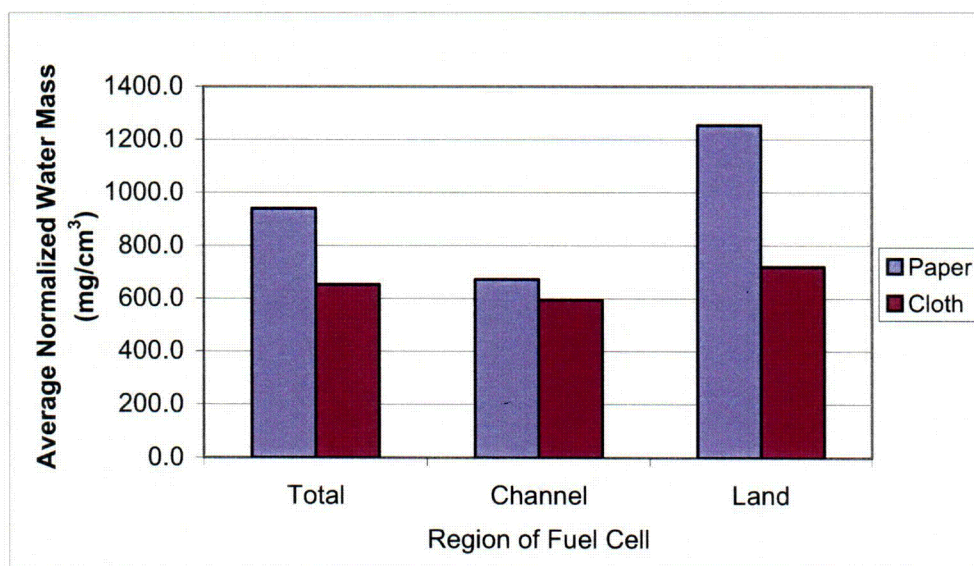


Figure 3. Water Mass Values Per Unit Volume of DM

CONCLUSIONS

Neutron radiography is an excellent non-intrusive technique to visualize the water distribution in a PEFC. The results of this study show that an increased flow rate can remove water from the cell, especially the channels and in the DM under the channels. Also, the cloth DM contained less water under the lands compared to the paper DM. This would make the cloth DM easier to purge since the water under the landings is more difficult to remove. These results have a deep impact on the design of automotive fuel cells to reduce the residual liquid water fraction in the porous media, which will help improve low temperature performance.

RELATED REFERENCES AND PRESENTATIONS

- [1] Turhan, A., Heller, K., Brenizer, J. S., Ünlü, K., and Mench, M. M., "Influence of operating parameters on liquid water distribution and flooding in a PEFC," *Abstract 942 Presented at the 208th Electrochemical Society Meeting*, Los Angeles, California, 2005.
- [3] Mench, M. M., "Advanced Diagnostics for PEFCs," *(Invited) Gordon Research Conference on Fuel Cells*, Bristol, RI., July 2004.

SOFT ERROR ANALYSIS TOOLSET (SEAT) DEVELOPMENT

Participants: V. Narayanan, Prof. of Computer Science and Engineering Dept.
M. J. Irwin, Prof. of Computer Science and Engineering Dept.
K. Ünlü, Prof. of Mechanical and Nuclear Engineering Dept.
Y. Xie, Prof. of Computer Science and Engineering Dept.

V. Degalahal, Ph.D, Intel Corp., Mobile Platforms Architecture and Development
S. M. Çetiner, Ph.D. candidate, Mechanical and Nuclear Engineering Dept.

Services Provided: Neutron Beam Laboratory

Sponsor NSF, Penn State Dept. of CSE, RSEC

INTRODUCTION

Soft errors, or single event effects (SEE), are transient circuit errors caused due to excess charge carrier induced primarily by external radiation. Radiation, directly or indirectly, may induce localized ionization that can flip the internal values of the memory cells. The major radiation source that causes this temporary malfunction in semiconductor devices is the cosmic rays.

Figure 1. A 65-nm DRAM (left) and a schematic that conceptualizes the soft error phenomenon (right). Electron-hole pairs created through ionization by radiation might get drawn to node terminals before they recombine in the substrate causing a transient glitch in the device node. This temporary pulse might flip the internal state of the memory bit.

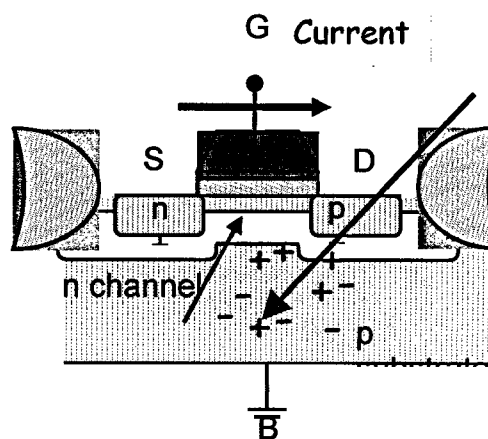
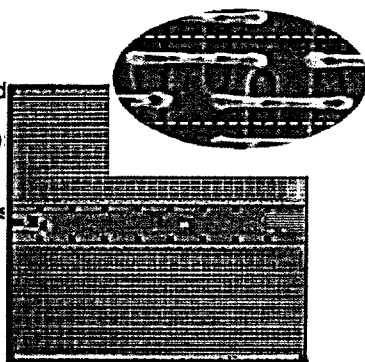


Figure 2. Integrated circuits (IC) are becoming a major component of modern societies.

Cosmic ray particles have the ability to either toggle the state of memory elements or create unwanted glitches in combinational logic that may be latched by memory elements. As supply voltages reduce and feature sizes become smaller in future technologies, soft error tolerance is considered a significant challenge for designing future electronic systems. For example, a 1 GB memory system based on 64Mbit DRAMs has a combined error rate of 3435 FIT (failure in 10^9 hours of operation) when using single error correction and double error detection. An even higher soft error rate of 4000 FIT was reported for a typical processor with approximately half of the errors affecting the processor core and the rest affecting the cache. Such errors also affect the fast growing FPGA (Field Programmable Gate Array) segment.

As earth's atmosphere shields most cosmic ray particles from reaching the ground and charge per circuit node used to be large, SEE on terrestrial devices has not been important until recently. The galactic flux of primary cosmic rays (mainly consisting of protons) is very large, about 100,000 particles/ m^2s as compared to the much lower final flux (mainly consisting of neutrons) at sea level of about 360 particles/ m^2s [1]. Only few of the galactic particles have adequate energy to penetrate the earth's atmosphere. However, with

continued scaling of feature sizes and the use of more complex systems, soft errors in terrestrial applications are becoming an increasing concern and have drawn attention since late 1990s.

The issue of SEE was first studied in the context of scaling trends of microelectronics in 1962 [2]. Interestingly, the forecast from this study that the lower limit on supply voltage reduction will be imposed by SEE is shared by a recent work from researchers at Intel [3]. However, most works on radiation effects, since the work in 1962, focused on space applications rather than terrestrial applications.

There have been various documented failures due to soft errors ranging from memories used in large servers and aircrafts to implantable medical devices like cardiac defibrillators [4]. A widely cited soft error episode involves L2 caches with no error correction or protection that caused Sun Microsystems' flagship servers to crash suddenly and mysteriously [5]. This problem resulted in loss of various customers for Sun Microsystems. More ominous than this failure can be errors in embedded devices such as cardiac defibrillators that are becoming an integral part of our society. As computing systems develop into indispensable part of various critical applications ranging from medical implants to fly-by-wire aircrafts, immunity against soft errors becomes more critical for the society as a whole.

The importance of dealing with the soft error problem can be evidenced by the large number of papers and articles that flooded the scientific community over the last decades. However, most researchers are impeded by access to realistic fault models and real soft error data. This limitation results from confidentiality of soft error data of chips tested by semiconductor companies and the limited access to accelerated soft error testing facilities for academics. Most commercial soft error testing in U.S.A. is performed at the Los Alamos test facility, access to which is expensive and cumbersome due to security clearances required.

THE IMPETUS BEHIND THE SEAT

Radiation-induced SEE may seem to be easily solved through techniques such as radiation-hardened processing. These kinds of countermeasures have been traditionally and successfully adopted to remedy radiation effects in space applications. However, they are not suitable for commercial manufacturers of terrestrial devices as many of the solutions consume more power, reduce manufacturability and severely influence IC performance [6]. Even space applications are moving away from the use of radiation hardened process technology. They are using commercial off-the-shelf components that employ soft error protection techniques at software and architecture level for cost and performance reasons. As a result, many researchers have been focusing on employing new soft error countermeasures ranging from process to software levels.

Advances in process technology such as adoption of silicon-on-insulator (SOI), elimination of boron-10 impurities are expected to mitigate the soft error problem to a certain extent. However, solutions at higher levels are still essential for reliable operation of the computing system. The lack of fault models that abstract the physical phenomena of soft errors accurately in a fashion that is accessible to computer engineers and the absence of tools that analyze the effectiveness of soft error countermeasures are affecting researchers in their quest for taming the soft error problem.

There is an obvious need for a community resource for researchers and industrial practitioners studying radiation-induced SEE on computing systems. Existing tools either do not address the problem in full extent or they are kept confidential by the sole proprietorship of commercial entities, and therefore are not available to the research community. The SEAT will serve a critical purpose in providing researchers of electrical, computer, information sciences or nuclear origin with an open, modular, flexible yet a comprehensive tool.

The SEAT has emerged as a complementary tool to furnish theoretical foundation to experimental radiation-induced soft error research at Penn State Breazeale Nuclear Reactor by Mechanical and Nuclear Engineering, and Computer Science and Engineering Departments. More details can be found in [7] in this

The strength of the SEAT is the fact that it is built upon the combined expertise of computer and nuclear engineers. The SEAT hierarchy starts with modeling the ionization effects of particle strikes on semiconductor devices, and then creates higher-level abstractions of these effects for analysis at the circuit and architecture level. This infrastructure will enable researchers working on circuit, architectural and software countermeasures for soft errors to obtain a better perspective of the physical phenomena, and help them tune their techniques accordingly. If the fault model used at architecture or circuit-level fails to model the SEE accurately, the underlying value of solutions proposed at higher abstractions become meaningless. In this report, we will present details of SEAT-DA, the device level abstraction of the toolset.

SEAT-DA TOOL

Soft error induced transient pulse generation is dependent on exact charge deposited by the neutron-Si interaction and its subsequent collection. SEAT-DA is a tool flow built on top of three different tools as shown in Figure 3. It models both charge deposition and charge collection as described in the following subsections.

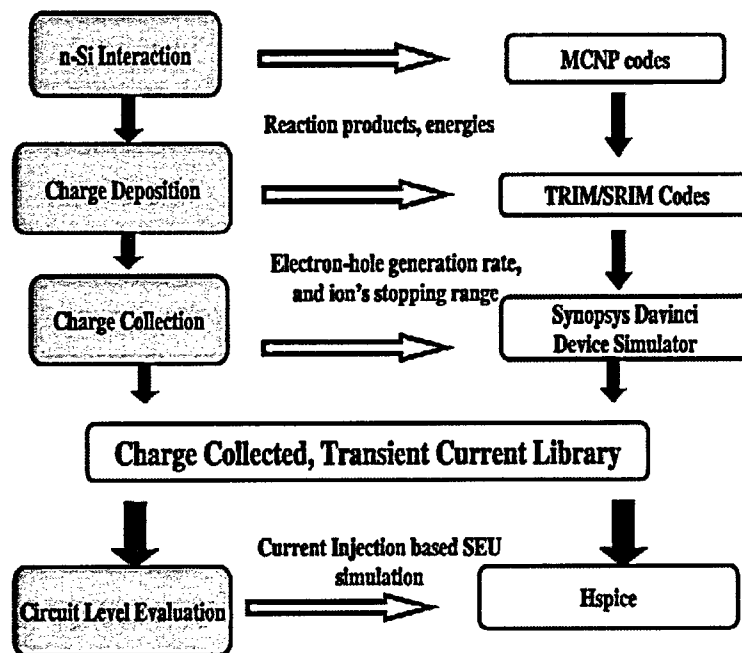
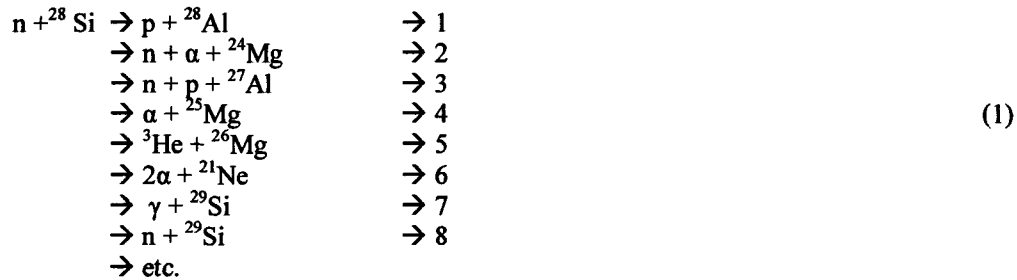


Figure 3. SEAT-DA Simulation Tool Flow

Charge deposition by neutron induced soft errors

To study n-Si interactions, we use the Monte Carlo N Particle (MCNP) toolset. Input to MCNP includes a model of silicon substrate and the description of the neutron flux. MCNP can be made to run with the right reaction codes and neutron data files to model various reactions. This feature is particularly useful as the neutron flux is dependent on the location and altitude, we may setup MCNP with the exact distribution of neutron flux at a given place to calculate the exact n-Si interaction. We have also created customized scripts that parse the MCNP output to identify the different reactions and their outputs. MCNP is used for studying neutron, photon, electron, or coupled neutron/photon/electron transport. This tool has been traditionally used in nuclear engineering for applications such as, reactor designs, radionuclide based imaging, and others. Neutron-Si reactions can be classified into two main groups: elastic and inelastic.

enters the nucleus and the unstable nucleus disintegrates to smaller particles. Many reactions are possible and various particles may be emitted (Please see Equation 1; we will refer to these reaction by the numbers given below).



Once the different reactions products are obtained, we use Transport of Ions in Matter (TRIM) simulator to calculate the charge deposited by these ions. Interfacing MCNP and TRIM together enables an accurate analysis of the charge creation. TRIM is used to calculate the stopping power of ions. TRIM identifies the range of these ions and the charge these ions are capable of depositing. Once the ion distribution resulting from a particle strike is known, its range and charge generation rate is calculated using TRIM. This generation rate is fed to a 3D device simulator to calculate the charge collected in a given region of the device. Among the above set of possible reactions, inelastic scattering produce byproducts that are heavier than the original neutrons, hence they deposit more charge as they travel in silicon. In terms of the susceptibility, transient pulse caused by the inelastic scattering is of higher magnitude than elastic scattering errors. For this reason, it can cause errors on even nodes with large capacitance, or alternatively will not be easily attenuated by the electrical and latching window masking effects. However, it should be noted that these occur fewer in numbers in comparison to the elastic scattering. However, in this work we just present the results from for inelastic reactions, as we believe these are the upper bound worst case scenarios that require to be addressed to ensure a reliable circuit operation. A circuit designed for these conditions will be immune to errors due the elastic scattering.

Charge collection

After the reaction products of n-Si interactions deposit charge, this charge may either recombine or get collected on the device terminal to generate current. For modeling charge collection we use Synopsys TCAD Davinci 3D device simulator. Davinci uses the physical model and equation interface (PMEI) to perform simulations that incorporate user-defined physical models and equations. The input to the 3D simulator includes the device structure, device parameters and device level equations. The charge may be collected in the device terminals by either drift or diffusion processes.

In the case where the ion track is sufficiently far from the space charge zone of the drain junction, the carriers generated in the track mainly move by diffusion. However, for charge collection, the most sensitive regions are reverse biased p/n junctions of the transistor. The high field present in a reverse-biased junction depletion region can collect the charge generated by the ion tracks through drift processes, leading to a transient current at the junction. An important phenomenon associated with the charge collection is called field funnel. Charge generated along the ion track can locally collapse the junction electric field due to the highly conductive nature of the charge track and separation of charge by the depletion region. Figure 8 shows the field in a device after the field has collapsed. The funneling effect can increase charge collection at the struck node by extending the junction electric field away from the junction and deep into the substrate such that charge deposited some distance from the junction can be collected through the efficient drift process.

In deep-sub-micron technology, another phenomenon termed as alpha-particle source-drain penetration effect (ALPEN) also contributes to the phenomenon of charge collection. Due to ALPEN, if a particle strike passes through both the source and the drain at near-grazing incidence, a significant but short-lived source-drain conduction current that mimics the "on" state of the transistor, is generated. However, in sub-100nm devices, when electron-hole pairs are generated there is a high probability that such a generator spans a region greater than the gate length. Hence, we will expand the definition of ALPEN to include these effects. In addition, we will refer to the processes of funneling and ALPEN as drift processes.

CONCLUSIONS AND FUTURE WORK

The SEAT seems to fill a critical need, particularly in research community. With its current stage, it received a great deal of interest from both the academia and industry. We received many positive critiques in a conference that we presented the SEAT the first time [9]. Many industry affiliates stated their interest in the tool.

Even though neutrons account for the majority of the cosmic particles at sea level, the contribution of other particles, particularly protons, become dominant to the soft error problem at higher altitudes. For a more thorough analysis and more extensive applicability, other particle interactions should also be incorporated into the simulation. At this stage of the tool, we managed to include proton flux in the cosmic rays into the analysis. This, however, does not include nuclear-level interactions of protons with the medium, but it does take into account their direct ionization effect. For better modeling of physics, nuclear interactions of protons with the host nuclei must be accounted for since this dominates proton-related single-event effects.

REFERENCES

1. J. F. ZIEGLER, *Terrestrial Cosmic Ray Intensities*, IBM Journal of Research and Development, v. 40, No: 1, pp. 19-39, 1996.
2. J. WALLMARK, S. MARCUS, *Minimum Size and Maximum Packaging Density of Non-redundant Semiconductor Devices*, Proceedings of IRE, 50, 1962.
3. S. BORKAR, T. KARNIK, V. DE, *Design and Reliability Challenges in Nanometer Technologies*, Proceedings of 41st Design Automation Conference, San Diego, 1994.
4. P. D. BRADLEY, E. NORMAND, *Single Event Upsets in Implantable Cardioverter Defibrillators*, IEEE Trans. Nucl. Sci., v. 45, pp. 2929-2940, Dec. 1998.
5. Sun Microsystems, *Soft Memory Errors and Their Effect on Sun Fire Systems*, 2002.
6. P. E. DODD, L. W. MASSENGILL, *Basic Mechanisms and Modeling of Single-event Upset in Digital Microelectronics*, IEEE Trans. Nucl. Sci., v. 50, pp. 583-602, June 2003.
7. N. VIJAYKRISHNAN, M. J. IRWIN, K. ÜNLÜ, V. DEGALAHAL, S. M. ÇETINER, *Testing Neutron-induced Soft Errors in Semiconductor Memories*, Breazeale Nuclear Annual Report, December 2004.
8. J. F. ZIEGLER, <http://www.srim.org/>
9. V. DEGALAHAL, S. M. ÇETINER, F. ALIM, N. VIJAYKRISHNAN, M. J. IRWIN, K. ÜNLÜ, *SESEE: A Soft Error Simulation and Estimation Engine*, 7th Int. Conf. on Military and Aerospace Programmable Logic Devices (MAPLD), September 8-10, 2004.

TESTING NEUTRON-INDUCED SOFT ERRORS IN SEMICONDUCTOR MEMORIES

Participants: N. Vijaykrishnan, Prof. of Computer Science and Eng. Dept.
M. J. Irwin, Prof. of Computer Science and Eng. Dept.
K. Ünlü, Prof. of Mechanical and Nuclear Eng. Dept.
V. Degalahal, Ph.D, Intel Corp., Mobile Platforms Architecture and Development
S. M. Çetiner, Ph.D. Candidate, Mechanical and Nuclear Eng. Dept.

Services Provided: Neutron Beam Laboratory

Sponsor: Department of Energy, INIE Mini Grant, RSEC, Penn State Dept. of CSE

INTRODUCTION

Soft errors are transient circuit errors caused due to excess charge carriers induced primarily by external radiations. Radiation directly or indirectly induces localized ionization that can flip the internal values of the memory cells. Our current work tries to characterize the soft error susceptibility for different memory chips working at different technology node and operating voltage.

BACKGROUND AND RELATED WORK

Advances in VLSI technology have ensured the availability of high performance electronics for a variety of applications. The applications include consumer electronics like cellular phones and HDTVs; automotive electronics like those used in drive-by-wire vehicles, and million dollar servers used for storing and processing sensitive and critical data. These varied applications require not only higher throughput but also dependability. Even if a microprocessor is shipped without any design errors or manufacturing defects, unstable environmental conditions can generate temporary hardware failures. These failures, called *transient faults*, cause the processor to malfunction during operation time. The major sources of transient faults are electromagnetic interference, power jitter, alpha particles, and cosmic rays. Studies in [1, 2] have shown that a vast majority of detected errors originate from transient faults. Even a single-bit error may eventually lead to a computation failure. Therefore, managing the soft errors is a critical problem to solve in fully realizing dependable computing.

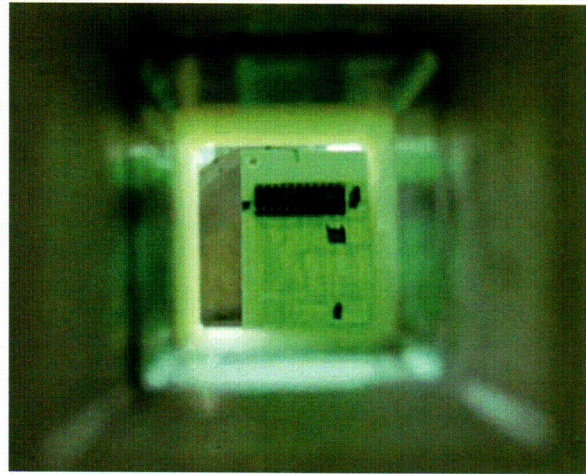


Figure 1. Test chip as seen through the narrow opening in the polyethylene/lead shield.

Soft error rate (SER) testing of devices has been performed for both neutron and alpha particles. Beam 30L of Weapon Neutron Research at the Los Alamos National Laboratory is a JEDEC prescribed test beam for soft errors, and is the only one of its kind. This beam is highly stable and it closely replicates the energy spectrum of terrestrial neutrons in the 2-800 MeV range while providing a very high neutron flux. The SER testing reported in literature recently were performed at this facility [4, 5]. However, the beam availability is limited. Alternatively in the past, experiments were carried out with alpha particles originating from ^{238}Th foil on 0.25 μm -generation SRAMs [7]. Elimination of borophosphosilicate glass (BPSG) and ^{10}B from the process flow in the 180-nm generation has made the low-energy (<1 eV) neutron SER negligible [3]. High-energy (1-1000 MeV) neutrons often dominate SER in advanced CMOS logic and memories. Hence, the need for accessible neutron testing facilities is critical for design of the next generation semiconductor devices.

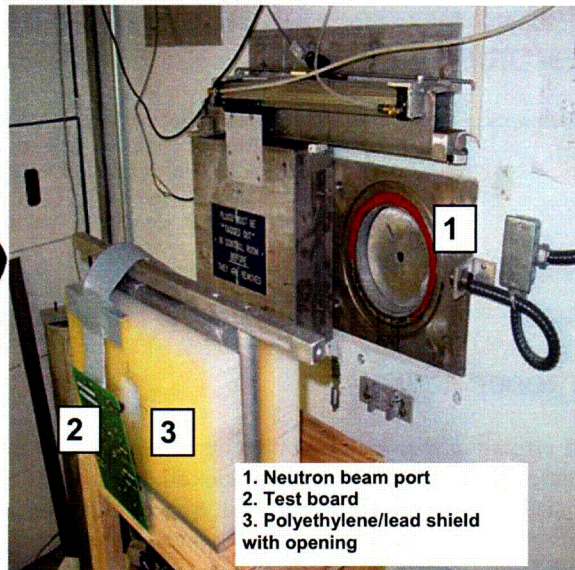
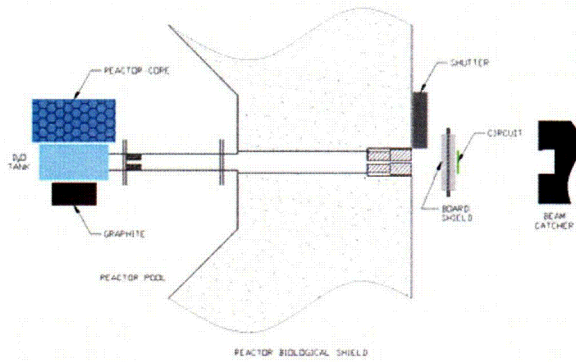


Figure 2. (Left) Simplified layout of the test board, beam tube and the reactor, (right) test chip placed in front of the beam tube with the polyethylene/lead shield for thermal neutron testing.

This study intends to observe the effect of ^{10}B and high-energy neutrons on soft error rate. In order to investigate the effect of boron-10 on SER, a thermal neutron beam is used as shown in Figure 2. For high-energy neutron testing, we intend to use the fast neutrons available near the reactor core by inserting a test circuit into a stand-up pipe adjacent to the reactor core face. This setup is shown in Figure 3.

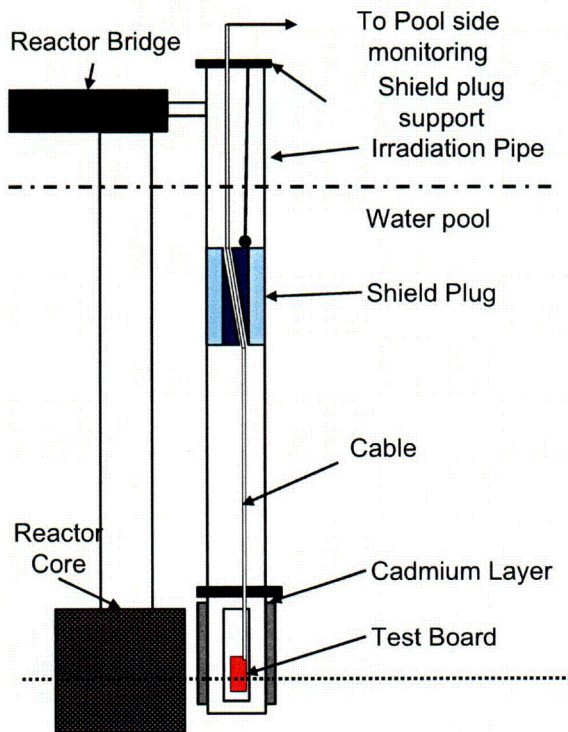


Figure 3. Fast neutron test setup near the reactor core.

EXPERIMENTAL SETUP AND RESULTS

Penn State Breazeale Nuclear Reactor was used as the neutron source in the experiments. The maximum rated power of the reactor is 1 MW in the continuous mode, and 2000 MW in the pulse mode. The reactor power is adjusted from 10 W to 1MW observe the soft error rate dependence on neutron flux. No pulse-mode operation has been performed. Figures 1 and 2 show the test chip and the experimental setup.

For the beam port that was used in the experiments, the beam tube looks at the D_2O tank to get a well-thermalized beam. The average thermal flux at the exit of the beam port is about 3×10^7 neutrons/cm²sec. The high neutron flux allows for accelerated testing of the phenomenon.

The experimental setup consists of a custom board interfaced with a computer through a GPIB card (from National Instruments). The board itself has off-the-shelf SRAM memory chips. The board is controlled through a LabVIEW interface. The controlling application consists of simple routines to read and write a user specified value across the whole memory. During the readout, it compares the written value to the value in each address. The

circuit board is secured in the beam cave, and connected to a PC outside using a 25-ft cable. This configuration allowed for continuous read-write, and for changing the operating conditions without interrupting the experiment.

The selected section of the board is tested on-line multiple times in the actual setup before the reactor is started. The board is exposed to neutron flux after the reactor reaches the stable power level.

As mentioned earlier, the neutron flux around the reactor core is much higher than that at the neutron beam ports. Therefore, the circuit board will also be placed by the periphery of the reactor core via a vertical standpipe in order to observe the effect of fast neutrons on soft error rate. A schematic drawing of fast neutron irradiation facility at PSBR is shown in Figure 3. The fast neutron flux at the core boundary is 5×10^{12} neutrons/cm²sec, and thermal flux is 1.3×10^{13} neutrons/cm²sec at 1MW steady state reactor operation. The reactor can be pulsed for a very short duration of time, around 10 milli-sec at its Full-Width Half-Maximum, at which it generates a fast flux of about 1×10^{16} neutrons/cm²sec at the core periphery. This amounts to about a ten order of magnitude increase in the fast flux. The time duration is very limited, yet the amount of fast flux is immense. The test circuits will be let inside the standpipe and the reading will be taken. In addition, the walls of the pipe will be covered with cadmium. Cadmium will absorb the thermal component of the flux so that the board is affected only by fast neutrons.

RESULTS AND DISCUSSION

The setup described in this report allows for accelerated testing of semiconductor memory devices with thermal and fast neutrons. The experiments and analyses have been performed only on soft errors due to thermal neutrons. Currently, a 16-kbit for Vendor A and a 4-Mbit memory from Vendor B were tested at various supply voltages and reactor power levels. The chip from Vendor A is rated to operate at 5V, but was found to operate as low as 3V. Figures 4 (a) shows the effect of changing the supply voltage on registered soft errors in one hour. A more salient behavior can be observed with the chip from Vendor B. Vendor B chip was known to be denser (4-Mbits compared to 16-kbits) and was expected to have higher soft error vulnerability. Figure 4 (b) shows the effect of supply voltage change on measured soft errors in one hour.

As presented in Equation 1 below, the soft error rate is expected to depend on the $Q_{critical}$ and hence on the operating voltage.

$$SER = Nflux * CS * \exp(-Q_{critical}/Q_s) \quad (1)$$

where Nflux is the intensity of neutron flux, CS is the area of cross section of the node, Q_s is the charge collection efficiency, $Q_{critical}$ is the charge that is stored at the node and hence is equal to $VDD * C_{node}$, where VDD is the supply voltage and C_{node} is the nodal capacitance. Figures 4 (a) and (b) confirm the exponential dependence of soft error rate on device operating voltage as well as other specifications of the device as pointed out by several authors before [7].

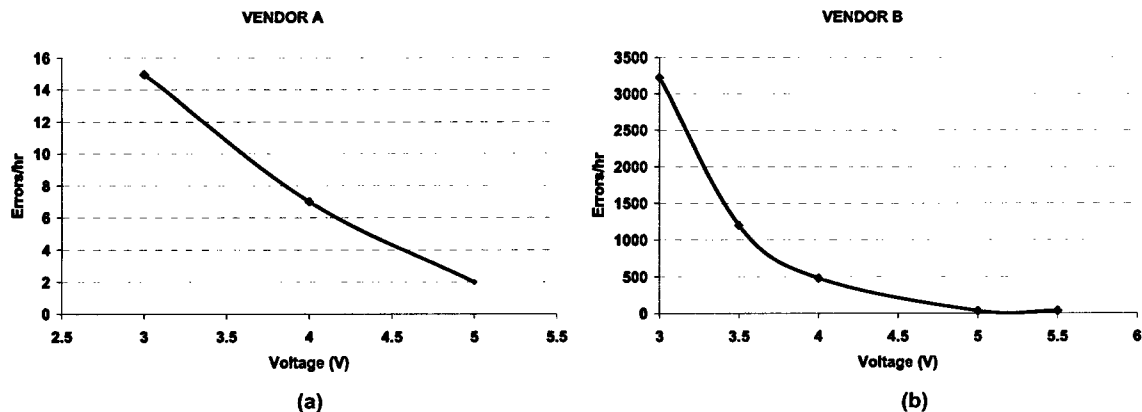


Figure 4. Effect of supply voltage on soft errors

While employing voltage scaling for power reduction, there is a reduction in the $Q_{critical}$ of the cell. Now, if all the other factors remained the same there should be a super-linear increase in the SER. However, based on the Figures 4, we see a linear increase in the SER for a corresponding decrease in the voltage. This is because for a change in supply voltage, the resultant current transient also changes. As the supply voltage reduces, the magnitude of the current changes. This affects the regenerative feedback of the SRAM cell. Thus, the soft error rate is inversely proportional to the supply voltage.

For examining the statistical accuracy of the accelerated tests, the tests were performed at various reactor power levels. Since the reactor power and the flux at the exit of the beam port are directly correlated, changing the reactor power effectively changes the neutron flux impinging on the test sample, hence is expected to increase the soft error rate. The results are presented in Figures 5 (a) and (b).

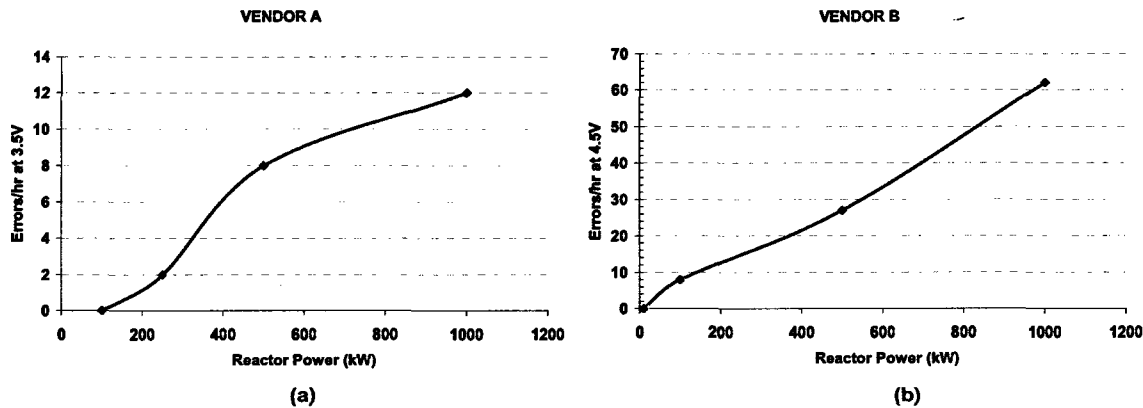


Figure 5. Effect of neutron flux on soft errors

Both figures prove that the soft error rate increases as the reactor power increases. That the soft error rate for the chip from Vendor A is not as linear as the chip from Vendor B is attributed to the relatively small size of the first one. Hence, for statistical accuracy of accelerated soft error rate measurements, it is suggested that the measurements be performed using high capacity chips.

FUTURE WORK

This report briefly summarizes the first phase of the study that focused only on the effect of ^{10}B fission caused by thermal neutron absorption on soft error rate. The elimination of BPSG layer in new device technologies and considerable reduction of ^{10}B content in the p-dopant significantly dropped the contribution of boron fission as a source of soft error. Therefore, for younger-generation technologies, one needs to take into account the high-energy neutron impact on device operation for proper soft error rate analysis.

In the later phase, the circuit will be placed by the periphery of the reactor core in order to observe the effect of fast neutrons on soft error rate. The fast neutron flux at the core boundary is 5×10^{12} neutrons/cm²sec, and thermal flux 1.3×10^{13} neutrons/cm²sec at 1-MW steady state reactor operation. Also, apart from memory chips, other processing circuits will also be put to test in similar fashion and the results observed.

The reactor can be pulsed for a very short duration of time, around 10 msec at FWHM, at which it generates a fast flux of about 1×10^{16} neutrons/cm²sec at the core periphery. This amounts to about a ten order of magnitude increase in the fast flux. The time duration is very limited, yet the amount of fast flux is immense. That might also reduce the experiment times significantly and help perform more tests with various technologies and designs.

REFERENCES

1. J. SOSNOWSKI, *Transient fault tolerance in digital systems*, IEEE Micro, v. 14 No. 1, pp. 24-35, February 1994.
2. D. P. SIEWIOREK, R. S. SWARTZ, *Reliable Computer Systems: Design and Evaluation*, 2nd edition, Digital Press, Burlington, MA.
3. R. BAUMANN, *The impact of technology scaling on soft error rate performance and limits to the efficacy of error correction*, IEDM '02 Technical Digest, IEEE International, pp. 329-332, 8-11 Dec. 2002.
4. P. HAZUCHA, T. KARNIK, J. MAIZ, S. WALSTRA, B. BLOECHEL, J. TSCHANZ, G. DERMER, S. HARELAND, P. ARMSTRONG, S. BORKAR, *Neutron soft error rate measurements in a 90-nm CMOS process and scaling trends in SRAM from 0.25- μm to 90-nm generation*, IEDM '03 Technical Digest, IEEE International, pp. 21.5.1-21.5.4, 8-10 Dec. 2003.
5. J. MAIZ, S. HARELAND, K. ZHANG, P. ARMSTRONG, *Characterization of multi-bit soft error events in advanced SRAMs*, IEDM '03 Technical Digest, IEEE International, pp. 21.4.1-21.4.4, 8-10 Dec. 2003.
6. N. SEIFERT, D. MOYER, N. LELAND, R. HOKINSON, *Historical Trend in Alpha-Particle induced Soft Error Rates of the Alpha Microprocessor*, IEEE 39th Annual International Reliability Physics Symposium, pp. 259-265, 2001.
7. P. HAZUCHA and C. SVENSSON, *Impact of CMOS Technology Scaling on the Atmospheric Neutron Soft Error Rate*, IEEE Transactions on Nuclear Science, v. 47, No. 6, pp 2586-2594, Dec. 2000.

NEUTRON ENERGY SPECTRA CHARACTERIZATION USING A HELIUM-3 NEUTRON SPECTROMETER

Participants: J.S. Brenizer, Professor of Mechanical and Nuclear Engineering
K. Únlü , Professor of Mechanical and Nuclear Engineering

C. Trivelpiece, Graduate Student

Services Provided: Neutron Beam Laboratory, Hot Cell Laboratory, PuBe & AmBe Neutron Sources

Sponsor: DOE-INIE

INTRODUCTION

Neutron beams are used in a variety of experimental methods at research reactors all across the United States. Such applications include: neutron imaging and neutron tomography, neutron depth profiling, neutron diffraction, neutron scattering etc. The aforementioned techniques employ neutron interactions, which are characterized by energy dependent cross sections. Accordingly, information characterizing the energy spectrum of these neutron beams is useful.

A Model 525-780 ^3He spectrometer was purchased from ORTEC and is currently being tested and calibrated at the Radiation Science and Engineering Center (RSEC). Current thermal neutron beam energy measurements are performed using a slow neutron chopper, which employs the time-of-flight technique. However, the maximum detectable neutron energy is bound by the mechanical limitations of the slow neutron chopper, specifically the rotational speed of the chopper disk. The helium-3 spectrometer provides the experimenter with the ability to characterize neutron energies in the hundreds of keVs to the MeV range. Figure 1 is a photograph of the ORTEC Model 525-780 ^3He Spectrometer. Appendix A is a schematic of the pulse processing circuit. The spectrometer included: two surface barrier detectors mounted 1 mm apart in side a sealed spectrometer head, a bottle of He-3 gas that allows for up to 80 refills of the spectrometer head at an internal pressure of 5 atm, the necessary nuclear instrumentation and the associated power supplies.

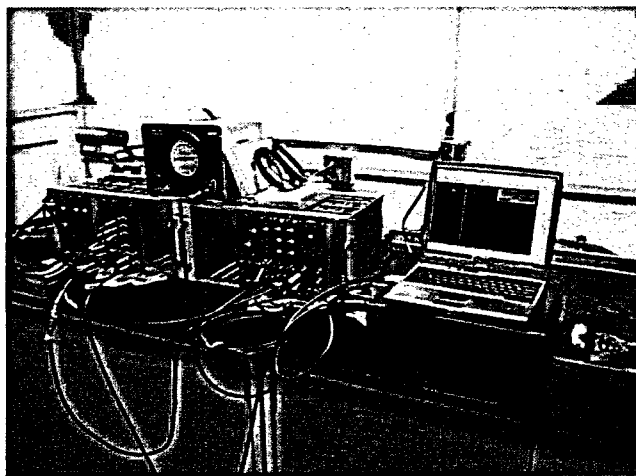


Figure 1: He-3 spectrometer with PCI expansion box and Dell Laptop used for data collection

The spectrometer utilizes the $^3\text{He}(n,p)^3\text{H}$ reaction. This is an exothermic reaction in which the resulting reaction products (a proton and a triton) share the Q-value of the reaction (764 keV) as well as the kinetic energy of the incident neutron. The “head” of the helium-3 neutron spectrometer contains two surface barrier detectors in a sandwich geometry. The energies of the reaction products are deposited in these

detectors and output pulses are generated. The height of the output pulses is directly proportional to the incident neutron energy. These pulses are processed by summing and coincidence circuits. The pulse height analyzer used in this system is an ORTEC TRUMP – PCI card. The ADC on this card is gated using the output from the coincidence circuit in the instrumentation and the neutron energy information is collected from the summing circuit. The system is made portable with the addition of a PCI expansion box from MAGMA electronics. This device houses the TRUMP – PCI card in a fashion similar to a regular desktop PC but connects to a laptop computer using a PCMCIA card. The raw neutron energy spectra from various sources (PuBe, AmBe, neutron beam) are collected and visually displayed using ORTEC’s MEASTRO – 32 MCA Emulator. A typical raw neutron energy spectrum is shown in Figure 2.

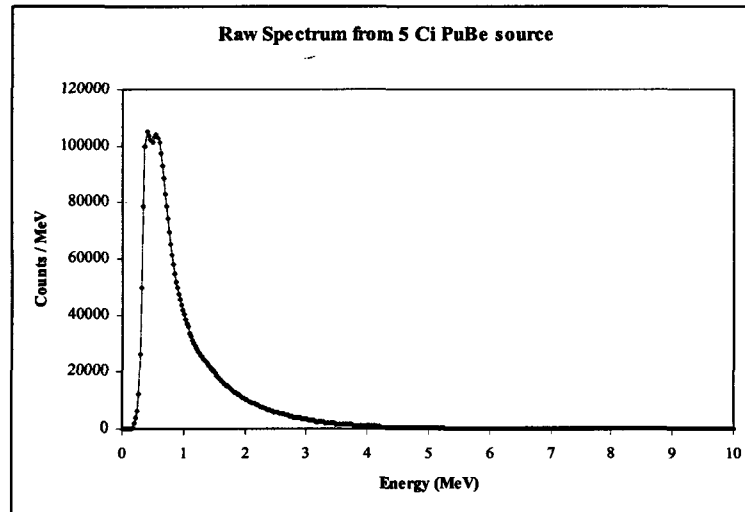


Figure 2: Raw neutron spectrum collected from 5 Ci PuBe source

The helium-3 neutron spectrometer is calibrated using an ORTEC Model 419 Precision Pulse Generator (pulser). The system was calibrated at ORTEC during the initial testing phases so that the pulse height dial reading on the front of the module corresponds to signal pulses from 0 to 10 MeV. The energy calibration in MEASTRO – 32 is preformed by obtaining multiple pulser peaks in a single spectrum and assigning energy values to each peak. The energies of the channels not in the peaks are extrapolated using a quadratic fitting process. Figure 3 shows a spectrum of pulser peaks used for a calibration.

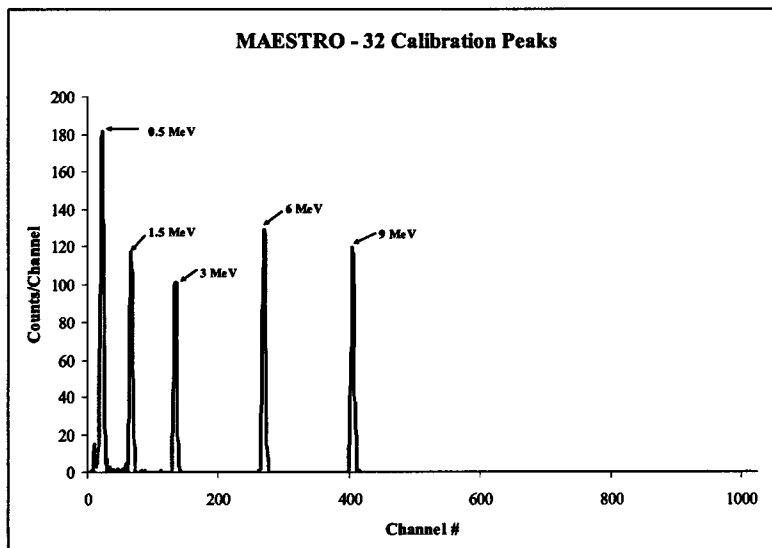


Figure 3: Peaks produce by pulser used in energy calibration procedure

Most of the measurements made to date were collected using a 5 Ci PuBe source located RSEC. The source is positioned in the same azimuthal plane (approximately 3 ft from floor) as the detector at a distance of 25 cm. Initial measurements were made with the detector and source much closer together in order to increase counting rates; however, indications of detector saturation were noticed, which is why the source was moved to 25 cm away from the detectors. At this distance the neutron flux incident on the detector (assuming point source and point detector for simplicity) is approximately $2.5 \times 10^7 \text{ n/cm}^2\text{s}$.

The raw spectral data (counts/channel or MeV), as shown in Figure 2, collected with the spectrometer is actually the number of (n,p) reactions per channel/energy for the spectrum collection time. While this is an accurate number in terms of (n,p) events occurring in the detector head, this information does not accurately represent the actual neutron spectrum emitted from the PuBe source (or from any other source).

Many phenomena must be considered when trying to extract the actual neutron spectrum from the information collected using the spectrometer. These considerations include the $^3\text{He}-\sigma_{n,p}$, the spectrometer efficiency and resolution, response functions of the detector, and so on. For simplicity, it was assumed that the reaction rate per MeV (RR), mentioned earlier, was related to the flux by the equation:

$$RR(E) = N\sigma(E)\phi(E) ,$$

where N is the number of helium – 3 atoms in the detector head and is relatively constant throughout the collection time. The $^3\text{He}-\sigma_{n,p}$ was acquired from ENDF/B and a polynomial fit was applied to the data in order to obtain energy dependent equations that could be used to unfold the neutron spectra. These polynomial fits are shown in Figure 4.

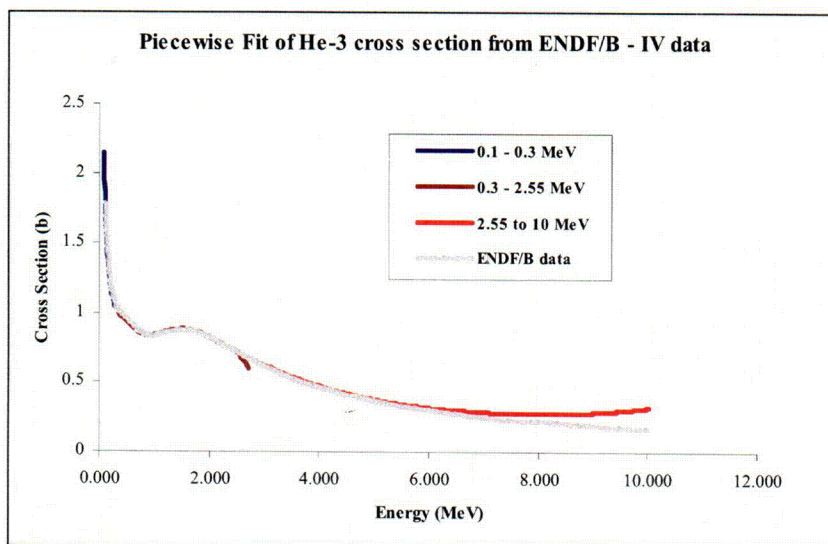


Figure 4: Polynomial piecewise fit to the ENDF/B cross section for the helium-3 (n,p) reaction

Another major consideration that was originally overlooked was the inclusion of the Q value of the reaction in the reported neutron energy. The raw data is shifted in energy by about 764 keV because sum of the kinetic energies of the proton and the triton is given by:

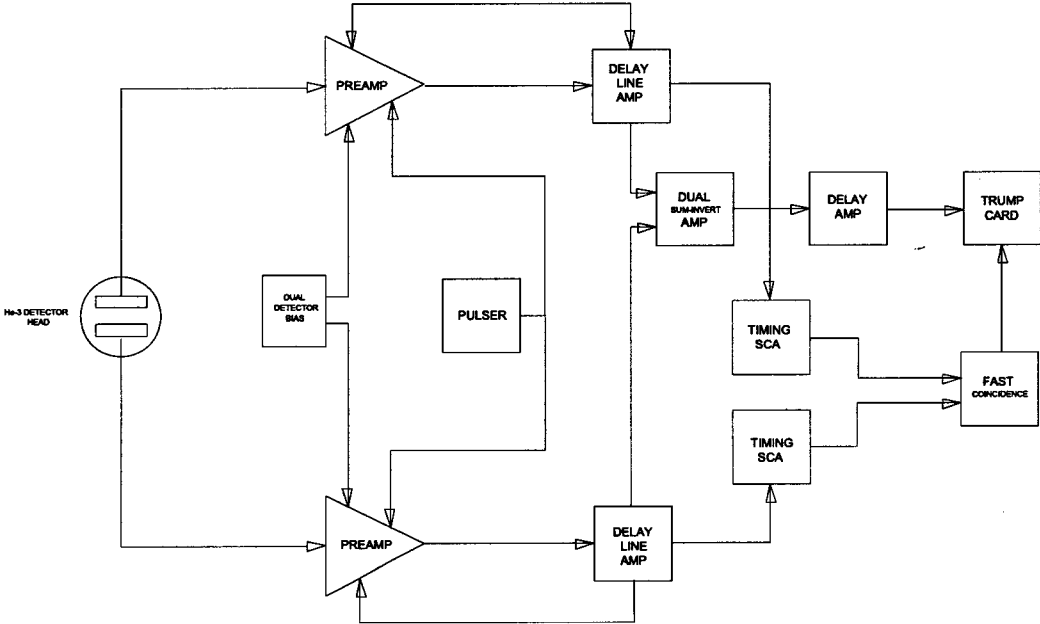
$$KE_{p,t} = KE_p + KE_t = KE_n + Q.$$

Neutrons with initial energies in the thermal range ($E = \sim 0$) will appear in the raw spectrum to have energies of 764 keV. This additional Q value energy can be subtracted during the energy calibration process so that the incident neutron's actual energy is recorded in the spectrum.

A current effort is underway to determine if the response function of the system should also be considered when unfolding the raw neutron spectra. The response of the spectrometer is likely a function of the system efficiency, which varies by several orders of magnitude for thermal and fast neutrons ($\epsilon = \sim 10^{-2}$ for thermal, $\sim 10^{-6}$ for fast).

As mentioned, there are still issues that need to be accounted for before a completely unfolded or deconvolved neutron spectrum can be obtained. The ultimate goal, once a neutron spectrum can be extracted from the raw data, is to combine the ORTEC Model 525 – 780 Neutron Spectrometer with the portable slow neutron chopper, which was developed at Ward Center for Nuclear Science at Cornell University and the RSEC at the Pennsylvania State University, into one unit that can be transported to different research neutron beams for characterization purposes.

APPENDIX A



THERMAL-HYDRAULIC ANALYSIS OF NEUTRON COOLING SYSTEMS

Participants: S. Yavuzkurt, Prof. of Mechanical and Nuclear Eng. Dept
K. Ünlü, Prof. of Mechanical and Nuclear Eng. Dept.
H. Melaku, Ph.D. student at Mechanical and Nuclear Eng. Dept

Services Provided: Neutron Beam Laboratory

Sponsor: DOE-INIE, RSEC, Penn State Mechanical and Nuclear Engineering Dept.

INTRODUCTION

Cold neutrons can be obtained in several ways. Only two cold neutron beam facilities were developed at the U.S. university research reactors, namely at Cornell University and the University of Texas at Austin. Both facilities used mesitylene moderator. The mesitylene moderator in the Cornell Cold Neutron Beam Facility (CNBF) [1] which is no longer available – was cooled by a helium cryorefrigerator via a copper cold finger to maintain the moderator below 30 K at full power reactor operation. The Texas Cold Neutron Source (TCNS) [2] also uses mesitylene moderator cooled via a thermosyphon containing neon. The operation of the TCNS is based on a helium cryorefrigerator, which liquefies neon gas in a 3 m-long thermosyphon. The thermosyphon cools and maintains mesitylene moderator at about 30 K in a chamber. Neutrons streaming through the mesitylene chamber are moderated and thus reduced in energy to produce a cold neutron distribution.

The basic principle used in both systems is similar. However, the thermal-hydraulic mechanism of removing the heat from the moderator chamber that is near the reactor core to the cold head that is placed outside the biological shield of the reactor is different. The CNBF system uses copper rod to transfer heat by conduction to the cold head. In the TCNS system the basic mode of heat removal involves conduction through the wall, free convection and mainly pool boiling of cold neon inside the thermosyphon. In this study the mechanisms of heat removal is analyzed and evaluated both analytically and using computational fluid dynamics and heat transfer codes mainly by using commercially available FLUENT [5] code. The advantages and disadvantages of each system will be determined. FLUENT [5] through parametric studies is being used to design a new Neutron Cooling System (NCS) for university research reactors and particularly for PSU reactor. In this paper, preliminary results of CFD simulation of TCNS are presented.

CURRENT STUDY

This study focuses on detailed thermal-hydraulic analysis of both the TCNS and the CNBF cooling systems, analytically and using standard commercial thermo-fluid dynamic code such as FLUENT6.1 [5]. At the current stage of this study, the transient cooling down process of the thermosyphon is being studied. By observing the earlier measured data [1] and using equilibrium model to derive neon temperature and mass flow rate, it has been concluded that the basic mechanism of the cooling down process consists of four dominant stages as shown in Figure 1: 1. Transient startup, 2. Cooling down of neon gas 3. Cooling down of the moderator, 4. Condensation and pool boiling. The neon temperature and mass flow rate were derived using ideal gas model from the measured pressure data and assuming thermodynamic equilibrium conditions.

The various models of heat transfer process are being developed in order to incorporate them into the FLUENT solver. The computational domain is prepared using GAMBIT software which is the default grid generation tool for FLUENT. Figure 2a and Figure 2b show the result of the temperature distribution at the inlet to the thermosyphon during the early stages of the cooling down process. Sufficiently fine computational grid sizes ranging from 60,000 to 120,000 cells depending on the flow regime were required to capture the high temperature gradient and for ease of convergence of the solution. However, this comes at the expense of calculation time for the transient system with a relatively large aspect ratio of the domain. In this case the computational domain is of 3.35 m long and of 19 mm diameter thermosyphon tube connected to a 6.5 l neon reservoir. Efforts are being made to reduce the skewness factor of the grid as low as possible by using hexagonal mesh wherever possible in the flow domain.

The computational result together with the experimental data obtained previously is expected to lead to a better design for the Penn State cold neutron source.

SET UP AND PREPARATION OF THE CFD SIMULATION

The default preprocessor software for Fluent which is GAMBIT was used to prepare the computational domain of the TCNS and generate the finite volume cells. The total number of cells of the flow domain was 6700 cells. The mesh sizes were varied according to the anticipated flow structure such that more cells were used wherever there is large velocity or temperature gradients. To take advantage of the flow symmetry and save computation time the analysis was made by splitting the above flow domain in half along the length of the tube. Symmetry boundary condition will then be applied along the cutting plane. In order to perform an accurate CFD simulation, all the boundary conditions at the various surfaces of the flow domain must be known. Due to the nature of the operational temperature range of the system, the cold head temperature can be affected by even a small exposed (un-insulated) thermocouple wire. The operation manual recommends that these wires should be thermally shielded. The amount of heat removed by the cryorefrigeration system at the cold head during the cooling down stages of the TCNS is not known. However, the temperature at the cold head during cooling down stages was measured previously[1] and this was taken as a temperature boundary condition for the CFD simulation. The temperature data was curve fitted and a "C" code was written to interface it within FLUENT as a UDF after compiling.

The geometry and material properties of the tube that connects the neon tank and the thermosyphon affect the heat transfer. In this revised simulation the length of the tube was increased to 5 m. The internal diameter of the tube is 3 mm. From the initial simulations it appears that the neon tube is a major heat load to the cooling system in the initial cooling period. The boundary condition at the surface of the neon tube was set to be room temperature of 300 K.

The reservoir was located outside the biological shield and hence the surface temperature should be assumed to be room temperature of 300 K. Since it is located inside the biological shield, the boundary condition for the thermosyphon wall was set to be an insulated wall.

The working fluid for the TCNS thermosyphon was neon gas. The initial condition of the gas is a room temperature of 300 K and pressurized to 10 atm. In this simulation neon was considered as an ideal gas and hence the ideal-gas model was selected for the variation of density in the simulation. In order to account for the continuous drop of absolute pressure in the system during cool down, the floating pressure option was activated. Previous simulations have shown that this was a major source of instability in the convergence of the simulation.

TWO-PHASE FLOW ANALYSIS

The condensation and boiling of the neon gas inside the thermosyphon should be modeled using the general two phase modules of FLUENT. This can be accomplished by using a two phase flow UDF to simulate the condensation and boiling inside the thermosyphon. Condensation on the inside wall of the cold head starts when the neon gas inside the thermosyphon reaches at or below the saturation temperature at the prevailing saturation pressure. Since the pressure inside the thermosyphon continuously changes the saturation temperature also changes continuously. The UDF that should be incorporated should account for the continuously changing saturation condition. The saturation temperature vs. pressure of neon was incorporated into FLUENT by using a curve fit.

PRELIMINARY RESULTS

The simulation result shown in figure 3 is the latest result of prediction of the absolute pressure in the neon reservoir. This simulation was carried out by taking the variation of physical and thermal properties of both aluminum and neon with temperature. The operating temperature and pressure range of the TCNS was about 28 K and 40 kPa respectively. At such a low temperature the thermal properties were found to be extremely sensitive to temperature. These effects were included during the simulation. From the result it was possible to see that the absolute pressure in the neon reservoir was accurate up to the beginning of condensation. At this point the simulation beyond the condensation point is being carried out. The

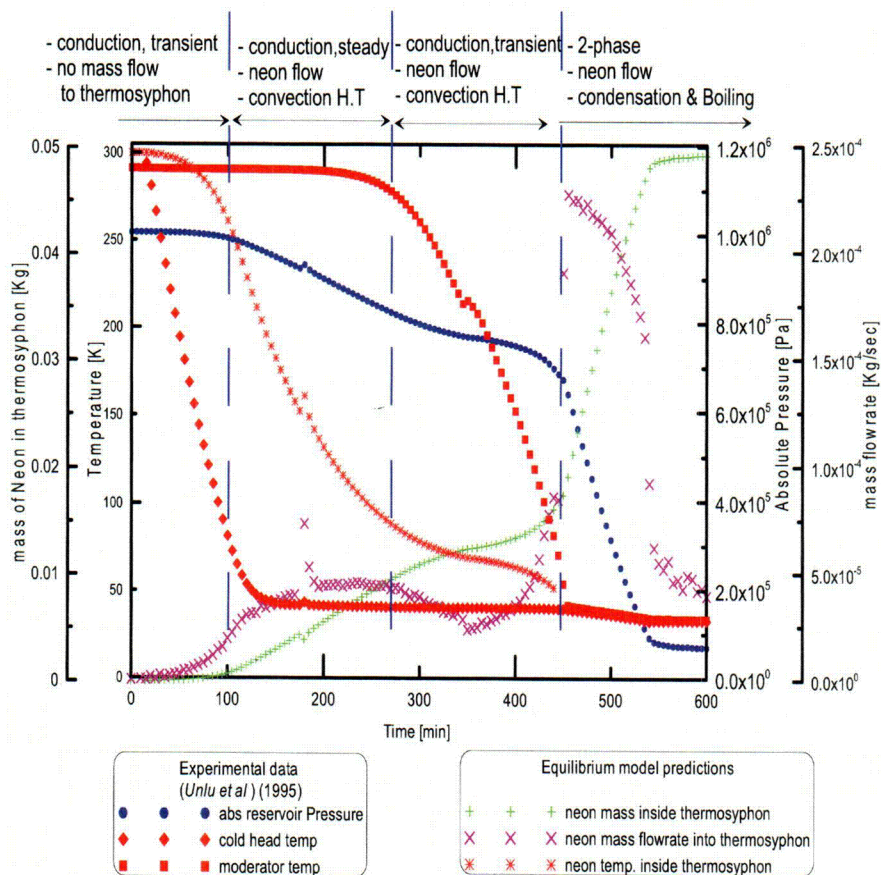


Figure 1. The thermal and flow properties of the TCNS at various stages of the cooling down process. The neon mass flow into the thermosyphon increases substantially at the beginning of the fourth stage when condensation starts

simulation result of the moderator temperature, that is not shown here was not in a good agreement with the data which suggests that there needs to be improvement to the condensation modeling. However initial results shown in Figure 4 show how the condensed neon liquid accumulates at the moderator end of the thermosyphon.

CONCLUSIONS

Neutronic performance of both the CNBF and TCNS systems are known and published previously. However, thermal and thermal-hydraulic behavior of both systems have never been analyzed in detail. Currently both the TCNS and the CNBF cooling systems are being analyzed in order to design and build a third generation mesitylene based cold neutron source at Penn State. The Penn State cold neutron source will be designed with a superior cooling system and an optimized cold neutron beam output. A parallel research to this proposed study is ongoing for the size and shape optimization of Penn State cold moderator chamber. An equilibrium analysis of the experimental data gave four distinctive thermal regimes when plotted as a function of time. These are being used to make the thermal modeling easier. Results from the initial analysis of the TCNS cooling system using FLUENT are encouraging. Following the characterization of the thermal behavior of both systems and parametric studies, a model will be developed for the best performance of university reactor based cold neutron source.

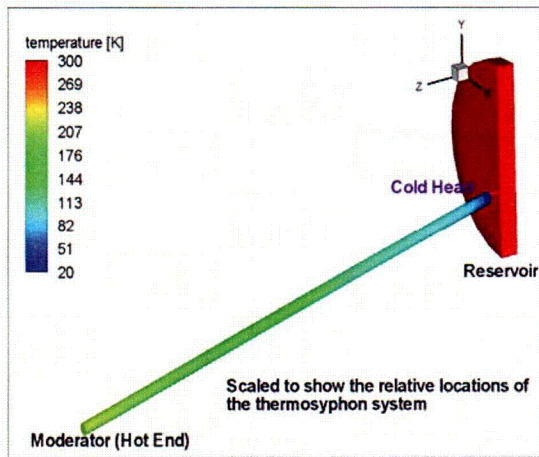


Figure 2a. Temperature distribution in the TCNS cold head, Moderator, Thermosyphon and Reservoir predicted using FLUENT code at the beginning of the cool down process

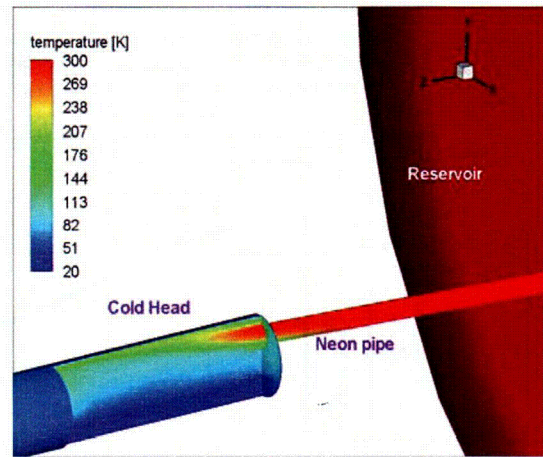


Figure 2b. Temperature distribution in the TCNS cold head predicted using FLUENT code at the beginning of the cool down process. Reservoir temperature remains constant

REFERENCES

1. K. Ünlü, C. Rios-Martinez, B. W. Wehring, "The University of Texas Cold Neutron Source," Nucl. Instr. and Meth., A 353, (1994),397
2. D. D. Clark, C. G. Quillet, and J. S. Berg, "On the Design of Cold Neutron Source," Nucl. Sci. Eng. 110 (1992) 445
3. C. Rios-Martinez, K. Ünlü, Thomas L. Bauer and B. W. Wehring, "Performance of neon thermosyphon in the Texas cold neutron source," Trans. Am. Nucl. Soc., 71 692 (1994)
4. C. Rios-Martinez, K. Ünlü, and B. W. Wehring, "Thermal-Hydraulic and Neutronic Performance of the Texas Cold Neutron Source," Sociedad Nuclear Mexicana, IV. Congreso Anual Memorias, Vol 1, 148 (1993)
5. FLUENT-Computer Code, FLUENT Inc. Centerra Park Lebanon, New Hampshire 03766

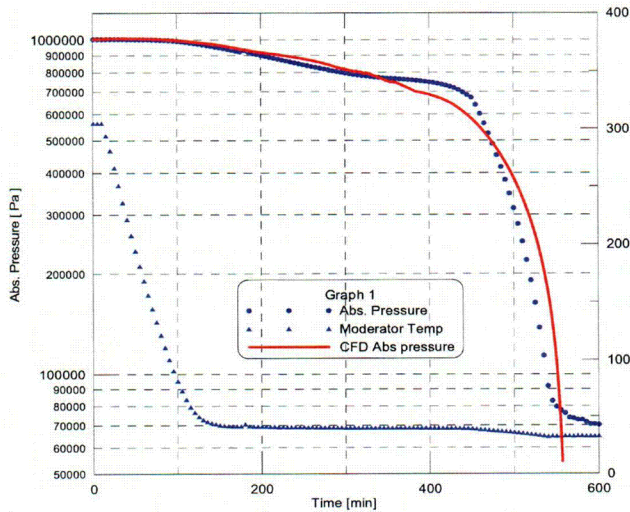


Figure 3 Comparison of simulation and experimental data of absolute pressure in thermosyphon during cool down

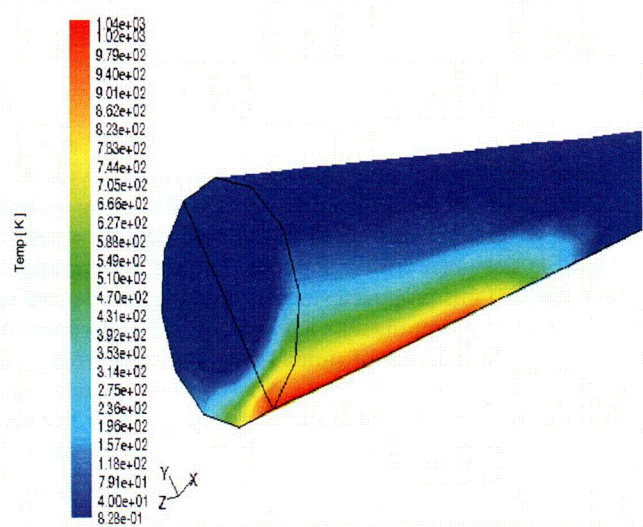


Figure 4 Condensation of neon inside TCNS thermosyphon

MODELLING OF EXISTING BEAM-PORT FACILITY AT PENN STATE UNIVERSITY BREAZEALE REACTOR BY USING MCNP

Participants: K. Ivanov, Prof. Mechanical and Nuclear Engineering Dept.
Y. Azmy, Prof. Mechanical and Nuclear Engineering Dept.
J. Brenizer, Prof. Mechanical and Nuclear Engineering Dept.
K. Ünlü, Prof. Mechanical and Nuclear Engineering Dept.

F. Alim, PhD Student, Mechanical and Nuclear Engineering Dept.
K. Bekar, PhD Student, Mechanical and Nuclear Engineering Dept.
J. Butler, MS Student, Mechanical and Nuclear Engineering Dept.

Services Provided: Neutron Beam Laboratory

Sponsor: DOE, Innovations in Nuclear Infrastructure and Education (INIE)

INTRODUCTION

The Radiation Science and Engineering Center (RSEC) facilities at the Pennsylvania State University (PSU) include the Penn State Breazeale Reactor (PSBR), gamma irradiation facilities, and various radiation detection and measurement laboratories. The PSBR is the nation's longest continuously operating reactor that went critical in 1955. The PSBR is a 1 MW, TRIGA with moveable core in a large pool and with pulsing capabilities. The core is located in a pool of de-mineralized water. When the reactor core is placed next to a D₂O tank and graphite reflector assembly near the beam port (BP) locations, thermal neutron beams become available for neutron transmission and neutron radiography measurement from two of the seven existing beam ports. With TRIGA fuel, only one beam port is at the centerline of the core active area, four beam ports are five inches below the centerline and two are eleven inches below the centerline (below the active fuel region). The PSBR beam port layout is shown in Figure 1. Only two beam ports are currently being used (beam ports shown as red in Figure 1). BP #4, which is located axially at the centerline of the reactor core, is used for research, primarily neutron radiography and radioscopy, and BP #7 with its lower neutron flux level is used for service activities involving neutron transmission measurements. Due to inherited design issues with the current arrangement of beam ports and reactor core-moderator assembly, the development of innovative experimental facilities utilizing neutron beams is extremely limited. Therefore, a new core-moderator location in PSBR pool and beam port geometry needed to be developed. A study is underway with the support of DOE-INIE funds to examine the existing beam ports for neutron output and to investigate new moderator and beam-port designs to produce more useful neutron beams.

The neutron beam ports of any research reactor are designed to transport neutrons generated in the core to the location of experimental equipment. The utility of the neutron beam is strongly dependent on the energy and angular characteristics of incoming neutrons at the beam port entry. Therefore, the optimization of the size and shape of the moderator chamber(s) and of the beam re-entry hole for a beam port enables obtaining higher neutron output through the beam tube with the desired energy, angular and spatial distributions. Such optimization calculations are being performed for the beam port facility of the PSBR to design a couple of new beam ports. In addition, a cold neutron source will be designed and a cold moderator chamber with a mesitylene moderator at cryogenic temperature placed into one of the neutron beam ports. Three cold neutron beams will be extracted using super-mirror neutron guides from this beam port.

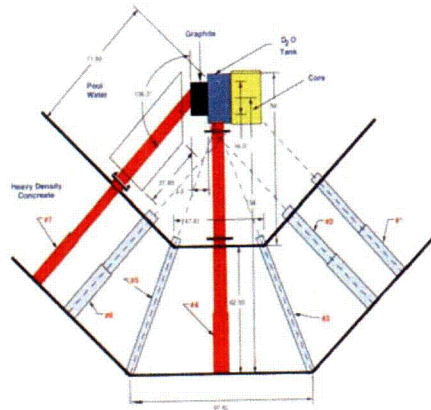


Figure 1. PSBR beam port layout with D₂O tank and graphite reflector

PSU METHODOLOGY AND CODE SYSTEM

Two different methodologies for neutronic modeling of the beam port facility at PSBR have been developed at PSU. The first methodology, is a Monte Carlo based model using MCNP5 [1], while the second model is a deterministic one using TORT [2]. Both models use a diffusion code as the source model for the beam port calculations. Core calculations were performed using a three-dimensional nodal diffusion code ADMARC-H [3], which utilizes a few-group cross-section library developed with HELIOS [4]. Next, beam port calculations are performed either with the MCNP5 or TORT. Separate interface programs have been developed at PSU to link the diffusion code output to the neutron transport code input [5-6]. The MCNP model consists of the D₂O tank, graphite reflector block, and beam tube with their surroundings. This methodology along with some preliminary results was presented at the PHYSOR 2004 conference [5]. The BP #4 configuration was modeled using MCNP. The output of the D₂O tank model is used as the incoming source into the BP #4 model. The results of the MCNP model were compared with the experimental data [7] demonstrating very good agreement. In addition a second model with MCNP5 has been developed in which not only the beam port calculations but also the core calculations were performed with MCNP [8]. This methodology and computational results obtained with it for the PSBR beam port configuration are reported in [9]. The TORT model and its verification by comparison with the results of the first MCNP5 model are presented in [6]. The reason for developing and validating these three alternative models is to use them simultaneously in the optimization of the design of the beam port facility. Having three sets of results, which indicate the same sensitivity trends and confirm the optimality of given design decision would increase the confidence in the optimization process.

Modular code package was prepared for the size and shape optimization of the beam tube device of the beam port facility at the PSBR. In the test cases, using the Min-max algorithm as an optimizer and the multidimensional, transport code TORT as a transport solver in the physics calculation, we optimize the shape of the D₂O moderator of the beam tube device. The modular nature of the optimization package has been illustrated, validation tests of the physics model, have been performed, and preliminary optimization calculation via the whole code package have been analyzed. Results obtained so far indicate that the drum-shaped D₂O moderator tank is over-designed in size and does not possess the almost hemi-spherical optimal shape computed by our new package.

RESULTS AND DISCUSSION

A study for the optimization of the beam port entry hole location for BP #4 has been performed.

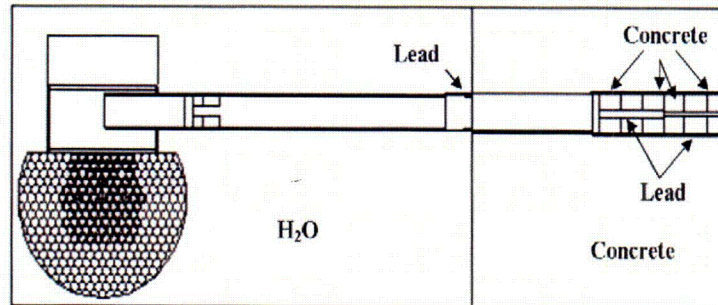


Figure 2. Combined model of core, D₂O and beam port

The location of the beam port entry into the D₂O tank is changed to observe the neutron flux dependence against the location change. The original location of the beam port is demonstrated in Figure 2. Axis of the beam port is changed with respect to this original location, which is shown in Figure 2. Figure 3 shows that the neutron flux increases monotonically as the beam port gets closer to reactor core. The depicted neutron spectra are calculated before bismuth insertion (see Figure 2).

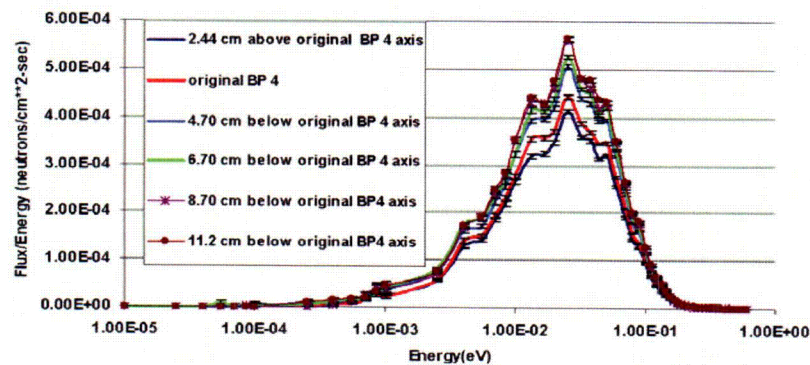


Figure 3. Neutron spectrum behavior with changing the location of beam port 4 entry into the D₂O tank

Another study has been performed to find the best configuration for the moderator tank to maximize the thermal neutron output while minimizing the gamma ray (photon) flux. Sensitivity calculations were performed by changing the dimensions of the moderator tank (in radius and in height separately) and by changing the material of the moderator (from D₂O to H₂O, aluminum, or graphite respectively). The obtained results indicate that both the neutron flux and photon flux decrease at the exit of the beam port entry hole when either the tank radius or the tank height increases. However, it was interesting to observe that the photon flux decreases more quickly than the neutron flux with the increase of the tank volume. Changing the moderator material does not change much the neutron flux but graphite generates smaller photon flux as compared to the other materials.

The third study performed concerns the best configuration for the graphite reflector assembly, which is attached to the D₂O on the side opposite to the core. Sensitivity calculations were performed by changing the shape of the reflector assembly and material of the reflector (the graphite is replaced by D₂O or H₂O). The highest neutron flux was obtained using graphite as reflector material and extra-side reflector.

In the fourth study, the modular optimization procedure is introduced and some preliminary calculations are obtained and analyzed. In the preliminary calculation, one of the beam ports of the PSBR was modeled with the TORT and MCNP codes and the results of both codes were compared. After validating the physics module, a manual optimization procedure was applied to obtain a simplified model or the optimization procedure. In the simplified model, the beam tube re-entry hole geometry and shape remain constant while generating new states by performing D₂O-H₂O replacement. The preliminary calculations show that the sequence implementing the optimization procedure is operational. Other optimizers can be easily mounted into the procedure and parallel execution can be simply performed in the physics module. The results confirmed the previous MCNP results that, the flux output increases when the beam tube is brought close to the core interface. In addition, no more D₂O is necessary to increase the flux output behind Bismuth disk.

CONCLUSIONS AND FUTURE WORK

Three alternative computation models have been developed at PSU for neutronic calculations and design optimization of the beam port facility at PSBR. The models have been validated by comparison with the available experimental data and model-to-model code comparisons. The main goal of the first optimization study being performed at PSU is to find the best location of the beam port entry position in the D₂O tank in terms of the maximum thermal neutron flux. The second study on finding best moderator configuration indicated that using graphite as a moderator material will lead to minimizing the photon flux at the exit of beam port entry hole. In the third study none of the reflector box modifications and material variations resulted in significant changes in terms of thermal neutron flux and photon flux. In the next step, the optimizer modules will be improved by allowing D₂O-AIR, AIR- H₂O replacement which means the size and shape of the beam-tube re-entry hole becomes variable. As a result, the modular optimization procedure search not only for the optimum shape of the D₂O moderator but also determines the shape of the beam re-entry hole.

REFERENCES

1. X-5 Monte Carlo Team, "MCNP - A General Monte Carlo N-Particle Transport Code, Version 5, Volume I: Overview and Theory", *LA-UR-03-1987*, April 24, 2003
2. W. Rhoades, et al, "The TORT Three-Dimensional Discrete Ordinates Neutron Photon Transport Code", ORNL, USA (1997).
3. K. Ivanov, N. Kriangchaiporn, "ADMARC-H Manual", *The Pennsylvania State University*, 2000..
4. "HELIOS Methods", *Studs vikScandpower*, 2000.
5. B. Sarikaya, et al, "Modeling of Existing Beam-port Facility at PSU Breazeale Reactor by Using MCNP5", Proc. of PHYSOR 2004, Electronic Publication on CD-Rom, April 2004.
6. K. Bekar, et al, "TORT Modeling of the Beam Port Facility of PSBR and Comparison with MCNP", TANSO 92, 2005.
7. J. H. J. Niederhaus, "A Single-Disk-Chopper Time-of-Flight Spectrometer for Thermal Neutron Beams." *M.S. Thesis, The Pennsylvania State University*, August 2003.
8. C. Tippayakul, N. Kriangchaiporn, K. Ivanov, C. F. Sears, B. Heidrich, M. Morlang, "Validation of the MCNP5 Core Model of the PSU Breazeale Research Reactor", *American Nuclear Society Topical Meeting in Monte Carlo*, Chattanooga, TN, 2005.
9. B. Sarikaya, et al, "Validation of the mCNP5 Models of the Beam Port Facility at PSBR", *American Nuclear Society Topical Meeting in Monte Carlo*, Chattanooga, TN, 2005.

AUTOMATED THREE-DIMENSIONAL MONTE CARLO BASED DEPLETION METHODOLOGY FOR PSBR CORE

Participants: K. Ivanov, Professor

C. Tippayakul, Graduate Student

The research is focusing on applying the Monte Carlo techniques for fuel management calculations of the PSBR core. The Monte Carlo code, MCNP5, is being mainly employed to analyze the PSBR core. In addition, the ORIGEN2.2 code has been coupled with the MCNP5 code in order to introduce the depletion calculation capability to the PSBR core analysis code system. The interfacing between the two codes is performed by a new developed code, TRIGSIM. The TRIGSIM code provides a convenient PSBR core analysis to users since it automatically generates both MCNP input and ORIGEN input from a simpler TRIGSIM input. The MCNP input for PSBR core is generated based on the geometry and the fuel composition of each fuel element provided by the TRIGSIM input. The TRIGSIM code calls the MCNP code to execute the calculation and extracts the MCNP output to generate ORIGEN input. Then the TRIGSIM code calls the ORIGEN code to execute the calculation and extracts the ORIGEN output to generate MCNP input for the new burnup step. The PSBR core loading 51 has been analyzed by the TRIGSIM code. The initial fuel composition of each fuel element is determined by utilizing the HELIOS-1.7 code to perform the burnup calculation. Furthermore, the calculation has been employed to analyze the new PSBR core loading 52.

New developments in this research will be included to the TRIGSIM code system in the future. These comprises of the development of Monte Carlo acceleration scheme for PSBR core, the generation of burnup cross section library for TRIGA fuel types and the development of the coupling Monte Carlo/Nodal methodology to efficiently provide better spatial distributions of the PSBR core.

Master's Thesis:

C. Tippayakul, K. N. Ivanov, C. F. Sears, G. M. Morlang and B. J. Heidrich "Automated three dimensional depletion capability for the Pennsylvania State University research reactor" PHYSOR2004, April 2004

C. Tippayakul, N. Kriangchaiporn, K. N. Ivanov, C. F. Sears, G. M. Morlang and B. J. Heidrich "Validation of the MCNP5 core model of the PSU Breazeale Research Reactor" Monte Carlo 2005 Topical meeting, April 2005

PARALLEL TRANSPORT MODEL BASED ON 3-D CROSS-SECTION GENERATION FOR TRIGA CORE ANALYSIS

Participants: K. Ivanov, Professor
N. Kriangchaiporn, Graduate Student
C. Tippayakul, Graduate Student

The research is focused on the development of an efficient three-dimensional (3-D) transport model for TRIGA core analysis based on the discrete ordinates (S_n) method. The S_n transport theory method is one of the most accurate numerical approximations for solving the linear Boltzmann equation. The first part of the study was completed for the development of multi-group cross-section generation methodology in 2-D geometry. The second part of this study is continued with the development of multi-group cross-section generation methodology for the TRIGA transport core model in 3-D geometry using the TORT code.

The selected fine-group structure for 3-D cross-section generation of 280-energy groups is the same structure we have obtained for the 2-D cross-section generation. The selected broad-group structure for 3-D cross-section generation consists of 26-groups. This result differs from the obtained broad group structure for 2-D cross-section generation, which consists of 18 groups. The 3-D geometry and presence of graphite in the 3-D unit fuel cell model required more groups in the fast energy range.

The PENTRAN calculations for the mini-core test problems and comparisons of results obtained using 2-D and 3-D cross-sections are being finalized. The implementation of the 3-D TRIGA core simulation will be accomplished. The new calculation scheme will be validated with Monte Carlo solutions.

Ph.D. Thesis:

N. Kriangchaiporn, K. Ivanov, A. Haghghat, and C.F. Sears (2003). "Parallel Transport Model based on 3-D Cross-Section Generation for TRIGA Core Analysis." *A Doctoral Thesis Proposal*. In progress.

Publications:

N. Kriangchaiporn, K. Ivanov, C. Sears, G. Morlang, and B. Heidrich. (2001). Advanced Fuel Management Code System for the Pennsylvania State University Breazeale Reactor (PSBR). TANSO. 85:415-417.

N. Kriangchaiporn, K. Ivanov, A. Haghghat, and C. Sears. (2004). Multi-Group Cross-Section Generation for TRIGA Core Analysis. TANSO.

ANTHROPOLOGY DEPARTMENT

NAA ANALYSIS OF PREHISTORIC METARHYOLITE ARTIFACTS FROM VIRGINIA AND MARYLAND

Participants: K. Hirth, Professor
G. Bondar, Ph.D. Candidate
J. Fleming, Undergraduate

Services Provided: Neutron Irradiation, Radiation Counters, Laboratory Space

The goal of this research is to trace distinctive artifacts manufactured from metarhyolite to known prehistoric quarries in North Carolina, Virginia, Maryland, and Pennsylvania. The artifacts of the Broadspear Horizon form a distinctive and intrusive element from 4,000 to 3,000 years ago in the archaeological record of this region. However, explanations for this cultural discontinuity vary.

This project tests the hypothesis that the prehistoric culture which produced these artifacts spread from south to north through the study area. Results of NAA of 65 artifacts from twenty-one archaeological sites in Virginia, and eight others from Maryland, will be matched to the extensive database of characterized source material from previous research at Penn State's Breazeale Reactor. Preliminary statistical results suggest that a transition point from southern sources (NC and VA) to northern sources (MD and PA) exists in the study transect just north of the Rappahannock watershed in Virginia. While these results generally conform with those from a parallel study of artifact form, and appear to support the hypothesis, the final implications of these results remain to be determined.



Figure 1: Metarhyolite broadspear from Watkins Island, Maryland (44FXH) in the Potomac River.



Figure 2: Metarhyolite broadspear from the Robinson Collection (44MCX32) along the Roanoke River in southern Virginia.

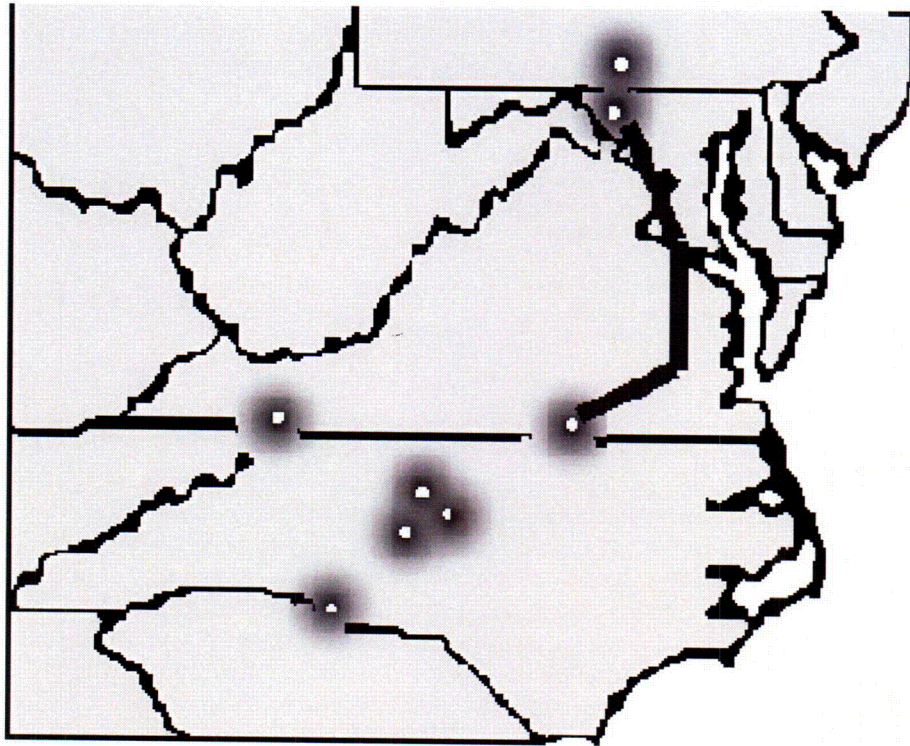


Figure 3: Location of the study transect along the upper limit of the Fall Zone in Virginia and Maryland.

Ph.D. Thesis:

Bondar, G.H., and K.G. Hirth, adviser. Tracing the Transitional: Examining Metarhyolite Use Along the Atlantic Seaboard During the Archaic-Woodland Transition. In progress.

BIOCHEMISTRY DEPARTMENT

THE USE OF HIGH-ENERGY GAMMA IRRADIATION TO EFFECT CRYOREDUCTION OF METTALLOENZYMES FOR SPECTROSCOPIC CHARACTERIZATION

Participants: M. Bollinger, Jr., Associate Professor
M. Green, Assistant Professor
R.B. Guyer, Research Technician
C. Krebs, Assistant Professor

J.C. Price, Graduate Student
L. Saleh, Graduate Student
K. Stone, Graduate Student

Services Provided: Gamma Irradiation

Sponsor: Project 1: grant GM 69657 from NIH to CK and JMB (\$ 256,000/year).
Project 2: grant GM 55365 from NIH to JMB (\$ 157,500 per year).
Project 3: grant GM 47295 to BHH (\$190,000/year).
Project 4: grant 39647-G3 from ACS/PRF to MTG (\$ 17,500/year).

Enzymes containing metal ions are wide-spread in nature and play a pivotal role in almost every aspect of life; they catalyze numerous biochemical transformations, such as key steps in the biosynthesis of DNA and antibiotics. The main purpose of our research program is to define the mechanisms on a molecular level, by which metallo-enzymes catalyze these reactions. To accomplish this goal, we employ time-resolved spectroscopic methods with the aim to identify and characterize reaction intermediates and thereby deconvoluting the catalytic mechanism.

Significant information about such species can be gained from studies of samples that have been exposed to gamma-irradiation (total dose 2 to 5 Mrad) at low-temperatures (77 K), a.k.a. 'cryoreduction'. It has been demonstrated (Davydov et al. JACS 1994, 116, 11120-11128 and references therein) that this procedure allows reduction of the metal clusters while retaining the geometry of the oxidized cluster, because the molecular motion of the radiolytically reduced metal center is impeded due to the low temperature.

This method is extremely valuable for the study of diamagnetic species, because they can be converted to paramagnetic species, which can then be interrogated in detail by paramagnetic methods, such as EPR, ENDOR, ESEEM, and Mössbauer spectroscopies. We employ this methodology to study the following projects:

- 1) We have recently used this method for the initial characterization of the first reaction intermediate in a mononuclear non-heme Fe-enzyme. In particular, the assignment that this species contains formally a high-spin Fe(IV) center was made possible by this technique. Additional information about the geometric and electronic structure will be obtained by the other, above-mentioned methods. Status: in progress
- 2) We have identified several peroxodiferric reaction intermediates in the reactions of non-heme diiron enzymes. Such species are believed to be key species in some of the non-heme diiron enzymes, and in order to gain insight into the reaction mechanisms detailed insight into the geometric and electronic structure is of high importance. We intend to employ the cryoreduction method to study the diamagnetic peroxodiferric species by the above paramagnetic methods. Status: in progress
- 3) In collaboration with Boi Hanh Huynh, Emory University, we will study the enzyme ferredoxin:thioredoxin reductase, which contains an unusual iron-sulfur cluster. Again, we will attempt to convert the diamagnetic cluster to a paramagnetic cluster by cryoreduction and gain information about this species by the above methods. Status: in progress
- 4) We use this method to study the geometric and electronic structure of ferryl-oxo reaction intermediates of P450 heme enzymes. These enzymes play a key role in numerous aspects of biology, and the elucidation of their structure is paramount for the understanding of their function. Status: in progress

Ph.D. Theses:

John C. Price, J. Martin Bollinger, Jr. (advisor), and Carsten Krebs (advisor):
Mechanistic and Structural Studies on Taurine: α -Ketoglutarate Dioxygenase

Lana Saleh, and J. Martin Bollinger, Jr. (advisor):
Oxygen Activation and Electron Transfer in the R2 Subunit of Ribonucleotide Reductase from *Escherichia coli*

Kari Stone, and Michael T. Green (advisor)
"Mechanism of Oxygen Activation by Chloroperoxidase"

Publications:

Price, J. C., Barr, E. W., Tirupati, B., Bollinger, J. M., Jr., and Krebs, C. The First Direct Characterization of a High-Valent Iron Intermediate in the Reaction of an α -Ketoglutarate-Dependent Dioxygenase: A High-Spin Fe(IV) Complex in Taurine/-Ketoglutarate Dioxygenase (TauD) from *Escherichia coli* *Biochemistry*, 42, 7497-7508, 2003

J. M. Bollinger, Jr. Characterization of a High-Spin Fe(IV) Intermediate in the Reaction of Taurine/-Ketoglutarate Dioxygenase (TauD)
Invited talk: 11th International Conference of Biological Inorganic Chemistry. Cairns, Australia, July 2003

Price, J. C., Barr, E. W., Tirupati, B., Bollinger, J. M., Jr., and Krebs, C. On the Identity of a Novel Fe(IV) Intermediate in the Catalytic Cycle of Taurine/-Ketoglutarate Dioxygenase (TauD)
Poster presentation by J.C. Price at the 11th International Conference of Biological Inorganic Chemistry, Cairns, Australia, July 2003

Price, J. C., Barr, E. W., Tirupati, B., Bollinger, J. M., Jr., and Krebs, C. Spectroscopic Characterization of a High-Spin Fe(IV) Intermediate in the Reaction of Taurine/-Ketoglutarate Dioxygenase (TauD)
Poster presentation by C. Krebs at the 11th International Conference of Biological Inorganic Chemistry, Cairns, Australia, July 2003

Carsten Krebs Mechanism of Oxygen Activation by Taurine/-Ketoglutarate Dioxygenase (TauD)
Invited talk: 227th Meeting of the American Chemical Society Anaheim, CA, March 2004

Michael T.Green Role of Thiolate ligation in P450 Enzymes.
Invited lecture: 3rd International Conf. on Porphyrins & Phthalocyanins(ICPP) New Orleans, July 2004

Kari Stone, Carsten Krebs, and Michael T. Green Role of Thiolate ligation in P450 Enzymes.
Poster presented by Kari Stone at the 3rd International Conference on Porphyrins and Phthalocyanins (ICPP) New Orleans, July 2004

Carsten Krebs Mechanism of Oxygen Activation by Taurine/-Ketoglutarate Dioxygenase (TauD)
Invited talk: 7th European Conference on Bioinorganic Chemistry Garmisch Partenkirchen, Germany, August 2004

Price, J. C., Barr, E. W., Tirupati, B., Bollinger, J. M., Jr., and Krebs, C. On the Identity of a Novel Fe(IV) Intermediate in the Catalytic Cycle of Taurine/-Ketoglutarate Dioxygenase (TauD)
Poster presentation by J.C. Price at the 7th European Conference on Bioinorganic Chemistry Garmisch Partenkirchen, Germany, August 2004

Michael T.Green Role of Thiolate ligation in P450 Enzymes.
Invited lecture at the 7th European Conference on Bioinorganic Chemistry Garmisch Partenkirchen, Germany, August 2004

Kari Stone, Carsten Krebs, and Michael T. Green Role of Thiolate ligation in P450 Enzymes.
Poster presentation by Kari Stone at the 7th European Conference on Bioinorganic Chemistry Garmisch Partenkirchen, Germany, August 2004

BIOLOGY

POST-DISPERSAL SEED REMOVAL OF *CARDUUS NUTANS* AND *C. ACANTHOIDES* BY SMALL MAMMALS AND INSECTS

Participants: Dr. Katriona Shea, Assistant Professor
Dr. Eelke Jongejans Postdoctoral Researcher

Ed Silverman Honor student

Services Provided: Gamma Irradiation

Sponsor: \$200 Honors Thesis Research Grant
\$1000 Schreyer Honors College Summer 2005 Research Scholarship

Invasive species have become a very important economic problem for American agriculture. Two common European thistles have become invasive species throughout the USA; these are the musk thistle (*Carduus nutans*) and the plumeless thistle (*Carduus acanthoides*). The two species are very closely related and have similar impacts on the fields that they invade. The plants grow in areas where the soil has been disturbed such as roadsides, heavily grazed fields and agricultural areas. The weeds displace favorable forage plants and the spines on the plants prevent cattle and other livestock from grazing around them.

A great deal is known about the demography and dispersal of *C. nutans* and *C. acanthoides*, but little is known about the post-dispersal seed removal. The post-dispersal seed-removal is a key determinant to the spatial spread of these weeds. Besides, in an area with a high magnitude of post-dispersal seed predation a smaller percentage of seeds that are dispersed will germinate. This is because the seeds are eaten and removed from the population of possible germinants.

In order to investigate what animals remove seeds and at what rate, we performed a series of field experiments in the summer of 2005. We displayed batches of 25 seeds on trays and monitored their removal. We aimed to exclude different groups of animals in different treatments: large-mesh cages were used to keep out large animals, small-mesh cages to exclude also voles and shrews and tanglefoot to refrain insects. Although the analyses of the data are still on-going, the preliminary results indicate that insects like ants and crickets remove most seeds already within 1 or 2 days. This indicates that thistle seeds are spread out quickly. Competition between sibling seedlings will therefore be rare, even when a flower head with seeds breaks off and falls to the ground. It is yet unknown what percentage of the removed seeds are actually eaten, but given that very many seeds are produced, even large predation rates may have a low cost compared to the benefit of the seeds being spread out.

In order not start a new infestation of thistle in the experimental field we first looked for a way to kill the thistle seeds without changing their texture or smell (so that the behavior of animals towards the seeds would not be changed). Candace Davison of RSEC helped us to determine what minimum level of gamma radiation kills a thistle seed. She tested a series of levels, and 1000 KR turned out to be just enough to kill all treated seeds. To be sure we conducted a preference test in the field. Irradiated seeds were removed at the same rate as untreated seeds. Therefore, all seeds used in the main field experiment were irradiated first.

Ph.D. Theses:

Honors' Thesis by Ed Silverman: Dispersal-Colonization Trade-off and Post-Dispersal Seed Predation in *Carduus nutans* and *C. acanthoides* Advisor: Dr. Katriona Shea

CIVIL AND ENVIRONMENTAL ENGINEERING DEPARTMENT

EFFECTS OF Zn(II), Cu(II), Mn(II), Fe(II), NO₃⁻ or SO₄²⁻ at pH 6.5 AND 8.5 ON TRANSFORMATIONS OF HYDROUS FERRIC OXIDE (HFO) AS EVIDENCED BY MÖSSBAUER SPECTROSCOPY

Participants:

G. Catchen, Professor
B.A. Dempsey, Professor
W. Burgos, Associate Professor

J. Jang, Postdoctoral Research Associate/Graduate Student
B. Park, Graduate Student

Services Provided:

Angular Correlations Lab, Laboratory Space

Sponsor:

Department of Energy, Natural and Accelerated Bioremediation Research Program, \$764,870

The objective of the research is to determine the effects of transition metals on transformation of hydrous ferric oxide (HFO) into more thermodynamically stable ferric oxides. Ferric oxides are important environmental adsorbents. In anoxic environments, ferric oxides with Fe(II) are important redox buffers. Transformation of HFO to more stable phases can result in decreased surface area and reduced redox potential.

In some experiments, HFO was precipitated in the presence of Cu(II), Zn(II), Mn(II) and/or Fe(II). In other experiments, Fe(II), NO₃⁻, and/or SO₄²⁻ were added to pre-formed HFO. Transmission ⁵⁷Fe-Mössbauer spectroscopy was used to monitor the phase changes. At pH 6.5 and 65 °C, HFO was transformed into hematite in the presence of Zn(II) or Mn(II). Both metals were significantly adsorbed for these conditions, occupying about 1.2 sorption sites per nm² of HFO surface. Transformations were not observed at pH 6.5 in the presence of Cu(II), which was weakly adsorbed (0.06 sites per nm²). No transformation occurred in the absence of Me(II) transition metals. At pH 6.5 and room temperature, HFO plus Fe(II) transformed into poorly crystalline goethite in the presence of chloride, into goethite and lepidocrocite in the presence sulfate, and into goethite and magnetite in the presence of nitrate. At pH 8.5 and room temperature, HFO that was formed with 0.033 or 0.33 mM Zn(II) and then aged with Fe(II) was transformed into magnetite that was depleted in octahedral Fe, i.e. non-stoichiometric or possibly mixed metal spinel, (Fe³⁺)^{IV}(Me_xFe²⁺_{1-x}Fe³⁺)^{VI}O₄. HFO that was aged with Cu(II) and Fe(II) was transformed into goethite and into magnetite that was also depleted in octahedral Fe. The transformations at pH 8.5 were completely inhibited by 3.3 mM Zn(II) and transformations were significantly decreased by 3.3 mM Cu(II). These results have extended observations of the transformation of HFO to neutral pH ranges and to lower concentrations of metals than previously reported.

Ph.D. Thesis:

Je-Hun Jang, "Chemistry of Environmentally Significant Phases of Oxides of Iron," Dept. of Civil and Environmental Engineering, The Pennsylvania State University, 2004.

Research Supervisor: Dr. Brian A. Dempsey

Publications:

Jang, Je-Hun, Brian A. Dempsey, Gary L. Catchen, and William D. Burgos, "Effects of Zn(II), Cu(II), Mn(II), Fe(II), NO₃⁻, or SO₄²⁻ at pH 6.5 and 8.5 on Transformations of Hydrous Ferric Oxide (HFO) as Evidenced by Mössbauer Spectroscopy," *Colloids and SurfacesA: Physicochem. Eng. Aspects*, **221**, 55-68 (2003).

ENGINEERING SCIENCE AND MECHANICS DEPARTMENT

STUDY OF THE CHARGE TRAPPING CHARACTERISTICS OF HfO₂/Si

Participants: P. Lenahan, Professor
A. Kang, Graduate Research Assistant

Services Provided: Gamma Irradiation

Sponsor: Semiconductor Research Corporation, \$250,000

Charge trapping is a major hurdle facing the integration of the high dielectric constant hafnium oxide material in complimentary metal-oxide-semiconductor devices. In collaboration with Sharp Labs of America and funded by the Semiconductor Research Corporation, we made magnetic resonance observations of the effects of flooding the dielectric material with charge carriers, i.e. through gamma irradiation. The irradiation generates several defect centers in the HfO₂ films, although the nature of these defects are still under investigation. It has been shown previously¹ that gamma irradiation induces charge trapping in HfO₂ devices, thus, the observed centers are likely linked to the charge trapping.

1. A.Y. Kang, P.M. Lenahan, and J.F. Conley, Jr., "The Radiation Response of the High Dielectric Constant Hafnium Oxide/Silicon System." *IEEE Trans Nucl. Sci.* **49(6)**, 2636 (Dec. 2002)

Master's Thesis:

A.Y. Kang, Electron Spin Resonance observation of trapping centers in the high κ hafnium oxide system. May 2004
Advisor: Patrick M. Lenahan

Publications:

A.Y. Kang, P.M. Lenahan, J.F. Conley, Jr., and Y. Ono, "Physical structure of trapped electrons in atomic layer deposited hafnium oxide using Hf(NO₃)₄ precursor." *34th IEEE Semiconductor Interface Specialists Conference*, Dec 4-6, 2003. Washington D.C.

A.Y. Kang, P.M. Lenahan, J.F. Conley, Jr., and Y. Ono, "Reliability Concerns for HfO₂/Si Devices: Dielectric Electron Traps." *International Integrated Reliability Workshop*, Oct. 20-23, 2003. Stanford Sierra Camp, Fallen Leaf Lake, CA.

MATERIALS SCIENCES AND ENGINEERING DEPARTMENT

ORTHOPEDIC BIOMATERIALS

Participants: E.A. Vogler, Professor
X. Liu, Ph.D. Student

Services Provided: Gamma Irradiation

Ph.D. Thesis:

Xiaomei Liu and Erwin Vogler, advisor. Influence of Growth Environment on Osteoblast Adhesion, proliferation, Morphology and Focal Adhesion Assembly

Publications:

Xiaomei Liu, Jung Yul Lim, Henry J. Donahue, Erwin A. Vogler. Influence of Substratum Surface Hydrophilicity/Hydrophobicity on Osteoblast Adhesion, Morphology, and Focal Adhesion Assembly. *Biomaterials*, submitted.

COMPARTMENTALIZED BIOREACTOR FOR BONE CELL CULTURE

Participants: E.A. Vogler, Professor
D. Ravi, Graduate Student
X. Liu, Graduate Student

Services Provided: Gamma Irradiation

COMPARTMENTALIZED BIOREACTOR FOR LONG-TERM CELL CULTURE

An advanced bioreactor permitting extended term culture of animal cells is reported. The bioreactor is based on the principle of simultaneous-cell-growth-and-dialysis that separates a cell growth chamber from a media reservoir by a dialysis membrane, thus compartmentalizing cell growth and cell nutrition functions. As a consequence of compartmentalization, the pericellular environment is unperturbed by continuous perfusion or punctuated re-feeding schedules and "luxury macromolecules" synthesized by cells are retained in a manner that more closely simulates the in vivo condition. Extended periods of unattended cell processing can thus occur during which secretion of various bioproducts and the development of extracellular matrix can be studied.

Long-term culture in a manner that does not disturb the pericellular environment is particularly significant for bone cells, since bone formation and remodeling is a complex cell-and-protein mediated process occurring over the time frame of weeks to months. With the goal of developing osteoinductive biomaterials as a specific application area, phenotypic behavior of a model human osteoblast cell line (hFOB 1.19, ATCC CRL-11372) and mouse calvaria derived osteoblast cell line (MC3T3, ATCC CRL-2593) cultured in the bioreactor was compared to that observed under conventional culture conditions. Attachment and growth of hFOB and MC3T3 cultured in the bioreactor was evaluated using optical microscopy, scanning and transmission electron microscopy (SEM/TEM). Differentiation was evaluated using Alkaline Phosphatase activity (ALP) staining and Von Kossa assay. hFOB cultured in the reactor for 15 days without sub-culturing formed up to 4 cell layers and stained for ALP activity. In sharp contrast, cells cultured for an equivalent period in conventional tissue culture flasks, also without subculture but re-fed every 2 days, exhibited continuous cell shedding, ruffled edges, and failed to form either multilayers or exhibit ALP activity. MC3T3 cultured in the bioreactor for 30 days, formed a tightly packed, dense layer of cells revealing uniform and extensive mineralization with Von Kossa assay. Results suggest that stable culture conditions afforded by the reactor has enhanced utility in the long-term culture of osteoblasts in terms of cell growth, proliferation and mineralized matrix deposition characteristics. The compartmentalized bioreactor thus shows promise as a tool for long-term culture conditions, and specifically for evaluation of bone-cell interactions with orthopedic biomaterials.

Ph.D. Thesis:

Thesis Title: Compartmentalized Bioreactor for long-term cell culture
Graduate Student: Dhurjati Ravi.
Advisor: Prof. Erwin A. Vogler.

Publications:

Ravi, D, Vogler E.A., Compartmentalized Bioreactor for Long-term Cell Culture, 7 th Annual New Jersey Symposium on Biomaterials, New Brunswick, NJ.

Ravi, D, Vogler E.A., Compartmentalized Bioreactor for Long-term Cell Culture, Biointerface, Annual Meeting of the Surfaces in Biomaterials Foundation, Baltimore, MD.

PLANT PATHOLOGY DEPARTMENT, FUSARIUM RESEARCH CENTER

Participants: J.Juba, Research Support Technologist

Services Provided: Gamma Irradiation

Carnation leaves are irradiated in the Cobalt-60 facility in order to provide a sterile growing medium for Fusarium species at the Fusarium Research facility. Nearly every project in our lab relies on the use of these leaves and as far as I know we are the only source of irradiated carnation leaves worldwide. We make them available to others in the Fusarium research community, charging fees to cover our costs. You might find some helpful information at <http://frc.cas.psu.edu/>.

Publications:

1. Garzón, C.D., Geiser, D.M., and Moorman, G.W. *Accepted with revision*. Analysis of AFLP and ITS sequence variation reveals a cryptic species boundary within *Pythium irregulare*. *Phytopathology*.
2. O'Donnell, K., Sutton, D.A., Rinaldi, M.G., Magnon, K.C., Cox, P.A., Revankar, S.G., Sanche, S., Geiser, D.M., Juba, J.H., van Burik, J.H., Padhye, A. and Robinson, J.S. *In Press*. Genetic Diversity of Human Pathogenic Members of the *Fusarium oxysporum* Complex Inferred from Gene Genealogies and AFLP Analyses: Evidence for the Recent Dispersion of a Geographically Widespread Clonal Lineage and Nosocomial Origin. *J. Clin. Microbiol.*
3. Garzón, C.D., Geiser, D.M., and Moorman, G.W. *In Press*. Diagnosis and population analysis of *Pythium* species using AFLP fingerprinting. *Plant Disease*.
4. Geiser, D.M., Lewis Ivey, M.L., Hakiza, G., Juba, J.H. and Miller, S.A. *In Press*. *Gibberella xylarioides* (anamorph: *Fusarium xylarioides*), a causative agent of coffee wilt disease in Africa, is a previously unrecognized member of the *G. fujikuroi* species complex. *Mycologia*.
5. Geiser, D.M., Jiménez-Gasco, M., Kang, S., Makalowska, I., Veerarahavan, N., Ward, T.J. Zhang, N., Kuldau, G.A., and O'Donnell, K. 2004. FUSARIUM-ID v.1.0: A DNA sequence database for identifying *Fusarium*. *European Journal of Plant Pathology* 110: 473-479.
6. O'Donnell, K., Ward, T.J., Geiser, D.M., Kistler, H.C., and Aoki, T. 2004. Genealogical concordance between the mating type locus and seven other nuclear genes supports formal recognition of nine phylogenetically distinct species within the *Fusarium graminearum* clade. *Fungal Genetics and Biology* 41:600-623.
7. Taylor, J.W., Blackwell, M., Geiser, D.M., Hibbett, D.S., James, T.Y., Lutzoni, F., O'Donnell, K.L., Porter, D., Spatafora, J.W., and Spiegel, F. 2004. The History of Fungi. *In: Assembling the Tree of Life*, Cracraft, J. and Donoghue, M.J., eds., Oxford University Press.
8. Geiser, D.M. 2004. Practical fungal molecular taxonomy: *In: Advances in Fungal Biotechnology for Industry, Medicine and Agriculture*. Tkacz, J. and Lange, L., eds. Kluwer Academic Publishers.
9. Geml, J. Geiser, D.M., and Royse, D.J. 2004. Phylogenetic relationships of the genus *Agaricus*. *Mycological Progress* 3: 157-176.
10. Jurjevic, Z., Wilson, D.M., Wilson, J.P., Geiser, D.M., Juba, J.H., Mubatenhema, W., Rains, G.C. and Widstrom, N. *In Press*. *Fusarium* species and fumonisin production on pearl millet and corn from Georgia, USA. *Mycopathologia*.

Seifert KA, Aoki T, Baayen RP, Brayford D, Burgess LW, Chulze S, Gams W, Geiser, D.M., de Gruyter J, Leslie JF, Logrieco A, Marasas WFO, Nirenberg HI, O'Donnell K, Rhéeder J, Samuels GJ, Summerell BA,

NORTHEAST TECHNOLOGY CORPORATION

TESTING OF BORAL UNDER CONDITIONS SIMULATING WETTING AND VACUUM DRYING IN SPENT NUCLEAR FUEL STORAGE CASKS

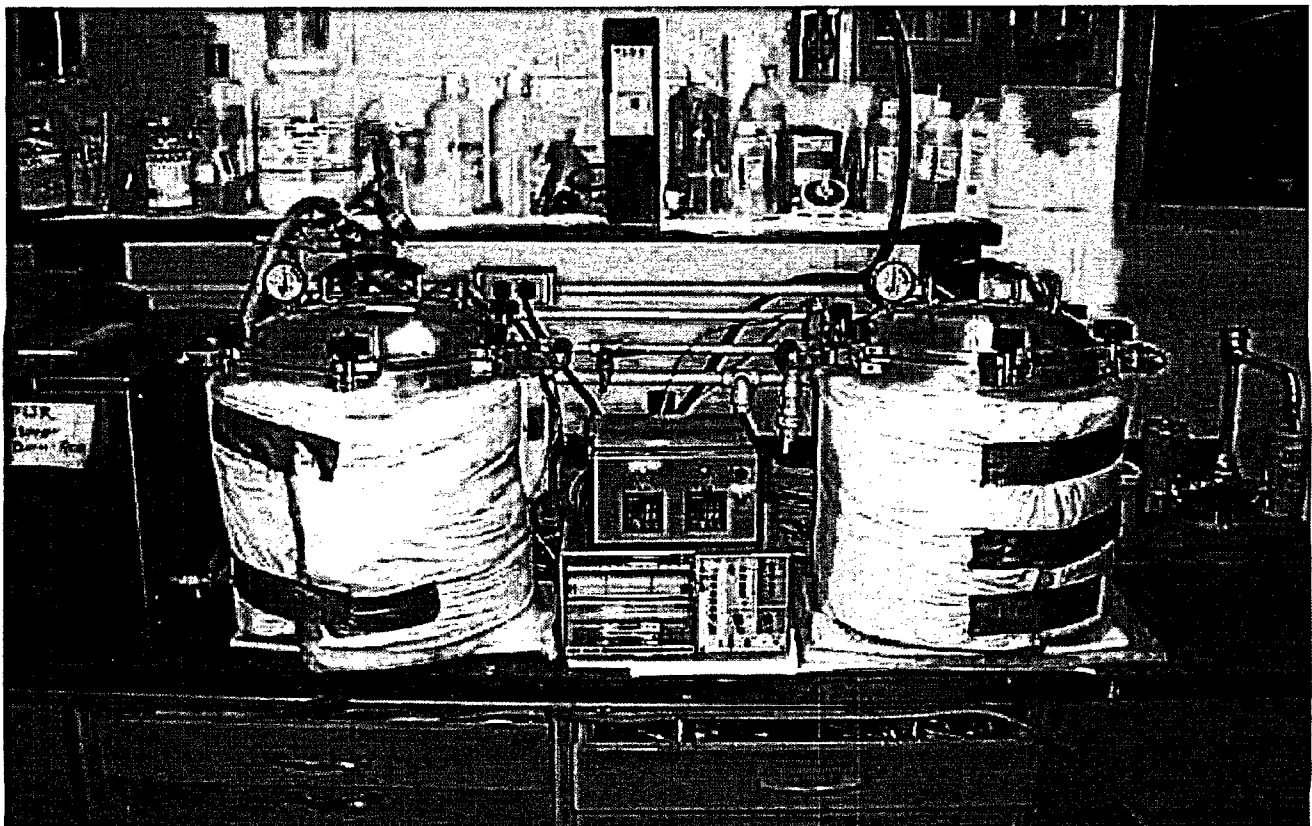
Participants: K. Lindquist, Ph.D.
D. Vonada

Services Provided: Laboratory Space

Sponsor: Electric Power Research Institute, AAR Cargo Systems, Inc., ENRESA

BORAL has been observed to develop large blisters in the aluminum cladding during vacuum drying. Equipment was constructed (Figure 1) to simulate the period when fuel is loaded and the multiple purpose canister (MPC) is in the pool and the BORAL is exposed to the pool water. Following exposure to the pool water the samples of BORAL are placed in a vacuum oven (Figure 2) and slowly brought to 550°F at a controlled rate. This simulates draining of the MPC and vacuum drying.

These studies evaluated BORAL processing variables, MPC drying conditions and as-fabricated BORAL attributes, which have an influence on the propensity for blister formation. The results of the work are providing the manufacturer of BORAL (AAR Cargo Systems, Inc.) with the basis for modifying process variables to provide a blister resistant material.



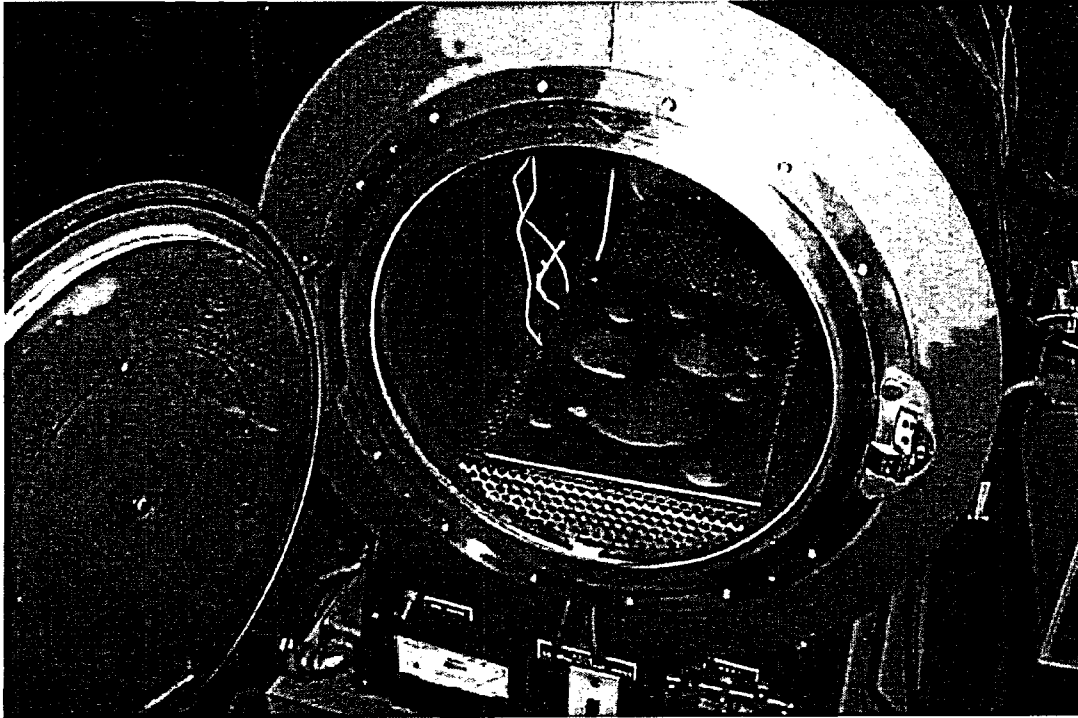


Figure 2: Vacuum Oven

Publications:

EPRI Report 1008441" BORAL Behavior under Simulated Cask Vacuum Drying Conditions", September 2003.

PHYSICAL CHARACTERIZATION OF NEUTRON ABSORBER MATERIALS

Participants: K. Lindquist, Ph.D.
D. Vonada
S. Leuenroth

Services Provided: Neutron Irradiation, Laboratory Space

Surveillance coupons from spent fuel pools at nuclear stations are tested and characterized with respect to their physical attributes. Materials tested include BORAL, Boraflex and borated stainless steel. A key attribute tested is the neutron absorption characteristics. This test is performed in the Neutron Beam Laboratory.

**SECTION B. OTHER UNIVERSITIES, ORGANIZATIONS AND COMPANIES
UTILIZING THE FACILITIES OF THE RSEC**

University or Industry	Type of Use
ADP Life Sciences	Gamma Irradiation
AMD-Cerium Laboratories	Neutron Irradiation
Clarion University	Neutron Activation Analysis
COGEMA	Neutron Radiography Neutron Radioscopy Neutron Transmission
Cornell University	Neutron Radioscopy
David Martin	Gamma Irradiation
Dupont-Stine Haskell	Gamma Irradiation
Eagle-Picher	Neutron Radiography Neutron Radioscopy Neutron Transmission
Exelon	Neutron Transmission
Fairchild Corporation, South Korea	Semiconductor Irradiation
FPL (Florida Power & Light)-Seabrook	Neutron Transmission
General Motors	Neutron Radiography Neutron Radioscopy
Hyundai (South Korea)	Neutron Radioscopy
Lockheed Martin	Semiconductor Irradiation
Mine Safety Appliance	Neutron Radioscopy
NETCO (Northeast Technology Corporation)	Neutron Radioscopy Neutron Transmission
Northrup-Grumman (formerly TRW)	Irradiation of Electronic Devices
NWT	Isotope Production
Physical Acoustics	Neutron Irradiation Gamma Irradiation
Powdermet	Neutron Transmission
Raytheon Company, Sudbury, MA	Irradiation of Electronic Devices
Raytheon Systems Company, El Segundo, CA	Irradiation of Electronic Devices
Toyota	Neutron Radioscopy
TRACERCO (formerly Synetix, Inc.)	Isotope Production
Tru-Tec	Isotope Production
University of Pittsburgh, Greensburg	Neutron Activation Analysis
University of Wisconsin	Neutron Activation Analysis
W.L. Gorr	Neutron Radiation

PUBLICATIONS



PUBLICATIONS

- K. Ünlü, P. I. Kuniholm, J. J. Chiment, D. K. Hauck, "Neutron Activation Analysis of Absolutely-Dated Tree Rings", *Journal of Radioanalytical and Nuclear Chemistry*, Vol. 264, No. 1 (2005) 21-27
- N. Pekula, K. Heller, P. A. Chuang, A. Turhan, M. M. Mench, J. Brenizer, K. Ünlü, "Study of water distribution and transport in a polymer electrolyte fuel cell using neutron imaging," *Nuclear Instruments and Methods in Physics Research A* 542, (2005) 134-141
- B. Sarikaya, F. Alim, K. Ivanov, K. Ünlü, J. Brenizer, Y. Azmy, "Verification of the MCNP5 Model of the Beam Port Facility at PSBR" *The Monte Carlo Method: Versatility Unbounded in a Dynamic Computing World*, Chattanooga, Tennessee, April 17-21, 2005, on CD-ROM, American Nuclear Society, (2005)
- J. Niederhaus, J. Brenizer, K. Ünlü, "Thermal Neutron Time-of-Flight Spectroscopy at Penn State using a Single-Disk Chopper", *PHYSOR 2004 -The Physics of Fuel Cycles and Advanced Nuclear Systems Global Developments* (2004)
- B. Sarikaya, F. Alim, K. Ivanov, K. Ünlü, J. Brenizer, Y. Azmy, "Modelling of Existing Beam Port Facility at PSU Breazeale Reactor by using MCNP", *PHYSOR 2004 -The Physics of Fuel Cycles and Advanced Nuclear Systems: Global Developments* (2004)
- S. M. Cetiner, K. Ünlü, G. Downing, "Development of time-of-flight neutron depth profiling at the Pennsylvania State University," *American Nucl. Soc. Trans.* Vol. 90, (2004) 311-312
- D.K. Hauck, K. Ünlü, P.I. Kuniholm, J.J. Chiment, "Uses of NAA: Gold Concentrations in Dated Tree Rings," *American Nucl. Soc. Trans.* Vol. 90, (2004) 320-321
- N. Pekula, M. M. Mench, K. Heller, K. Ünlü, J. Brenizer, "Neutron Imaging of Two-phase Transport in a Polymer Electrolyte Fuel Cell," *American Nucl. Soc. Trans.* Vol. 90, (2004) 309-310
- S. M. Cetiner, K. Ünlü, V. Degalahal, N. Vijaykrishnan, M. J. Irwin, "Testing Neutron-Induced Soft Errors in Semiconductor Memory," *American Nucl. Soc. Trans.* Vol. 91, (2004) 825-826
- K. Ünlü, C. Rios-Martinez, "Cold Neutron PGAA Developments at University Research Reactors in The USA," *Journal of Radioanalytical and Nuclear Chemistry*, Vol. 265, No. 2 (2005) 329-338
- K. Bekar, Y. Y. Azmy, K. Ünlü, "TORT Modelling of the Beam Port facility of PSBR and Comparison with MCNP," *American Nucl. Soc. Trans.* Vol. 92, (2005) 151-152
- M. Habte, S. Yavuzkurt, K. Ünlü, "Thermal-Hydraulic Analysis of Neutron Cooling Systems," *American Nucl. Soc. Trans.* Vol. 92, (2005) 170 -172
- F. Alim, B. Sarikaya K. Bekar, K. Ivanov, K. Ünlü, J. Brenizer, Y. Azmy, "Optimization of Beam Port Facility at PSBR," *American Nucl. Soc. Trans.* Vol. 92, (2005) 149-150
- K. Ünlü, S. M. Cetiner, G. Downing, "Development of Time-of-Flight Neutron Depth Profiling at the Pennsylvania State University," Accepted for publication in *Journal of Radioanalytical and Nuclear Chemistry* (2005)
- V. Degalahal, L. Li, N. Vijaykrishnan, M. Kandemir and M. J. Irwin. To appear. *Soft Errors Issues in Low Power Caches. /IEEE Transaction on VLSI.*

S. Srinivasan, A. Gayasen, N. Vijaykrishnan, M. Kandemir, Y. Xie, M. J. Irwin. November 2004. Improving Soft-error Tolerance of FPGA Configuration Bits. /Proceedings of the International Conference on Computer Aided Design/ (ICCAD-2004). pp. 107 – 110. San Jose, CA.

R. Ramanarayanan, N. Vijaykrishnan, Y. Xie, M. J. Irwin. September 2004. Soft Errors in Adder Circuits /Proceedings of the Annual Military and Aerospace Applications of Programmable Devices and Technologies Conference / (MAPLD'04). Washington D. C.

V. Degalahal, N. Vijaykrishnan, M. J. Irwin, S. Cetiner, F. Alim, K. Unlu. September 2004. Soft Errors Simulation and Estimation Engine. /Proceedings of the Annual Military and Aerospace Applications of Programmable Devices and Technologies Conference (MAPLD'04)./ Washington D. C.

L. Li, V. Degalahal, N. Vijaykrishnan, M. Kandemir, M. J. Irwin. August 2004. Soft Error and Energy Consumption Interactions: A Data Cache Perspective. /Proceedings of the International Symposium on Low Power Electronics and Design (ISLPED 2004)./ pp. 132-137. Newport Beach, CA.

A. Turhan, P.A. Chuang, K. Heller, J. S. Brenizer, and M. M. Mench, "The nature of flooding and drying in polymer electrolyte fuel cells," *Journal of Electrochemical Soc.* (submitted) 2005.

P. A. Chuang, A. Turhan, K. Heller, J. S. Brenizer, T. A. Trabold, and M. M. Mench, "The nature of flooding and drying in polymer electrolyte fuel cells," *Proceedings of the Third International Conference on Fuel Cell Science, Engineering and Technology, symposium*, paper #74051, Ypsilanti, MI, May 2005.

N. Pekula, K. Heller, P.A. Chuang, A. Turhan, M. M. Mench, J. S. Brenizer, and K. Ünlü, "Study of water distribution and transport in a polymer electrolyte fuel cell using neutron imaging," *Proceedings of the 5th International Topical Meeting on Neutron Radiography (ITNMR-5)*, Munich, Germany, September 2004.

M. M. Mench, A. Turhan, K. Heller, K. Ünlü, J.S. and Brenizer, "INIE Big-10 consortium enabled research: a new physical model of two-phase transport in polymer electrolyte fuel cells using neutron imaging at Penn State," *Accepted for presentation in the Fall ANS meeting and publication in Trans American Nuclear Society*, November, 2005.

A. Turhan, P.A. Chuang, K. Heller, J.S. Brenizer, K. Ünlü, M.M. Mench, and T. Trabold, "Liquid water distribution and flooding as a function of flowfield design in a PEFC," *Abstract 1014 Presented at the 208th Electrochemical Society Meeting*, Los Angeles, California, 2005.

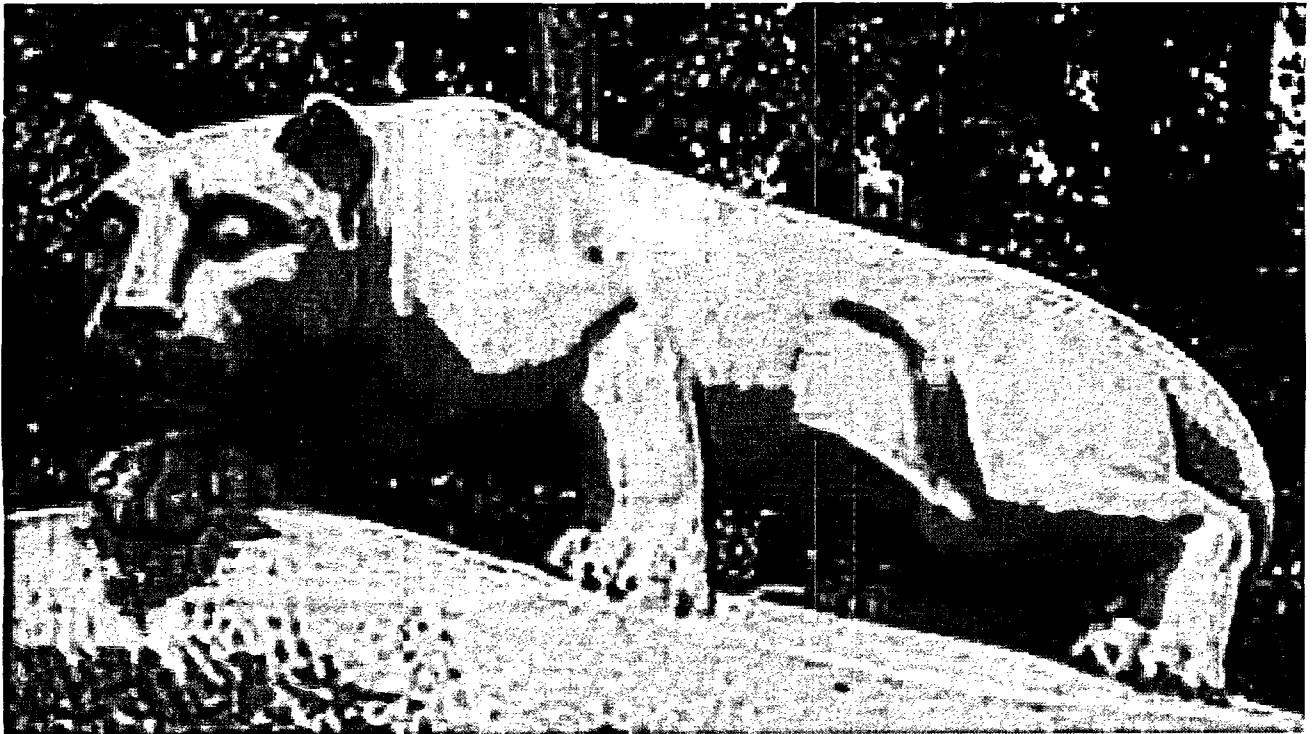
J. S. Brenizer, M.M. Mench, K. Heller, K. and Ünlü, "Neutron imaging at Penn State: past, present and future," (invited) *Presented at the Joint Meeting of the National Organization of Test, Research, and Training Reactors and the International Group on Research Reactors, Special session honoring the Pennsylvania State University Breazeale Reactor 50th Anniversary*, September 12-16, 2005.

P.A. Chuang, A. Turhan, K. Heller, J.S. Brenizer, M.M. Mench, T.A. Trabold, "The nature of flooding and drying in polymer electrolyte fuel cells," *Presented at the Third International Conference on Fuel Cell Science, Engineering and Technology*, Ypsilanti, MI, 2005.

A. Turhan, P.A. Chuang, K. Heller, J.S. Brenizer, M.M. Mench, and T.A. Trabold, "Water distribution at onset of flooding and dry-out in PEFCs," *Presented at the 207th Electrochemical Society Meeting*, Quebec Canada, 2005.

M. M. Mench, "Advanced Diagnostics for PEFCs" (Invited) *Gordon Research Conference on Fuel Cells Bristol, RI.*, July 2004.

APPENDICES



APPENDIX A

Personnel Utilizing the Facilities of the Penn State RSEC.

Faculty (F), Staff (S), Graduate Student (G), Undergraduate (U), Visiting Professor (VP), Visiting Scholar (VS), Faculty Emeritus (FE), Post-Doctoral (PD), High School Student (HS)

COLLEGE OF AGRICULTURE	
Plant Pathology:	
Juba, Jean	S

COLLEGE OF EARTH & MINERAL SCIENCE	
Energy & Geo-Environmental Engineering	
Phelps, Mwita	G
Narayananm, Beepa	G
Geology	
Horodyskyj, Lev	G
Kump, Lee	F

COLLEGE OF ENGINEERING	
Civil & Environmental Engineering:	
Burgos, William	F
Dempsey, Brian	F
Jang, Je-Hun	PD
Park, Byungtae	G
Computer Science & Engineering	
Degalahal, Vijay	G
Irwin, Mary Jane	F
Narayanan, Vijay Krishnan	F
Xie, Yuan	F
Electrical Engineering:	
Ramanarayanan, R.	G
Engineering Science & Mechanics:	
Hawk, Gavin	G
Kang, Andrew	G
Lenahan, P.	F
Mechanical & Nuclear Engineering:	
Alim, Fatih	G
Azmy, Yousry	F
Brenizer, Jack	F
Bryan, Mac	S
Catchen, Gary	F
Cetiner, Sacit	G
Chang, Jong	G
Chaung, Abel	G
Cimbala, John	F
Corbin, Elise	U
Daubenspeck, Thierry	S
Davison, Candace	S

Mechanical & Nuclear Engineering:	
Decker, Chanda	U
Edwards, Bob	F
Flinchbaugh, Terry	S
Hauck, Danielle	G
Heidrich, Brenden	F
Heller, A. Kevin	G
Hochreiter, Larry	F
Hoover, Jared	U
Ivanov, Kostadin	F
Kim, Soowhan	G
Kowal, J.J.	G
Koziol, Adam	U
Kriangchaiporn, Natekool	G
Melaku, H.	G
Mench, Matt	F
Morlang, G. Michael	G
Motta, Arthur	F
Portanova, Alison	S
Rankin, Paul	S
Rickert, Bret	U
Roh, Bumook	G
SariKuya, B.	G
Schwarz, Eric	U
Sears, C. Frederick	F
Sebastiani, Patrick	U
Shields, Dan	G
Skilone, Dan	U
Slaybaugh, Rachel	U
Talley, Ashley	U
Tippayakul, Chanatip	G
Tobin, Dan	G
Trivelpiece, Cory	G
Turhan, Ahmet	G

Mechanical & Nuclear Engineering	
Tyree, Chris	G
Ünlü, Kenan	F
Vincenti, John	S
Wilmot, Aaron	U
Yavue, Kurt	S
Yilmaz, Serkan	G
Yocum, Doug	U
Zangara, Anthony	U
Zerr, Robert	U

COLLEGE OF LIBERAL ARTS	
Anthropology	
Bondar, Greg	G
Fleming, J.	U
Hirth, K.	F

COLLEGE OF SCIENCE:	
Biochemistry	
Bollinger, M.J., Jr.	F
Green, M.	F
Guyer, R.B.	S
Krebs, Carsten	F
Price, J.C.	G
Saleh, L.	G
Stone, K.	G
Biology	
Jongejams, Eelke	PD
Li, Wuxing	G
Shea, Katriona	F
Silverman, Ed	U
Chemistry	
Allcock, Harry	F
Chalkova, Elena	S
Gerlach, Denise	U
Phelps, Mwita	G
Materials Sciences & Engineering Dept.	
Liu, Xiaomei	G
Ravi, Dhurjati	G
Vogler, Erwin	F

OFFICE OF ENVIRONMENTAL HEALTH AND SAFETY	
Bertocchi, Dave	S
Boeldt, Eric	S
Hermann, Greg	S
Linsley, Mark	S
Morlang, Suzanne	S
Wiggins, Jim	S

INDUSTRIES, ETC.

ADP Life Services	Roy Hammerstedt A.T. Philips
AMD-Cerium Laboratories	Tim S. Hossain
COGEMA	Pascale Adabie Gilles Bonnet Jean-Francoise Giraldi Laurent Hansel Jean Oudut
Cornell University	Mark Dinert Peter Kuniholm
David Martin	David Martin
Dupont-Stine Haskell	Valeyri Rotarenco
Eagle-Picher	Monte Hart Jerry Houdyshell Sandi Rushin
Exelon – Oyster Creek	Sharmi Hari
FPL (Florida Power & Light)-Seabrook	Alan Merrill
Fairchild Corporation, South Korea	Jiwall Joung
General Motors	Tom Trabold
Hyundai (South Korea)	Taewon Lim Inchul Hwang Seoho Choi
Lockheed Martin	Alex Bogorad Larry Bruccoliere Robert Gigliuto Surindu Seehra
Mine Safety Appliance	David Backfisch Zane Frund Jim Hendrickson
NETCO (Northeast Technology Corporation)	S. Leuenroth Ken Lindquist Doug Vonada
Northrup-Grumman (formerly TRW)	Frank Cornell Don Randall
NWT	Hank Helmholtz Jerre Palino
Physical Acoustics	Caesar Bascora Weiming Dai Jim Esposito
Powdermet	Andrew Shaman Raj K. Singh
Raytheon Company, Sudbury, MA	Jacques Casteel
Raytheon Systems Company, El Segundo, CA	Ed Craig
Toyota	Ida Atsushi Katsuhiko Kinoshita Kazuki Kuwabara Hiroyuki Matsumoto Seiichi Matsumoto Tori Mitshito Yasahiko Miwata Koji Ohshita Seiji Yamada Yasuhiro Yamamoto

TRACERCO	Mike Boone Ray Peacock Judy Seabrook Scott Vidrine
Tru-Tec	Chris Bocage Mike Flinniken Eric Growney
University of Pittsburgh, Greensburg	Tony Boldurian Jessica Kunes Brett Marion Tim Savisky
University of Wisconsin	David Blanchard
W.L. Gorr	Uwe Beuschu Simon Cleghorn Will Johnson Ron Reid

APPENDIX B Formal Tour Groups

TOUR GROUP	DATE	# IN TOUR
VIEW	07/01/04	28
EHS	07/02/04	2
Prospective Student	07/02/04	2
Personal	07/04/04	5
Electric Boat Corp.	07/06/04	1
PGSAS	07/06/04	36
PGSAS	07/06/04	34
Personal	07/08/04	2
VIEW	07/08/04	23
ARL	07/09/04	2
Personal	07/09/04	3
Nuclear Science and Technology	07/12/04	4
Nuclear Science and Technology	07/12/04	12
Nuclear Science and Technology	07/12/04	4
Personal	07/12/04	1
Nuclear Science and Technology	07/13/04	16
Nuclear Science and Technology	07/14/04	19
Occupational Medicine	07/19/04	1
DOE & Geo-Environmental Engr.	07/21/04	1
FBI	07/21/04	1
Toyota	07/23/04	3
Former Student & Family	07/26/04	2
Guts	07/27/04	17
Slice of Science	07/27/04	4
Boy Scouts	07/30/04	26
DOE	07/30/04	5
Spend a Summer Day	07/30/04	13
Supply Source	08/02/04	1
Telecommunications	08/04/04	2
Spend a Summer Day	08/06/04	5
Spend a Summer Day	08/06/04	1
NASA	08/09/04	1
NucE Student	08/13/04	1
Personal	08/13/04	1
Engineering Services	08/17/04	3

TOUR GROUP	DATE	# IN TOUR
Grier School	08/17/04	1
PRE ADT	08/18/04	12
NucE Grad Student	08/24/04	1
Nuclear Engineering	08/25/04	1
Personal	08/26/04	1
MNE	08/30/04	3
Cornell University	08/31/04	2
Messinger Brg.	08/31/04	1
GM	09/01/04	2
Freshman Seminar	09/02/04	18
Personal	09/02/04	1
Cornell University	09/03/04	1
Electro-Optics Center	09/03/04	1
Food Science	09/05/04	20
Freshman Seminar	09/06/04	18
Interview	09/07/04	1
Interview	09/07/04	1
MNE Grad Students	09/07/04	7
NucE Student	09/07/04	1
Interview	09/08/04	1
Freshman Seminar	09/09/04	1
Student	09/13/04	1
Hacettepe University	09/14/04	1
NucE 401	09/15/04	7
Radiation protection Conference	09/15/04	4
Radiation Protection Conference	09/15/04	3
Boy Scouts	09/21/04	17
NucE 401	09/22/04	13
Personal	09/22/04	1
AREVA	09/23/04	3
Cold Neutron Source Meeting	09/23/04	1
Central VA Gov. School	09/24/04	21
NucE 401	09/24/04	13
Prospective Student	09/27/04	2
Home school Group	09/28/04	7

APPENDIX B

Formal Tour Groups

TOUR GROUP	DATE	# IN TOUR
Biology Dept.	09/29/04	1
Interview	09/30/04	1
NucE 301	10/01/04	34
Parents Weekend Open House	10/02/04	211
Cogema	10/05/04	1
ASTM	10/06/04	13
Cold Neutron Source Meeting	10/07/04	1
Intern	10/07/04	1
NETCO	10/07/04	1
Personal	10/07/04	2
WPSX	10/07/04	1
Biology Dept.	10/08/04	1
Genetics Department	10/08/04	1
HMS Sultan	10/08/04	3
Lockheed Martin	10/08/04	3
Prospective Student	10/08/04	2
ASME	10/11/04	4
College of Engineering	10/14/04	1
Nuclear Concepts Alumni	10/14/04	1
Oak Ridge National Lab	10/14/04	1
CLC	10/15/04	25
Prospective Student	10/15/04	2
NucE Student	10/16/04	2
Personal	10/16/04	1
Personal	10/16/04	1
Westinghouse Scholars	10/16/04	59
NucE 401	10/18/04	13
Boalsburg Elementary	10/19/04	19
Boalsburg Elementary	10/20/04	21
Research Associate	10/21/04	1
ROTC	10/21/04	18
ROTC	10/21/04	10
Personal	10/22/04	2
Personal	10/22/04	2
Greensburg Salem High School	10/25/04	25

TOUR GROUP	DATE	# IN TOUR
Personal	10/25/04	1
Property Inventory	10/25/04	2
Property Inventory	10/26/04	2
E-House	10/28/04	19
Tau Beta Pi	10/28/04	25
St. Mary's Area High School	10/29/04	19
Vice President of Research Office	10/29/04	1
MNE Recruits	10/30/04	2
Westinghouse Scholars	10/30/04	71
Physics	11/01/04	1
Houserville Elementary	11/02/04	21
Houserville Elementary	11/02/04	50
MNE Prospective Student	11/03/04	1
Virginia MiniGrant	11/04/04	44
Purdue University	11/05/04	1
Dirk Maurer	11/08/04	1
Prospective Student	11/08/04	2
Interview	11/09/04	1
Interview	11/09/04	1
ME Student	11/09/04	1
ALCAN	11/10/04	5
GM-Fuel Cell Activities	11/10/04	4
Interview	11/10/04	1
Mike Smoyer	11/10/04	1
Personal	11/10/04	4
Italian Seminar Speaker	11/11/04	2
Public Information	11/12/04	1
WSHI	11/13/04	72
ARL Tour	11/18/04	8
Christensen Family	11/18/04	3
Student	11/18/04	1
Student	11/18/04	1
Engineering Mechanics	11/19/04	2
Guy Anderson	11/19/04	1
Mine Safety Appliances	11/19/04	3

APPENDIX B Formal Tour Groups

TOUR GROUP	DATE	# IN TOUR
Personal	11/19/04	1
NRC	11/29/04	1
EASI House	11/30/04	27
Prospective Student	11/30/04	3
Geosciences	12/02/04	2
Wisconsin Seminar Speaker	12/02/04	2
Education Class	12/07/04	9
NucE Student	12/10/04	2
Student	12/13/04	1
DEP	12/15/04	1
Engineering Mechanics	12/16/04	2
Bechtel/Engineering Mechanics	12/20/04	3
University Police	12/21/04	19
Engineering Mechanics	01/03/05	2
Personal	01/04/05	1
University Police	01/04/05	18
Kane High School	01/07/05	18
NucE 450	01/10/05	1
Berwick High School	01/13/05	8
MNE Grad Student	01/13/05	1
Porta Medic	01/13/05	1
Purdue University	01/13/05	1
Toyota	01/13/05	2
Toyota	01/14/05	2
Materials Club	01/17/05	5
Beam Port Meeting	01/18/05	1
NucE 450	01/18/05	26
Panera	01/18/05	1
ANS	01/19/05	1
Mechanical Engineering	01/19/05	1
Boy Scouts	01/22/05	14
Seminar Speaker	01/27/05	2
Students	02/01/05	2
DOD	02/03/05	1
Department Speaker	02/04/05	1

TOUR GROUP	DATE	# IN TOUR
Geosciences	02/04/05	2
Personal	02/04/05	1
Mechanical Engineering	02/07/05	1
Friends School	02/09/05	22
Brockway High School	02/11/05	13
Personal	02/11/05	1
Bioengineering	02/15/05	1
Department Speaker	02/17/05	1
Chemistry	02/18/05	1
NR Fuel Cell Meeting	02/18/05	1
Blue Chip Recruiting	02/19/05	1
Spring Grove High School	02/23/05	3
Environmental Engineering	02/24/05	6
Personal	02/25/05	1
Engineering Open House	02/26/05	218
TruTec	02/28/05	2
Aerospace Engineering	03/02/05	1
Personal	03/02/05	1
Department Speaker	03/03/05	1
Flow Media	03/03/05	1
PSU NR Meeting	03/04/05	1
Biology	03/11/05	1
Biology	03/11/05	2
Biology	03/15/05	1
Personal	03/16/05	1
Punxy High School	03/16/05	16
Ambulance	03/17/05	7
CPI	03/18/05	14
PJSAHS	03/21/05	8
Altoona Organic Chemistry	03/22/05	8
Middle School Students	03/22/05	13
Prospective Student	03/22/05	3
Biology	03/25/05	2
Ohio State Reactor	03/25/05	2
University Police	03/25/05	1

APPENDIX B Formal Tour Groups

TOUR GROUP	DATE	# IN TOUR
State College High School	03/29/05	24
IE 408W	03/30/05	24
IE 408W	03/31/05	24
IE 408W	03/31/05	7
IE 408W	03/31/05	12
Seminar Speaker	03/31/05	3
State College High School	03/31/05	37
Fuel Cell Group	04/01/05	1
IU-9	04/01/05	7
Penn State Students & Faculty	04/02/05	4
VIEW	04/02/05	32
VIEW	04/02/05	30
Personal	04/04/05	1
Energy	04/05/05	1
Radiation Class	04/05/05	1
Prospective Student	04/06/05	3
Department Speaker	04/07/05	3
Lycoming College	04/07/05	26
NIST	04/07/05	1
Personal	04/07/05	1
Personal	04/08/05	3
Prospective Student	04/08/05	2
University Police	04/08/05	1
Boy Scouts	04/09/05	54
ARL Tour	04/11/05	1
Personal	04/11/05	1
Moshannon Valley	04/12/05	16
Personal	04/12/05	1
Shuenke	04/12/05	3
Lock Haven	04/14/05	18
Prospective Student	04/14/05	4
University of Toronto	04/14/05	1
Coughlin High School	04/15/05	19
Bald Eagle High School	04/18/05	14
Prospective Student	04/18/05	2

TOUR GROUP	DATE	# IN TOUR
Toyota	04/18/05	2
Tyrone Middle School	04/19/05	37
Tyrone Middle School	04/19/05	36
BMB	04/20/05	2
The Strange Family	04/25/05	4
Williamson High School	04/25/05	17
Prospective Student	04/26/05	2
Red Lion Christian School	04/26/05	5
Elk County Catholic School	04/27/05	43
Take Your Daughters/Sons to Work	04/28/05	76
HMS Sultan	05/03/05	5
Administrative Services	05/05/05	10
Kyunghea University	05/05/05	1
St. Mary's Area High School	05/06/05	24
Director of Development	05/09/05	10
Personal	05/09/05	1
Marion Center High School	05/11/05	8
Public Information	05/11/05	1
PSU Student and family	05/13/05	8
PSU Student and family	05/13/05	4
PSU Student and family	05/13/05	8
PSU Student and family	05/13/05	3
PSU Student and family	05/13/05	7
PSU Student and family	05/13/05	3
University of Manchester	05/13/05	4
Chartiers-Houston High School	05/16/05	7
Geosciences	05/17/05	1
Ligonier Valley High School	05/17/05	19
Engineering Science and Mechanics	05/18/05	2
Northeastern High School	05/18/05	14
Henderson High School	05/19/05	35
Spring Grove High School	05/20/05	18
Personal	05/21/05	1
Union City High School	05/23/05	24
University Press	05/23/05	1

APPENDIX B Formal Tour Groups

TOUR GROUP	DATE	# IN TOUR
Elizabeth Forward High School	05/24/05	12
DOE	05/25/05	1
Pittsburgh Public Schools	05/25/05	57
Science Magazine	05/25/05	1
Hyundai	05/26/05	1
Personal	05/27/05	1
Geosciences	06/01/05	1
McMaster University	06/01/05	2
Federal Investigative Service	06/08/05	1
Time Capsule	06/08/05	1
Chemistry	06/09/05	1
Chemistry	06/09/05	1
GORE	06/09/05	2
Secret Service-Bush Visit	06/10/05	1
Personal	06/13/05	2
Personal	06/14/05	2
Toyota	06/14/05	2
University Police	06/15/05	2
Prospective Student	06/17/05	3
Prospective Student	06/21/05	2
Biology	06/28/05	2
FBI-Personnel Investigation	06/28/05	1
MNE Interim Department Head	06/28/05	1
Benchmark Group	06/29/05	14
Chemistry	06/29/05	1
Upward Bound	06/30/05	8